

OBSERVATIONS OF SHORT PERIOD
INTERNAL WAVES IN MASSACHUSETTS BAY

by

53.

DAVID HALPERN

B.Sc., McGill University

(1964)

SUBMITTED IN PARTIAL FULFILLMENT
OF THE REQUIREMENTS FOR THE
DEGREE OF DOCTOR OF PHILOSOPHY

at the

MASSACHUSETTS INSTITUTE OF TECHNOLOGY

January, 1969

Signature of Author
Department of Meteorology
January 10, 1969

Certified by . /
Thesis Supervisor

Accepted by
Chairman, Departmental Committee
on Graduate Students

Lindgren

WITHDRAWN
FROM
MIT LIBRARIES

OBSERVATIONS OF SHORT PERIOD
INTERNAL WAVES IN MASSACHUSETTS BAY

by

David Halpern

Submitted to the Department of Meteorology on January 10, 1969
in partial fulfillment of the requirements for the degree of
Doctor of Philosophy

ABSTRACT

Short period (7-minutes) temperature fluctuations were measured in 82 m of water from instrumented buoys moored 9 km west of a prominent sill in Massachusetts Bay. The high frequency oscillations begin with a large abrupt rise in temperature and persist for about three hours. The average time interval between the onset of successive groups of high frequency fluctuations was 12.4 hours. Prior to their onset the temperature is steady. The high frequency fluctuations are coherent and of uniform phase in the vertical direction. The distribution of the rms vertical displacements corresponds to the eigenfunction of the first mode of internal waves, which was computed from measurements of density and velocity. Long crested, short wavelength, dark narrow surface bands were related to the high frequency temperature fluctuations. Groups of high frequency large amplitude fluctuations occurred in velocity measurements made 200 m from the temperature instrumented buoys. The high frequency fluctuations occurring at regular intervals of time seem to be internal waves of mode one propagating in the same direction with respect to the moving medium.

Thesis Supervisor: Henry M. Stommel
Title: Professor of Oceanography

TABLE OF CONTENTS

List of figures	iv
List of tables	vii
Introduction	1.
Data acquisition	10.
Analysis of data	15.
1. Spectral analysis	30.
2. Coherency analysis	41.
Internal wave model	48.
Appendix A: Field program	60.
Appendix B: Data format	67.
Appendix C: Temperature and salinity measurements at Station T	72.
Appendix D: Velocity measurements	84.
Appendix E: Temperature measurements from a towed thermistor	95.
Appendix F: Problems for further investigation	97.
Acknowledgements	98.
References	99.
Biographical sketch	103.

LIST OF FIGURES

Figure	Title	Page
1	Location chart of Station T.	2.
2	Vertical section across Station T.	4.
3	Contour chart of Station T.	5.
4	Temperature measurements at 11.1 m (July 28 to August 2, 1966).	7.
5	Temperature measurements at nine depths (July 30-31, 1966).	8.
6	Oblique air photographs of surface bands.	9.
7	Temperature instrumented Richardson buoy.	11.
8	Speed measurements at 10.6 m (July 13-17, 1967).	17.
9	Directions measured at the time of individual maxima in the speed measurements.	18.
10	Temperature measurements of a towed thermistor.	22.
11	Temperature measurements at 10 m (July 25-27, 1967).	24.
12	Temperature measurements at nine depths (July 26, 1967).	25.
13	Vertical distributions of average temperature, standard deviation, mean density, and mean Brunt-Väisälä frequency (July 25-27, 1967).	26.
14	Simultaneous measurements of surface bands and temperature (July 26, 1967).	29.
15	Contours of spectral density on a frequency-depth plot.	35.
16a	Contours of spectral density on a frequency-depth plot.	36.
16b	Power density spectrum.	36.
17	Contours of spectral density on a frequency-time plot.	38.

Figure	Title	Page
18	Power density spectrum.	40.
19	Complex vertical coherency.	46- 47.
20	Vertical distributions of the amplitude of the vertical velocity of internal waves of mode one, mean density, and mean horizontal velocity.	55.
21	Ten-minute averages of Richardson number, vertical shear, and Brunt-Väisälä frequency.	57.
22	Thermal front.	58.
A1	Location of buoys at Station T (1966).	63.
A2	Location of buoys at Station T (1967).	66.
C1	Average vertical distribution of temperature at Station T.	73.
C2	Vertical distribution of salinity (1966).	77.
C3	Vertical distribution of salinity (1967).	78.
C4	Temperature measurements at 11.1 m below the surface at Station T between July 6 and 9, 1966.	80.
C5	Temperature measurements at 10 m below the surface at Station T between July 13 and 17, 1967.	81.
C6	Temperature measurements at 10 m below the surface at Station T between July 25 and 27, 1967.	82.
D1	Histogram of speed measurements (Station T; July 13-17, 1967).	85.
D2	Histogram of direction measurements (Station T; July 13-17, 1967).	86.
D3	Histogram of speed measurements (Stellwagen Bank; July 24-28, 1967).	87.
D4	Histogram of direction measurements (Stellwagen Bank; July 24-28, 1967).	88.

Figure	Title	Page
D5	Histogram of speed measurements (11 km east of Stellwagen Bank; August 22-25, 1967).	89.
D6	Histogram of direction measurements (11 km east of Stellwagen Bank; August 22-25, 1967).	90.
D7	Speed measurements at 25.8 m below the surface at Station T (July 13-17, 1967).	92.
D8	Speed measurements at 42.6 m below the surface at Station T (July 13-17, 1967).	93.
E1	Pattern of thermistor towing in Massachusetts Bay (September 19, 1967).	96.

List of Tables

Table	Title	Page
1	Statistics of the initiation of the high frequency temperature fluctuations.	16.
2	Mean and standard deviation of the speed measurements.	20.
3	Ensembled averaged statistics of the high frequency temperature fluctuations.	41.
4a	Values of $\Delta\phi$ for different coherences.	45.
4b	Values of upper and lower limits for different coherences.	45.
5	Harmonic number of coherence estimate greater than .47.	45.
6	Eigenvalues computed for velocity and density distributions shown in figure 20.	54.
A1	Moored buoy results at Station T (1966).	63.
A2	Location of velocity measurements.	65.
A3	Moored buoy results (1967).	66.
B1	A listing of a temperature-tape.	69.
B2	A listing of Fortran IV statements that sort the data.	70.
B3	A listing of a current meter-tape.	71.
C1	Minima and maxima temperatures.	74.
C2	Average temperature at the surface and for depths greater than 50 m.	74.
C3	Salinity measurements at Station T.	76.
C4	Comparison of 49 hours of temperature measurements obtained at buoys T1 and T2 between July 25-27, 1967.	79.
C5	Times of initiation of high frequency temperature fluctuations.	83.

Introduction

A form of organized fluctuations occurring in a stably stratified fluid and having periods varying from minutes to the half-pendulum day is internal gravity wave motion. These waves participate in the general variability of the ocean (Fofonoff, 1967), although the extent of participation is unknown. They may provide a sink for the ordinary tide (Munk and Macdonald, 1960, p.219; Cox and Sandstrom, 1962), and they represent a possible mechanism for mixing the ocean waters below the surface layer (Munk, 1966; Woods, 1968).

A complete statistical description of internal waves is both difficult and expensive, for it requires lengthy time series of a conservative property at many depths and at many horizontal locations. Haurwitz (1953) has shown that many identifications of internal waves may have been incorrect because the duration of the measurements was short and the fluctuations could have represented random or disorganized motion. Measurements exhibiting significant coherency (Sabinin and Shulepov, 1965) have been established less often than those containing a lack of coherency (Haurwitz et al, 1959; White, 1967).

During the 1966 summer, buoys instrumented for recording temperature at nine different depths were moored in 82 m of water 9 km west of a (magnetic) north-south trending submarine sill known as Stellwagen Bank (figure 1). This location (called

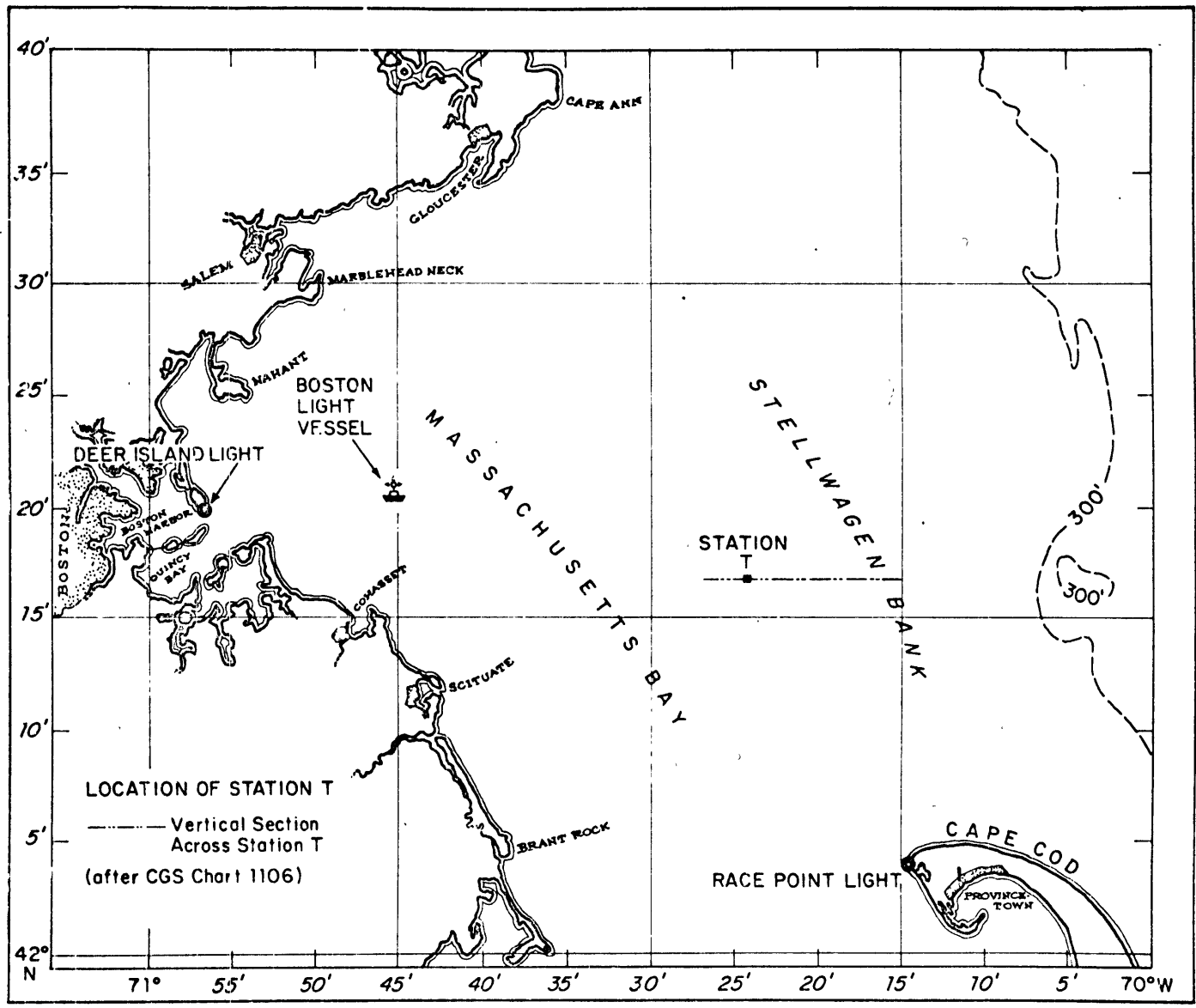


Figure 1.

Station T) was situated in the center of a basin which extended half-way to the sill (figures 2 and 3). Stellwagen Bank has a uniform depth (27 m) along its crest, reaches to the bottom of the seasonal thermocline (Bigelow, 1927) and separates Massachusetts Bay from the Gulf of Maine. Massachusetts Bay, isothermal in winter, contains a well developed thermocline in summer. The location of Station T was chosen on the supposition that tidal flow over a submarine ridge represented a likely method of producing internal waves (Pickard, 1954, 1961; Long, 1954; Defant, 1961, p.559). Atmospheric disturbances are virtually nonexistent during the summer months.

Groups of high frequency temperature fluctuations occurring at regular intervals of time were recorded at Station T on both occasions that field measurements were conducted during the 1966 summer. Figure 4 is a Calcomp plot containing sequential (sampling interval = 2 minutes) temperature measurements at 11.1 m below the surface between July 28 and August 2, 1966. The high frequency fluctuations begin with a large abrupt rise in temperature and persist for about three hours. The time of maximum flood in Boston Harbor occurs about 70 minutes earlier than the initiation time of the high frequency fluctuations. Figure 5 contains the vertical distribution of temperature in a single 18-hour period. The onset of the feature occurred simultaneously at all depths. During the 1966 summer two flights were made over the buoys and on both occasions a pattern of multiple surface

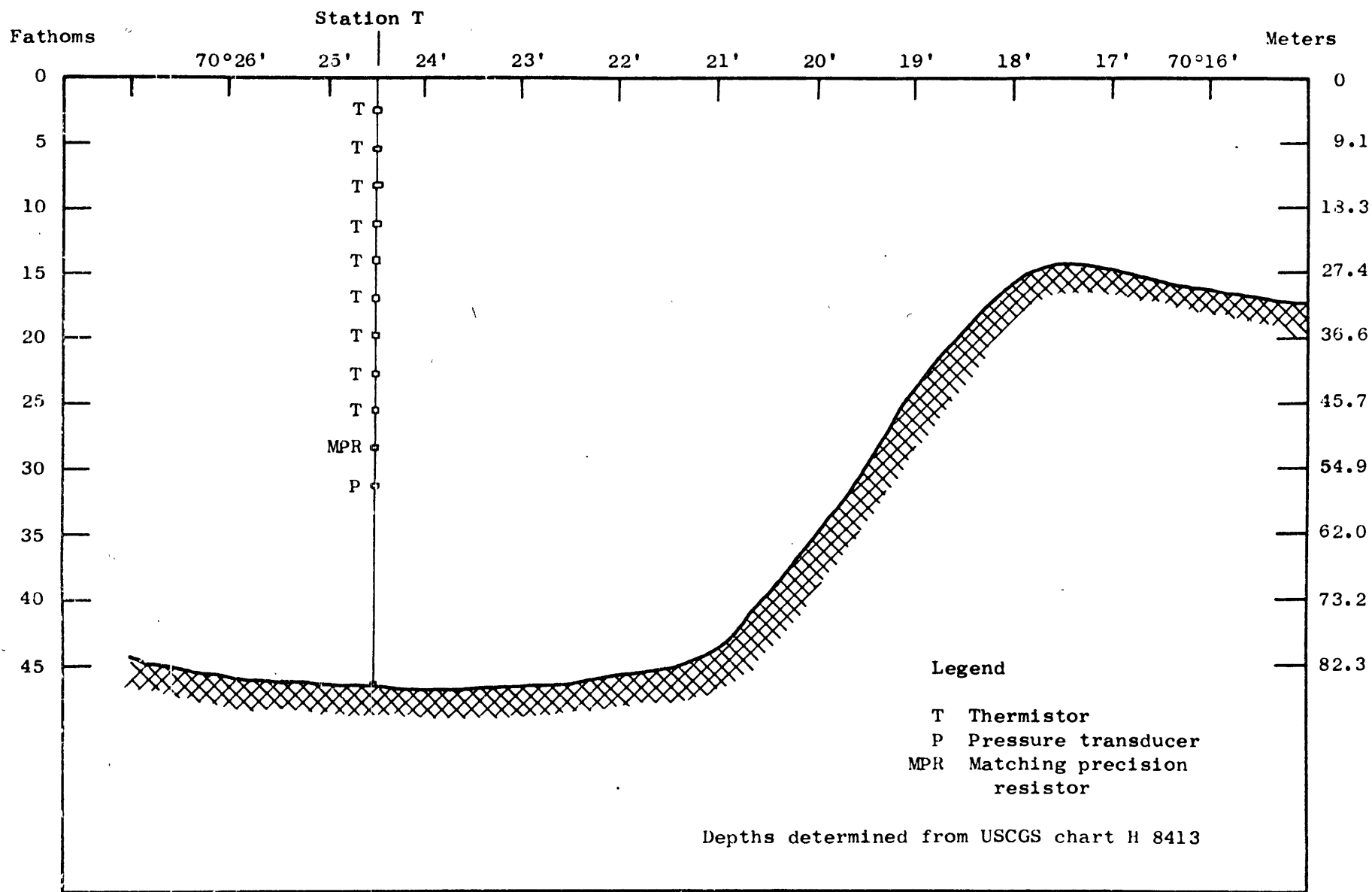


Figure 2. Vertical section across Station T

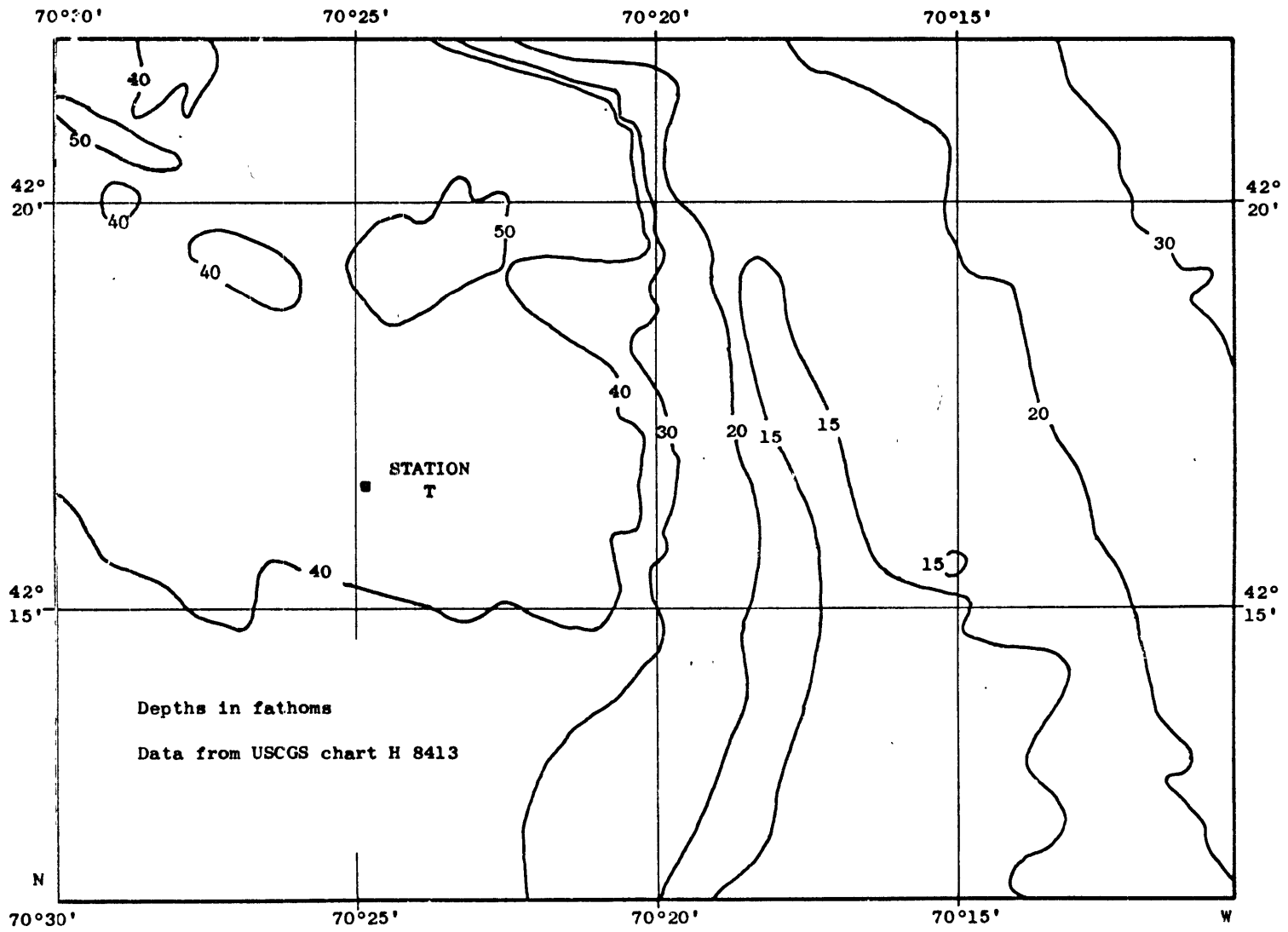


Figure 3. Contour chart of station T and surrounding area

bands was viewed (figure 6). The high frequency fluctuations and the surface bands were investigated during the 1967 summer by means of (1) temperature and velocity measurements from moored buoys, (2) a towed thermistor, (3) aerial surveys, and (4) auxiliary data such as salinity and BT's; this paper describes the results.

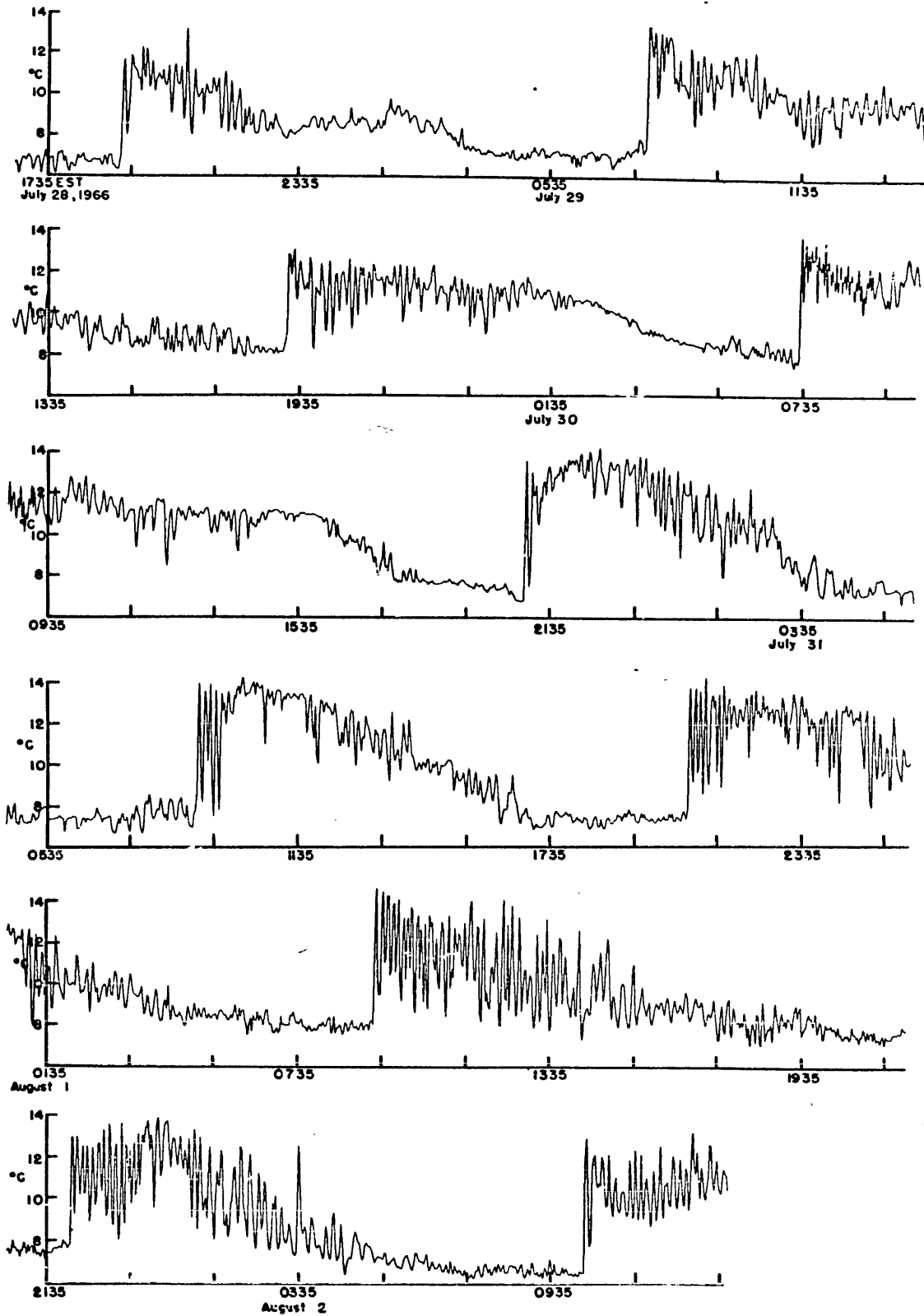


Figure 4 . A Calcomp plot of 3600 temperature measurements at 11.1m at Station T (buoy A) between July 28 and August 2, 1966. The sampling interval was 2-minutes.

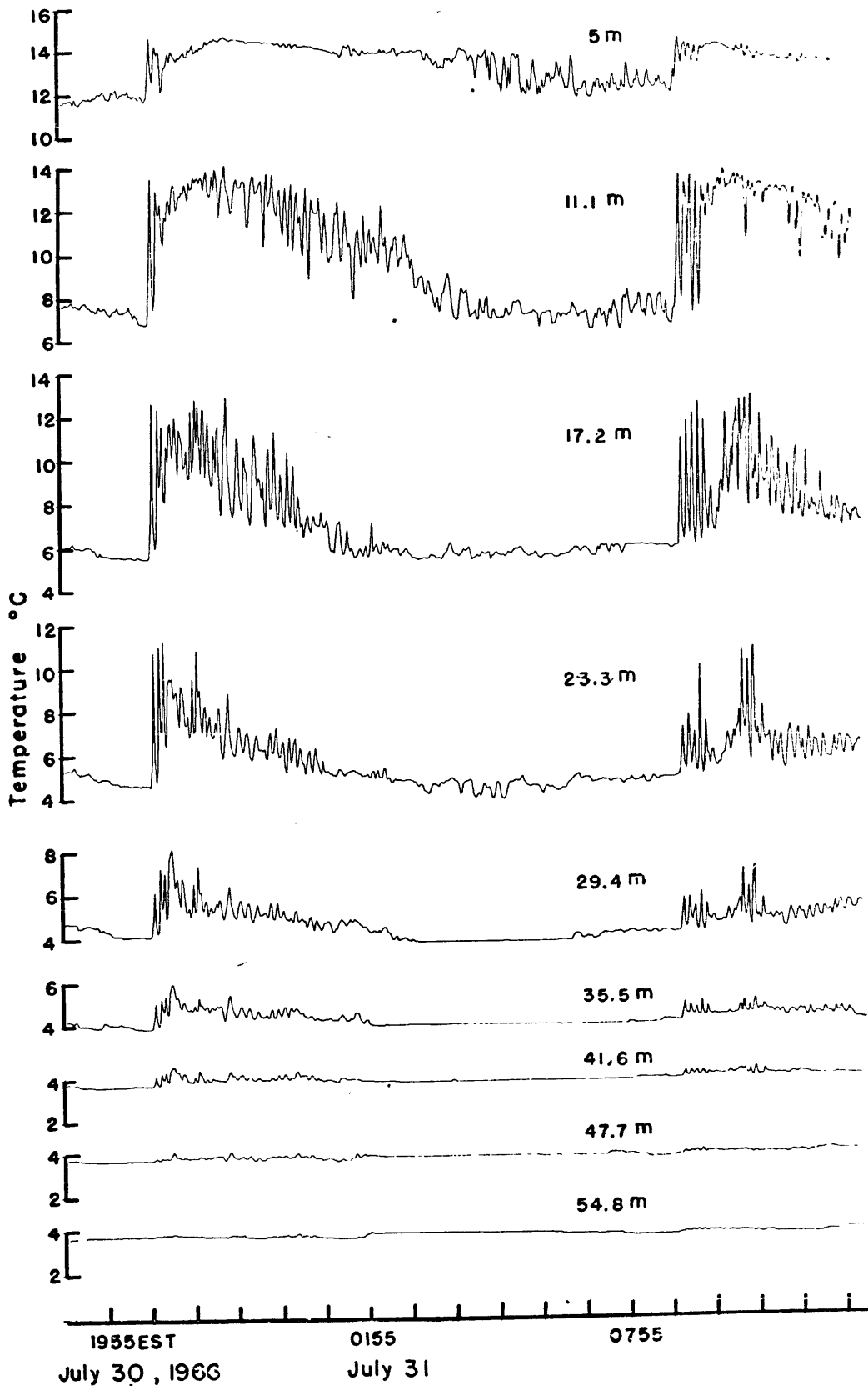
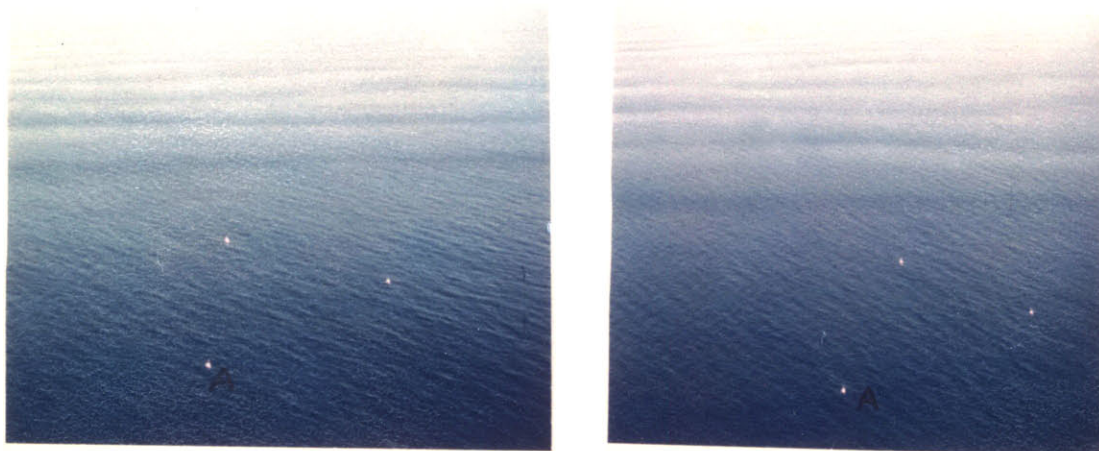
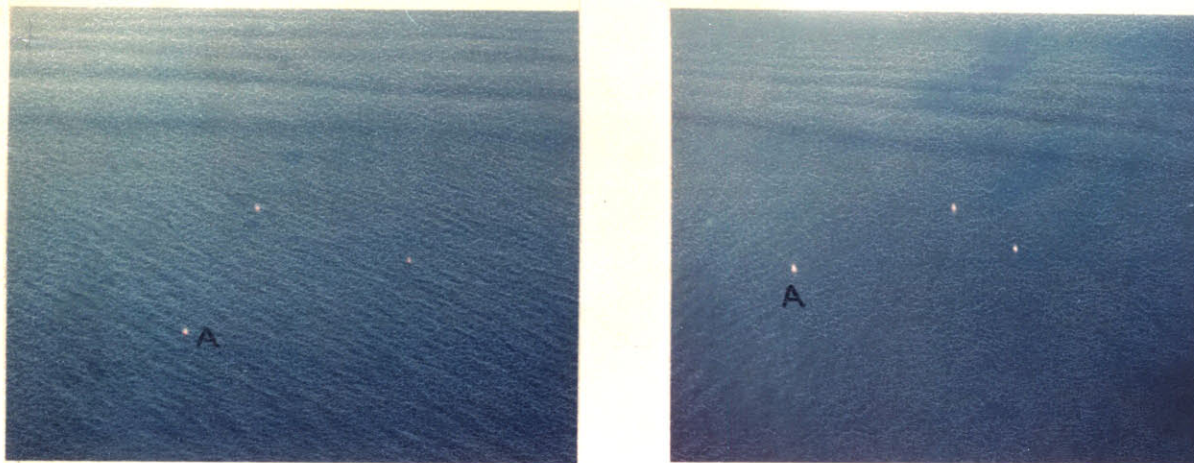


Figure 5 . A Calcomp plot of synchronous temperature measurements at 9 depths. The sampling interval was 2-minutes. (Buoy A)



August 3, 1966. Approximately 1100 EST. Altitude 700 feet.



August 18, 1966. Approximately 1030 EST. Altitude 800 feet.

Oblique air photographs of surface bands approaching Station T.

Figure 6

Buoy A is identified in all photographs.

Data Acquisition

Three Richardson buoys (Richardson et al, 1963) were instrumented for measuring temperature at Station T. The buoy consisted of a 10-foot tripod tower mounted onto an 8-foot outside diameter toroidal doughnut (figure 7). Designed to operate in regions of great depth, it had an ultimate buoyancy of 6000 pounds, but in shallow water it was subject to tipping. The stability was increased by attaching nine 50-pound weights to the bottom of the toroid. The buoy bridle and ground tackle were constructed from 1/2-inch proof coil chain (breaking strength = 13,200 pounds) and the mooring line consisted of 5/16-inch aircraft cable (breaking strength = 9800 pounds). An 800-pound Stimson anchor (Richardson et al, 1963) was used, and in the silty bottom it developed a holding power much in excess of its weight.

Nine thermistors, one pressure transducer and a reference resistor were mated to a multiconductor cable, with the uppermost thermistor 5 m below the water surface. The thermistor cable was loosely attached to the aircraft cable with swivel snap hooks and escaped the dynamic tensions encountered by the mooring line (Paquette and Henderson, 1965). A 3/8-inch chain bridle prevented the development of tensions between the temperature recording digitizer and the thermistor cable.

Two models of the Geodyne temperature recording digitizer (Perry and Smith, 1965 a,b) were used. One type stored the data on a 150-foot roll of 16 mm Kodak film and had a storage capacity

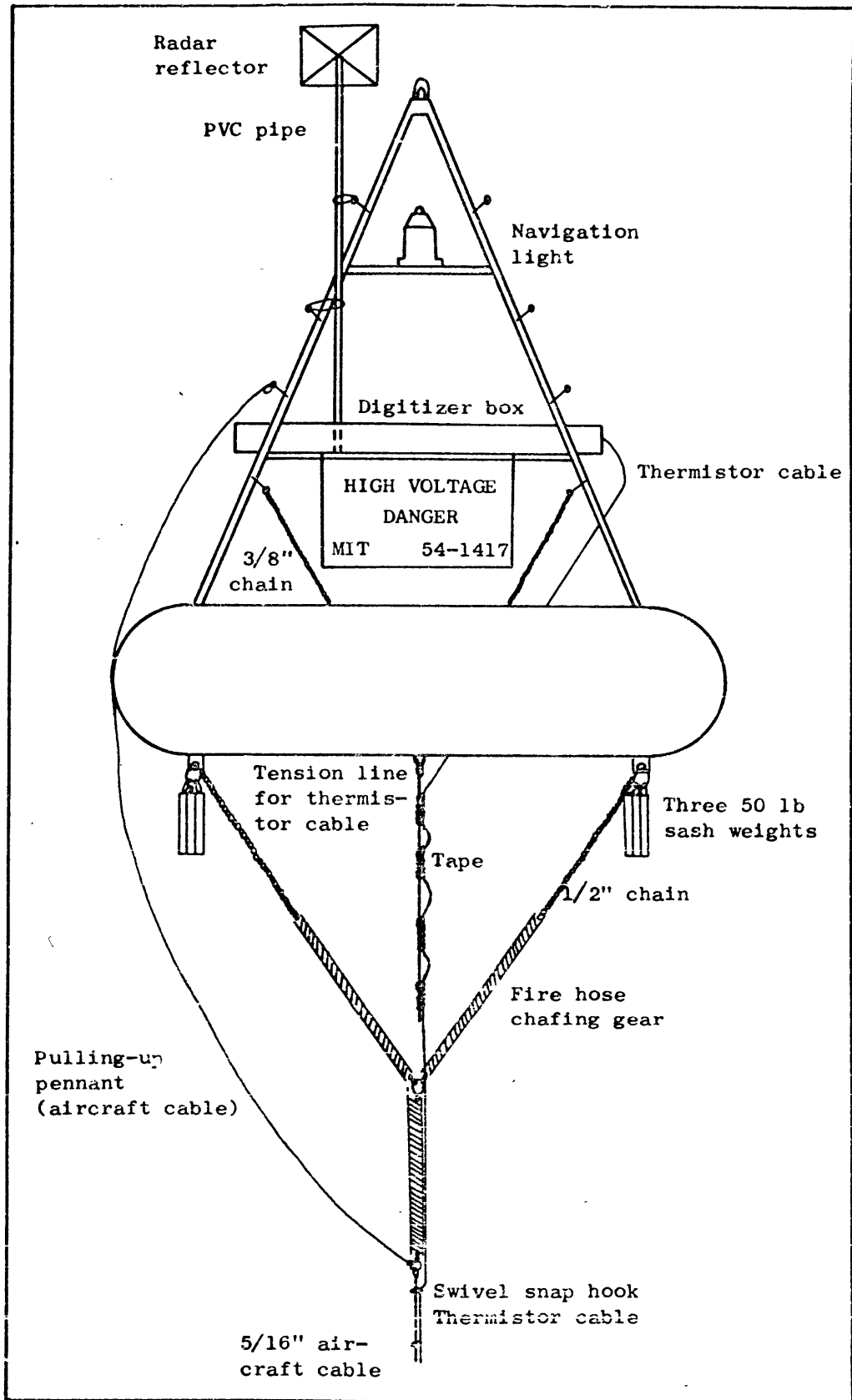


Figure 7. A typical temperature recording buoy used at Station T

of 7500 samples; the other used a 394-foot, 4-inch, 2-track closed loop magnetic tape which could contain 10,000 samples. During an experiment each instrument recorded between 100,000 and 140,000 observations because 14 sensors were measured at each sampling interval. A reference resistor, time, and temperature were measured inside the instrument. The data, recorded as electrical resistances in binary format, was processed by Geodyne Corporation and stored on 7-track magnetic tapes compatible to IBM equipment. Subsurface temperature values greater than 20°C or less than 2°C were considered erroneous measurements and were replaced by linear interpolation using the preceding value and the next value. About 1/2 % of a time series contained these errors. The pressure transducer and sensor recording time failed to operate properly throughout the measurement program.

In 1967 velocity was measured at three separate locations using three Geodyne film-recording current meters (Richardson et al, 1963) suspended from a Richardson buoy. Velocity and temperature were measured at the same time at Station T. The current meters were also placed on Stellwagen Bank and 11 km east of the Bank. Velocity measurements consist of 50-second averages of speed and direction each minute.

Mooring motion produces horizontal and vertical displacements of the sensors which appear in fixed depth observations as noise (Webster, 1964). The vertical displacements of the thermistors that occur when a buoy moves from a position over the anchor to

an equilibrium position were estimated by the method described by Fritzlaff and Laniewski (1964) and Pode (1951). A mean velocity distribution at Station T was determined from the conservation of mass applied to fixed depth observations at Station T and on Stellwagen Bank. The value for the combined wind and water drag on the buoy was calculated assuming that 1/4 of the buoy was submerged with 0° tilt. The vertical displacements computed for the upper six thermistors are (in descending order): .05, .43, .85, .97, 1.09, and 1.21 m. The high frequency fluctuations are not influenced by heaving of the buoy due to the tide. Many periods of observations occurred during calm, glassy sea conditions. Horizontal excursions of the thermistors can be neglected because the water is inhomogeneous only in the vertical.

In 1966 only one instrumented buoy system operated successfully and in 1967 only one of the systems failed to operate. The precision and accuracy of temperature measurements were .02°C and .05°C, respectively. The sampling characteristics of the 1967 measurements were: $\Delta t = .5$ minutes, $\Delta z = 5$ m, $\Delta x = 100$ m, record length = 2-1/2 days; in 1966, $\Delta t = 2$ minutes, $\Delta z = 6.1$ m, record length = 5 days. The amount of aliasing was reduced by the thermistors, which had time constants of about one minute. The two buoys which recorded data in 1967 were separated by 100 m along an east-west line which was perpendicular to the crest of Stellwagen Bank. The

horizontal spacing was estimated from the surface bands which had been aeriaily viewed in 1966. The measurement of the travel time (order $5\Delta t$) for events moving from buoy T2 to buoy T1 was unsuccessful. Experimental method introduced an uncertainty of $2\Delta t$, the time of individual events could be identified only within Δt , and the identification of similar events was difficult because the measuring systems differed.

Analysis of the Data

The groups of high frequency temperature fluctuations viewed in figures 4 and 5 were observed throughout the data. Daily values of mean temperature and standard deviations were quasi-stationary. No temperature inversions were observed in any portion of the measurements. The temperature and the increase in temperature occurring at the initiation of the high frequency fluctuations were uniform (Table 1). The time interval between the initiation of 29 groups of high frequency fluctuations was 12.4 hours and the standard deviation was 30 minutes.

Figure 8 contains a Calcomp plot of the speed measurements recorded at 10.6 m below the surface at Station T between July 13 and July 17, 1967. Groups of large amplitude high frequency fluctuations occurring at 12.4-hour intervals were also measured at 25.8 m and 42.6 m below the surface; they were absent from speed measurements recorded on Stellwagen Bank and at 11 km east of the Bank. The time origin of the velocity data had been destroyed by film exposure, and at each depth the onset of a group of large amplitude high frequency speed fluctuations was made to coincide. The measured directions shown in figure 9 occur at the time of individual maxima of the large amplitude high frequency fluctuations in the speed measurements. Current direction is referred to true north and is specified as the direction toward which the current is flowing. The time averaged

Table 1

STATISTICS OF THE INITIATION OF THE HIGH FREQUENCY TEMPERATURE FLUCTUATIONS

	July 6-9, 1966 z = 11.1 m		July 28-Aug 3, 1966		July 13-17, 1967 z = 10 m		July 25-28, 1967	
	T	ΔT	T	ΔT	T	ΔT	T	ΔT
	Temperature ($^{\circ}\text{C}$)							
Mean	7.6	7.7	7.3	6.1	7.8	6.1	7.8	7.2
SD	1.3	1.0	0.5	0.7	0.3	0.5	0.3	0.6
Maximum	10.2	8.6	8.0	7.0	8.2	6.8	8.4	8.0
Minimum	6.2	5.4	6.3	4.7	7.4	5.5	7.5	6.5
Number (N)	6		10		5		5	
	z = 17.2 m				z = 15 m			
Mean	5.0	5.1	6.2	6.1	6.6	6.8	6.4	4.8
SD	0.5	2.5	0.8	0.9	0.2	0.5	0.4	1.8
Maximum	5.6	9.1	6.5	8.0	7.0	7.6	6.8	7.5
Minimum	4.2	2.0	5.6	5.0	6.4	6.2	5.7	2.6
Number (N)	6		10		5		5	

T Temperature directly prior to the onset of the high frequency fluctuations
 ΔT Increase in temperature at the onset of the high frequency fluctuations
z Depth below the surface
SD Standard deviation

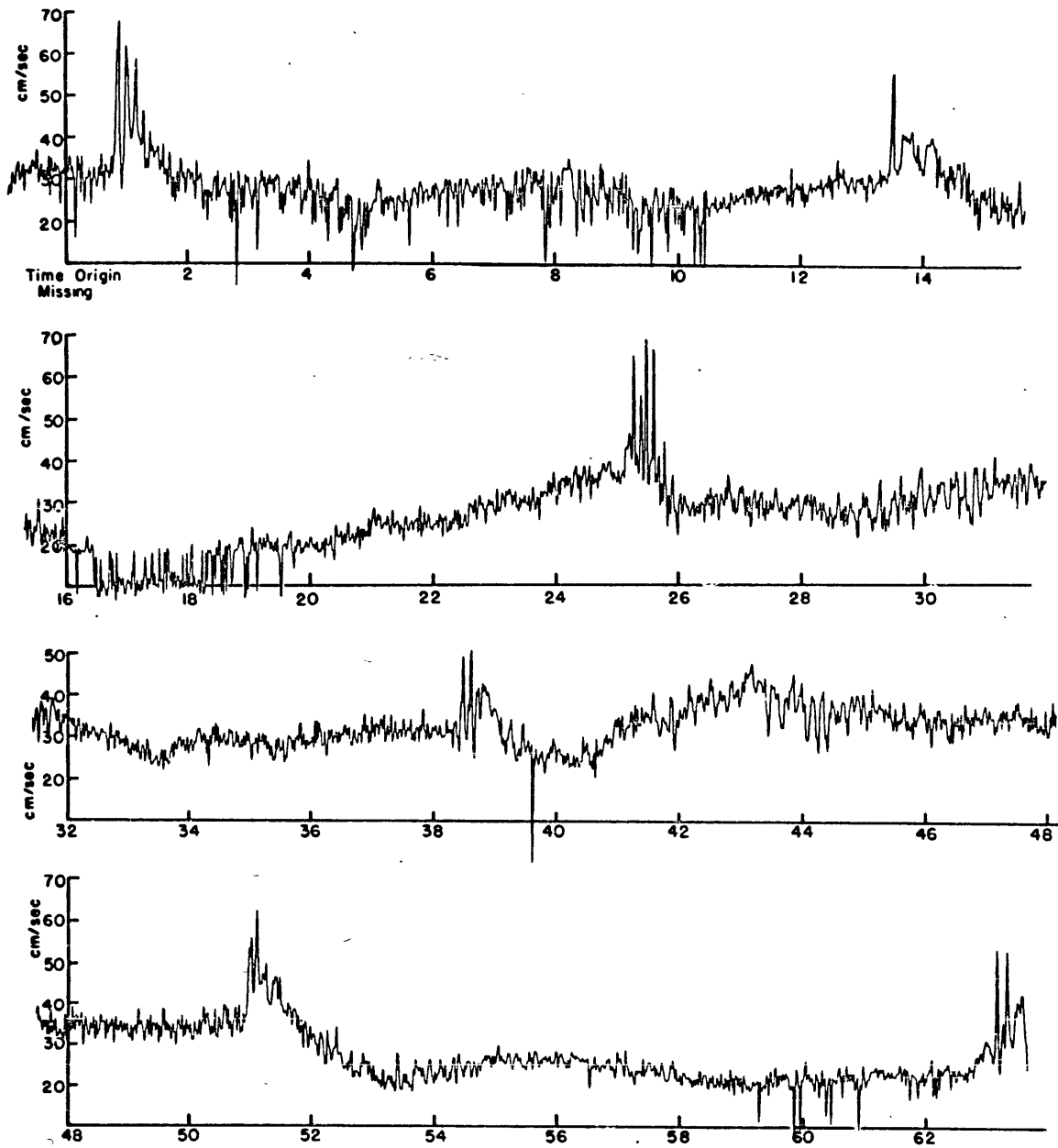


Figure 8 . A Calcomp plot of 3900 speed measurements at 10.6m at Station T between July 13-17, 1967. The time origin is missing and the interval between tick marks on the abscissa is 2-hours.

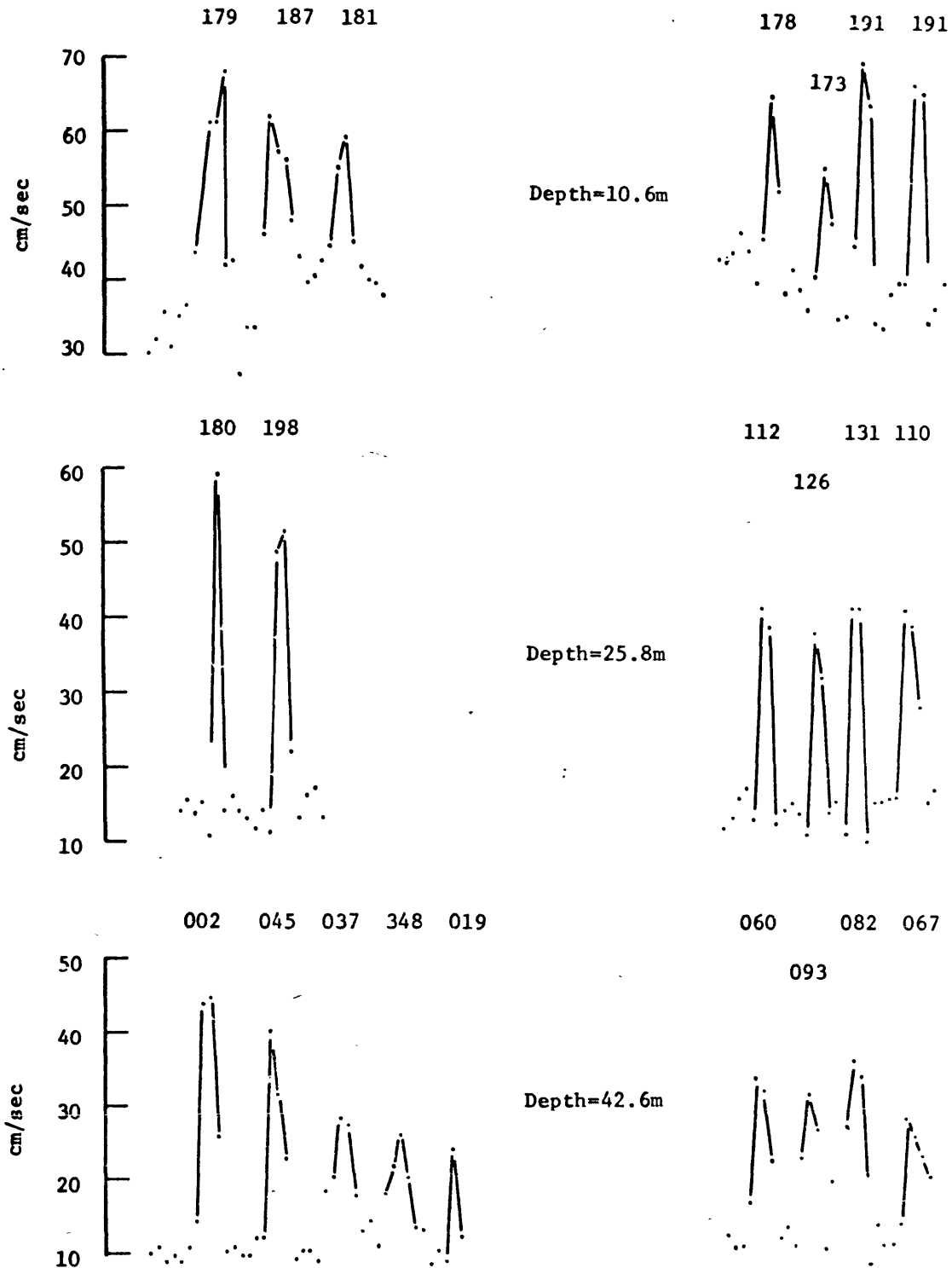


Figure 9 . A plot of speed (ordinate) and time (abscissa) for two groups of large amplitude high frequency speed fluctuations at three depths at Station Y. The time interval between each point is 1-minute and the direction (degrees; referred to true north) measured at the time of the peak value is given above each peak. These groups occur at hour 1 and hour 25 in figure 8.

velocities measured during the 2-hour interval directly prior to the onset of the first group (left portion of figure 9) were (33 cm/sec; 130°) at 10.6 m, (15 cm/sec; 223°) at 25.8 m, and (10 cm/sec; 202°) at 42.6 m. At each of the three depths the range (maximum - minimum) in the average direction was 55° . In the absence of the mean current, the computed velocities occurring at the time of the individual maxima of the first group in figure 9 were (46 cm/sec; 213°) at 10.6 m, (39 cm/sec; 155°) at 25.8 m, and (50 cm/sec; 020°) at 42.6 m. Although a reversal in the computed directions occurs between the measurements at 42.6 m and those at the other two depths, the dominant north-south component is perplexing because the regularly occurring groups of large amplitude high frequency fluctuations in the speed and temperature measurements are considered to arise from the same process. Observations of long-crested narrow surface bands suggested that the high frequency temperature fluctuations represented two-dimensional (vertical and east-west directions) motion which moved westward. Measurements from a towed thermometer also indicated that the high frequency temperature fluctuations moved westward.

The mean and standard deviation of the speed measurements are given in Table 2. The omnidirectionality of the Savonius rotor produces an average speed greater than the true average (Hunkins, 1967; Hansen, 1964). A study of the speed and direction histograms indicates that Stellwagen Bank does not restrict

the tidal flow to the thermocline region. During flood tide the water below the thermocline on the east side of the sill participates in the flow over the Bank producing a uniform flow from surface to bottom on the sill. The westward flow then diffuses in the vertical direction and at Station T a vertical shear has developed above the sill depth. The flow at 10 m below the surface on both sides of the sill is more complicated because the current contains a rotary component. A rotary component is also present in the measurements at 25.8 m and 42.6 m at Station T. It is surprising that the large values of tidal speed measured on Stellwagen Bank have been unnoticed (Bigelow, 1927; Haight, 1942; U.S. Coast and Geodetic Tidal Current Tables, 1967).

Table 2

AVERAGE AND STANDARD DEVIATION OF THE SPEED MEASUREMENTS

Station T			Stellwagen Bank			East (11 km) of Stellwagen Bank		
July 13-17, 1967			July 24-28, 1967			August 22-25, 1967		
Depth m	Aver cm/sec	SD	Depth m	Aver cm/sec	SD	Depth m	Aver cm/sec	SD
10.6	28.9	7.8	7.6	41.3	11.3	10.6	28.2	11.7
25.8	15.0	4.0	15.2	35.0	13.0	25.8	20.9	8.3
42.6	13.4	4.4	22.8	35.4	16.5	42.6	17.1	8.3

A thermistor, which was able to respond to fluctuations whose lengths were 100 m or greater, was towed at 16 m below the surface in the vicinity of Station T on September 19, 1967. The position error of the vessel was at least 2 km. The temperature sections are shown in figure 10; each section is a retracing of the actual observations. An initiation of high frequency fluctuations, similar to the observations obtained from the buoys, was measured at 1020 and 1133 EST, and beginning at 1133 EST, six narrow surface bands were seen from the tow vessel. The apparent westward velocity of the abrupt increase in temperature was (100 ± 45) cm/sec. The amplitude of the rapid rise in temperature increased as it moved into shallower water. The constant temperature with minimum value measured close to the sill between 1630 and 1840¹ EST occurred during ebb tide, indicating that a group of high frequency temperature fluctuations was not generated by reflection as the tide left Massachusetts Bay.

The measurements obtained at Station T between July 25 and July 28, 1967 will be described; this portion of the data was chosen only because the aerial survey of the surface bands occurred during this period. Figure 11 is a Calcomp plot of the sequential (sampling interval = .5 minutes) temperature measurements recorded at 10 m below the surface between July 25 and July 27, 1967. Figure 12 shows the distribution of temperature at nine depths during a 14-hour period on July 26, 1967. Figure 13

¹ The vessel was stopped between 1757 and 1820 EST.

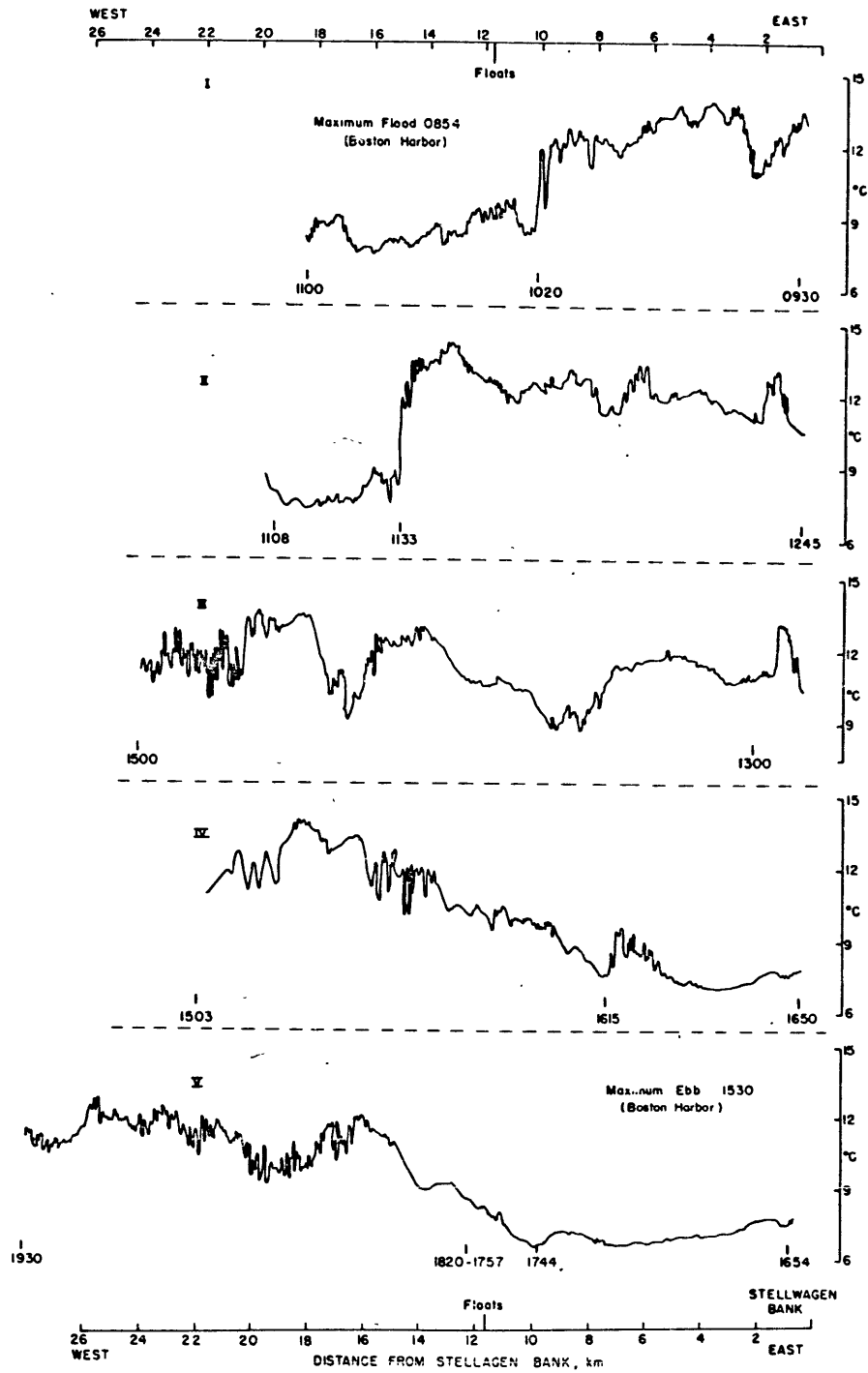


Figure 10 . Temperature measurements from a thermistor towed at 16m on September 19, 1967.

describes the vertical distribution of mean temperature, standard deviation, mean density and mean Brunt-Väisälä frequency for the period July 25 to July 28. The time-averaged Brunt-Väisälä frequency is defined by

$$N^2(z) = -\frac{g}{\rho_0} \frac{d\rho_0}{dz} \quad (1)$$

where ρ_0 is the mean density. The sequential temperature measurements recorded between July 25 and July 27 were used to evaluate the mean temperature and standard deviations at 5-meter intervals from 5 m to 45 m below the surface. At depths greater than 45 m the temperature distribution was measured from a single bathythermograph lowering on July 28. A salinity cast consisting of eight Van Dorn water sampling bottles (Van Dorn, 1956) spaced at 10-meter intervals was conducted on July 28. Density was computed from Knudsen's Formula (Lafond, 1951, p.91) using the mean values of temperature and the single measurement of salinity. A thermal gradient exists between 5m and 25 m below the surface, and below the sill depth the temperature is nearly isothermal. It is not surprising that the amplitude of the high frequency temperature fluctuations and the standard deviations are greatest in the region of maximum temperature gradient. The distribution of salinity (not shown) contained a halocline above the sill depth.

In figure 11 the period of the high frequency fluctuations appears to increase with time for the group initiated at 1336,

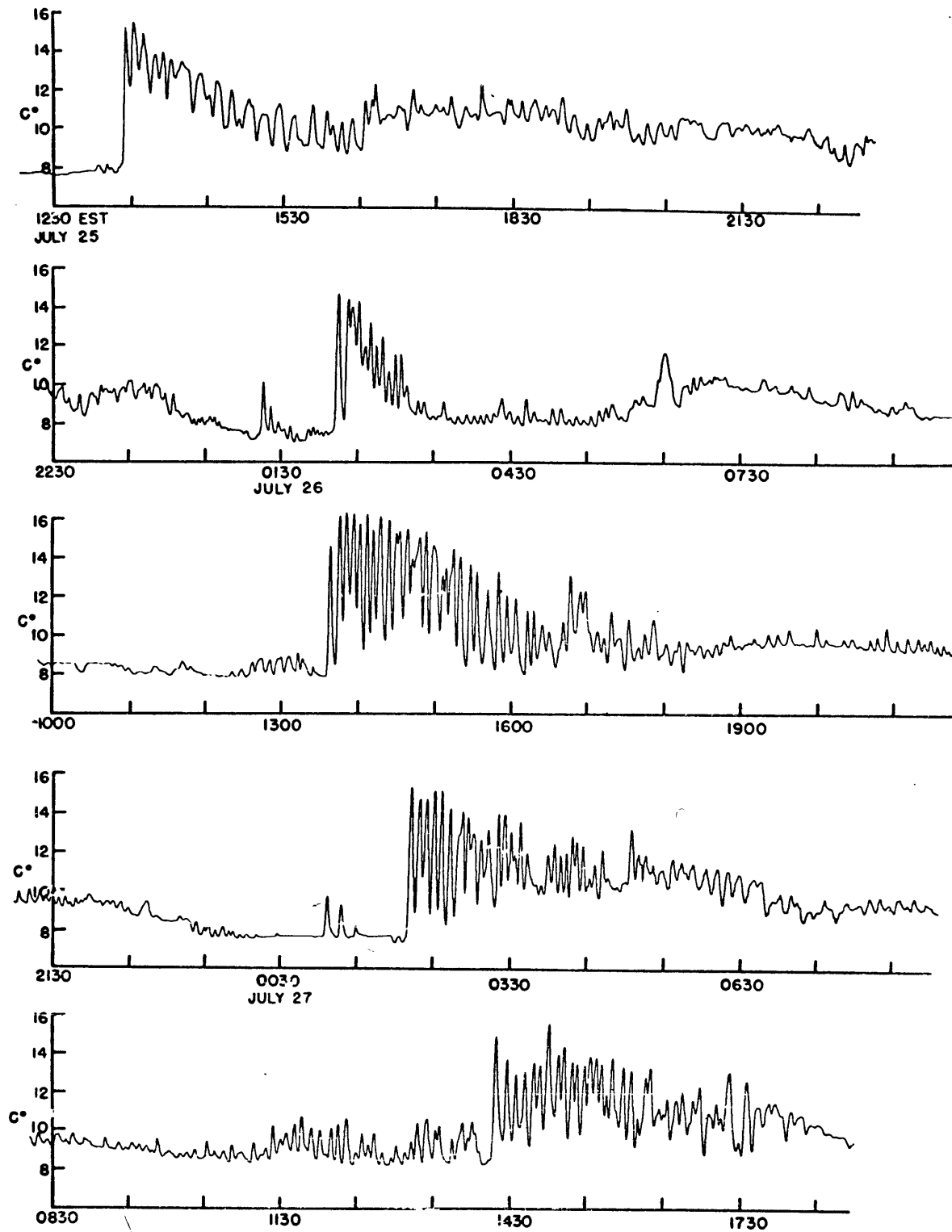


Figure II . A Calcomp plot of 6400 temperature measurements at 10m at Station T (buoy T2) between July 25 and July 27, 1967. Sampling interval was 30-seconds.

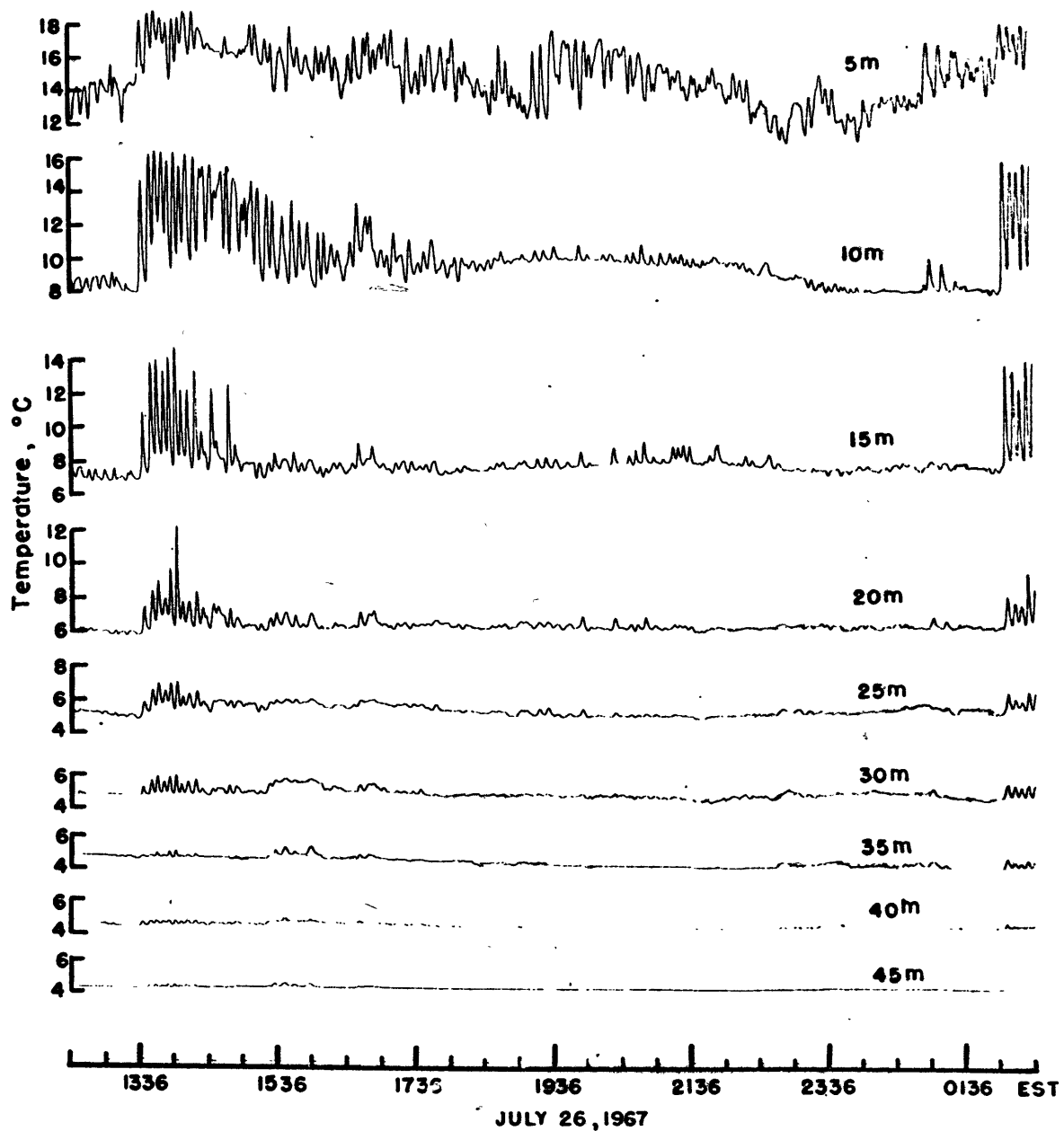


Figure 12 . A Calcomp plot of synchronous temperature measurements at 9 depths. Sampling interval was 30-seconds. (buoy T2)

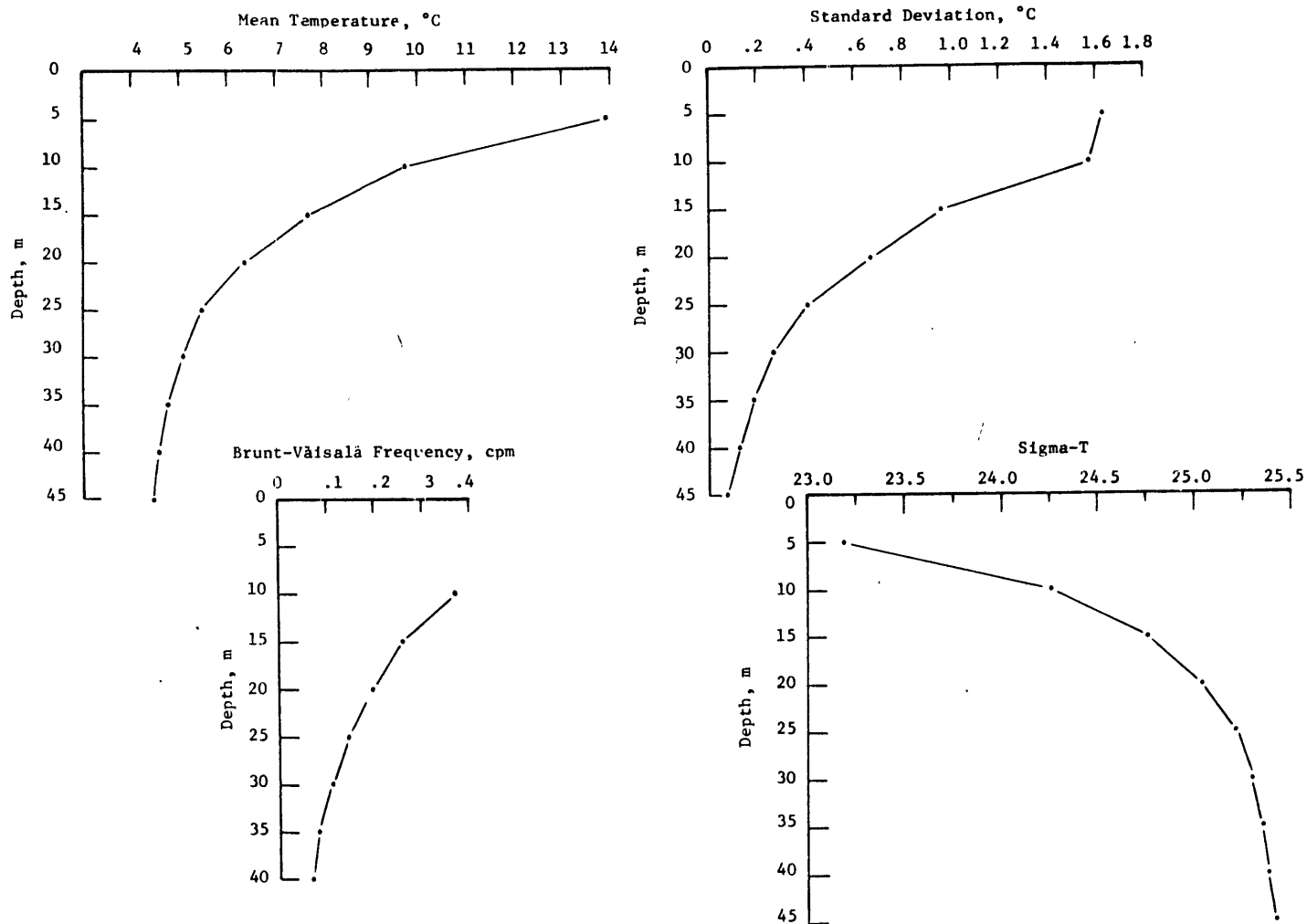


Figure 13. Average vertical distribution of temperature, density, and Brunt-Väisälä frequency at Station T between July 25 and July 27, 1967.

July 26; the opposite effect may be true for the group beginning at 1414, July 27.

Using the Woods Hole Oceanographic Institution heliocourier, a pattern of multiple surface bands was examined from an altitude of 700 feet between 1335 and 1500 EST on July 26, 1967. Figure 14 contains aerial photographs of the surface bands in the vicinity of buoys T1 and T2 and temperature measurements obtained at 10 m below the surface from the eastern buoy (buoy T2). Numbers on the photographs identify particular bands, i.e., a "1" designates the lead band. The arrival time of the lead band at the buoys coincided (within ± 2 minutes) with the onset time of the high frequency temperature fluctuations. The westward speed of individual bands was determined by measuring their travel time between the buoys. The accuracy of a travel time measurement was ± 30 seconds. In figure 14 narrow band "2" moved from the eastern buoy to twice the distance separating the buoys in five minutes beginning at 1345 EST. Band "3" travelled 100 m in two minutes beginning at 1350 EST. The average speed determined from a total of four travel time measurements was (88 ± 20) cm/sec. The distance separating the narrow bands was (175 ± 25) m. The crests of the bands paralleled Stellwagen Bank and exhibited the same curvature. Their length was 9.75 km and their northern edge occurred about 2.5 km north of Station T. Each narrow band consisted of about 30 m of choppy water. When the moored buoys were in the bands

Figure 14. Simultaneous measurement at Station T of surface bands and high frequency temperature fluctuations on July 26, 1967. T* represents 1336 EST, the onset time of the high frequency temperature fluctuations. The dark narrow bands represent the surface bands.

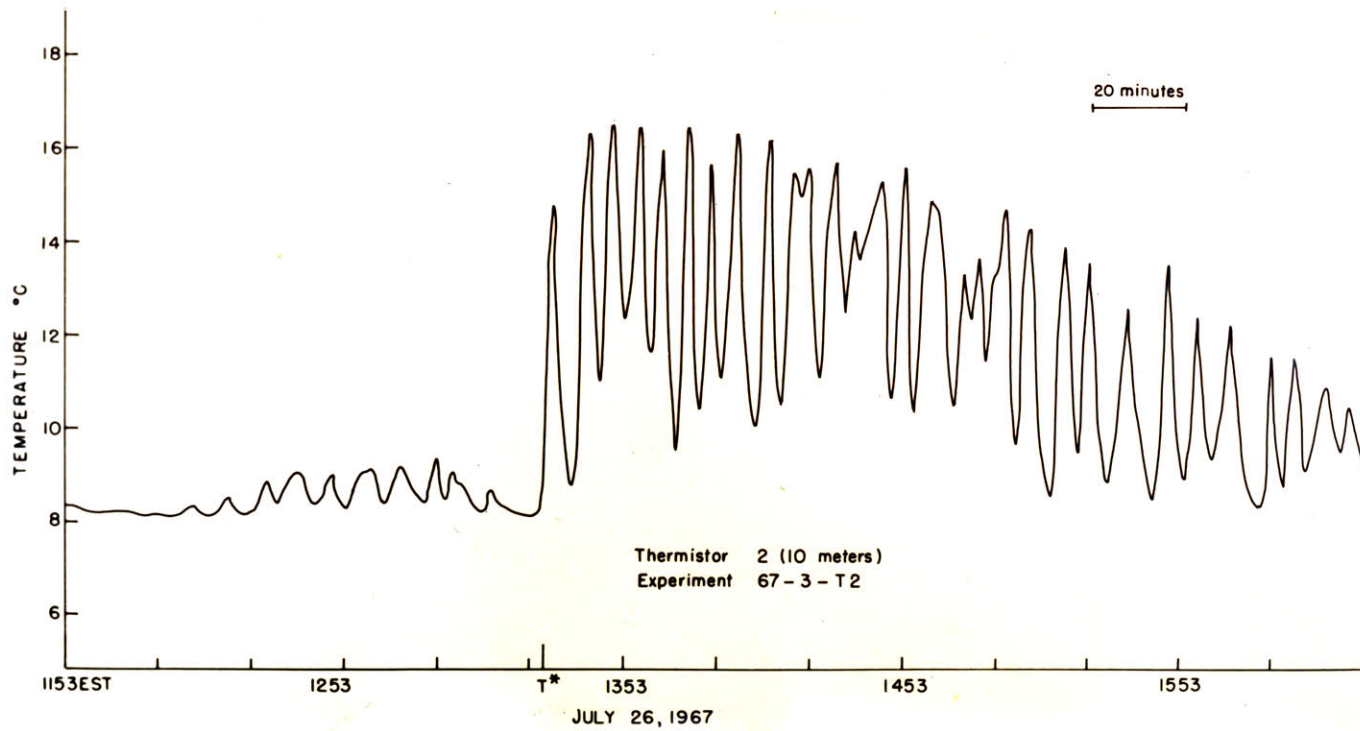
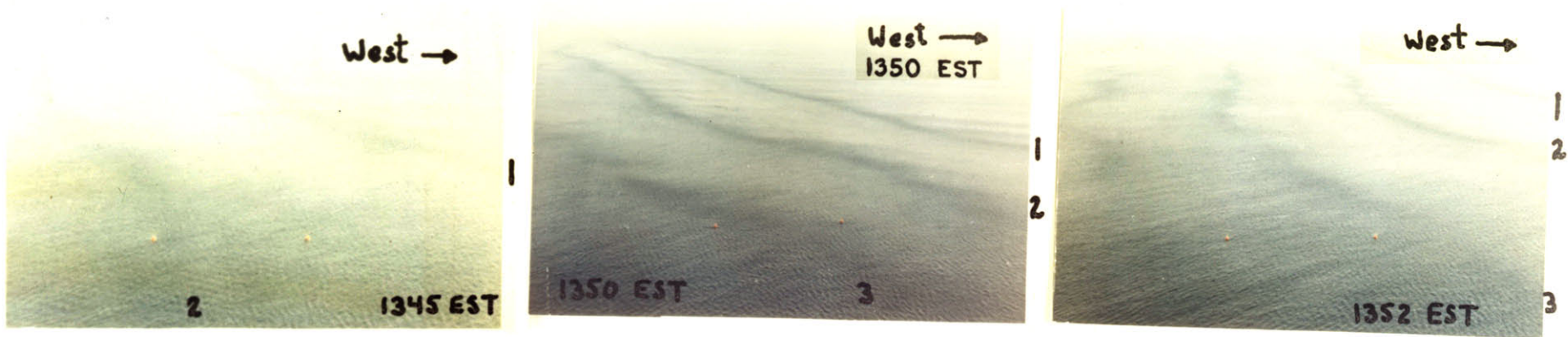


Figure 14.

they rolled to and fro, but they remained virtually motionless during the intervals of slightly rippled or calm water. The narrow bands are similar to bands of ruffles on smooth water (Shand, 1953; Pickard, 1961; Frassetto, 1964) and do not represent slicks of calm water in a wind rippled sea (Ewing, 1950; Lafond, 1962). Both types of surface features have been associated with near surface short period internal waves.

1. Spectral Analysis

Estimates of the spectra of the high frequency temperature fluctuations recorded between July 25 and July 27, 1967 (figures 11 and 12) were computed by a method described by Welch (1967) and Bingham et al (1967). The time series was divided into five sections; each section was multiplied by a window; a modified periodogram was computed for each section; Bartlett-Daniell estimates of the spectral density function were formed from the periodograms.

The normalized, complex, finite Fourier transform of a series of N temperature measurements is

$$A_k = \frac{1}{N} \sum_{i=0}^{N-1} T_i^* e^{(-2\pi j) \frac{ik}{N}} \quad \begin{matrix} i, k = 0, 1, 2, 3, \dots, (N-1) \\ j = \sqrt{-1} \end{matrix} \quad (2)$$

where T_i^* is the i^{th} temperature measurement. Equation (2) can

be written as

$$A_k = a_k + j b_{k+1} \quad k = 0, 2, 4, \dots, (N-2) \quad (3a)$$

or
$$A_k = a_n + j b_n \quad n = 0, 1, 2, 3, \dots, \frac{N}{2}-1 \quad (3b)$$

where (a_n, b_n) are the n^{th} Fourier coefficients of the time series. The raw periodogram of a discrete time series is the sequence of values $(a_n^2 + b_n^2)/\Delta f$ that are attached to the frequencies, or harmonics, $f_n = \frac{n}{N\Delta t}$. The fundamental resolution separating the harmonics is

$$\Delta f = \frac{1}{N\Delta t} \quad (4)$$

The zeroth harmonic is the D.C. component or mean value of the series. The direct computation of the Fourier coefficients was performed by a Fortran IV subroutine (IBM, 1967) which utilizes the Fast Fourier Transform (Cooley and Tukey, 1965) and which limits the number of data values to a power of two. Each periodogram ordinate describes the energy within the band $f_n \pm \frac{\Delta f}{2}$ with two degrees of freedom. The periodogram is a poor estimate of the spectrum (Hinich and Clay, 1968). Daniell estimates (Madden, 1963) with ν degrees of freedom were formed by averaging $\nu/2$ periodogram ordinates. This smoothing decreases the resolution between harmonics, but increases the

stability of the estimates. The stability was further increased by (ensemble) averaging the Daniell estimates from each of the sections.

Each section was multiplied, before taking the Fast Fourier Transform, with a window that slowly tapered the time series towards zero at both ends. A window suggested by Welch (1967) was selected. This data window is very close in shape to the Hanning (Blackman and Tukey, 1958) or cosine arch spectral window, and defined by

$$W_i = 1 - \left[\frac{i - \frac{N-1}{2}}{\frac{N+1}{2}} \right]^2 \quad (5)$$

Using the initiation of the high frequency temperature fluctuations as origins for the individual sections, the temperature record was divided into five 8-hours, 32-minutes (i.e., 1024 values) segments such that 3-hours, 1-minute occurred prior to the origin. Each member was adjusted to zero mean and zero linear trend by (1) removing the mean value from the entire section, (2) subdividing the section into 17 segments of 30-minutes length beginning with the third data point, (3) removing the mean value from each segment, and (4) removing the mean value from the zero linear trend data together with the first and last two data values. The trend in the variance had not been altered. Each section was then multiplied by

equation (5) and the modified Fourier coefficients were computed for the sequence of values $(W_i \cdot T_i)$, where T_i represents the adjusted temperature series. The amplitude of the n^{th} harmonic of the modified periodogram, denoted by P_n , was computed from

$$P_n = \frac{1}{U} \frac{(\bar{a}_n^2 + \bar{b}_n^2)}{\Delta f} \quad n=1,2,3,\dots,\frac{N}{2}-1 \quad (6)$$

where (\bar{a}_n, \bar{b}_n) are modified Fourier coefficients of the series $(W_i \cdot T_i)$. U is a dimensionless correction factor introduced to compensate for the data window and is defined by (Welch, 1967)

$$U = \frac{1}{N} \sum_{i=0}^{N-1} W_i^2 \quad (7)$$

Bartlett-Daniell estimates of 30 degrees of freedom were obtained in the following manner: (1) Daniell estimates of 6 degrees of freedom were computed for each of the five sections.

$$P_n^6 = (P_{n-1} + P_n + P_{n+1}) / 3.0 \quad n=3,5,8,\dots \quad (8a)$$

The superscript designates the number of degrees of freedom. A re-indexing of the harmonic number yields the equivalent relation

$$\begin{array}{ccc}
 P_n^6 & \longleftrightarrow & P_g^6 \\
 n=3,5,8,\dots & & g=1,2,3,\dots
 \end{array}
 \quad (8b)$$

(2) Bartlett-Daniell spectral density estimates of 30 degrees of freedom were formed by ensemble averaging the estimates P_q^6 , i.e.,

$$P_g^{30} = \frac{1}{5} \sum_1^5 P_g^6 \quad (8c)$$

Spectral density estimates of 60 and 120 degrees of freedom were then formed by averaging the ordinates P_q^{30} in blocks of two or four.

Spectral density estimates of 60 degrees of freedom occurring in the interval 146-minutes to 2.16-minutes are shown in a contour diagram (figure 15) in which depth and frequency are coordinates and lines are drawn through points of equal spectral density. The amplitude of the high frequency temperature fluctuations is largest at 10 m below the surface, decreases in both directions, and has periods between six and eight minutes. This is not surprising since the Calcomp plots of the observations indicated a similar result. The valley occurring between the two $15-(^{\circ}\text{C})^2/\text{cpm}$ peaks is observed with greater resolution in a contour diagram (figure 16a) and spectral density function (figure 16b) drawn from estimates of 30 degrees of freedom. The two peaks, possibly reflecting

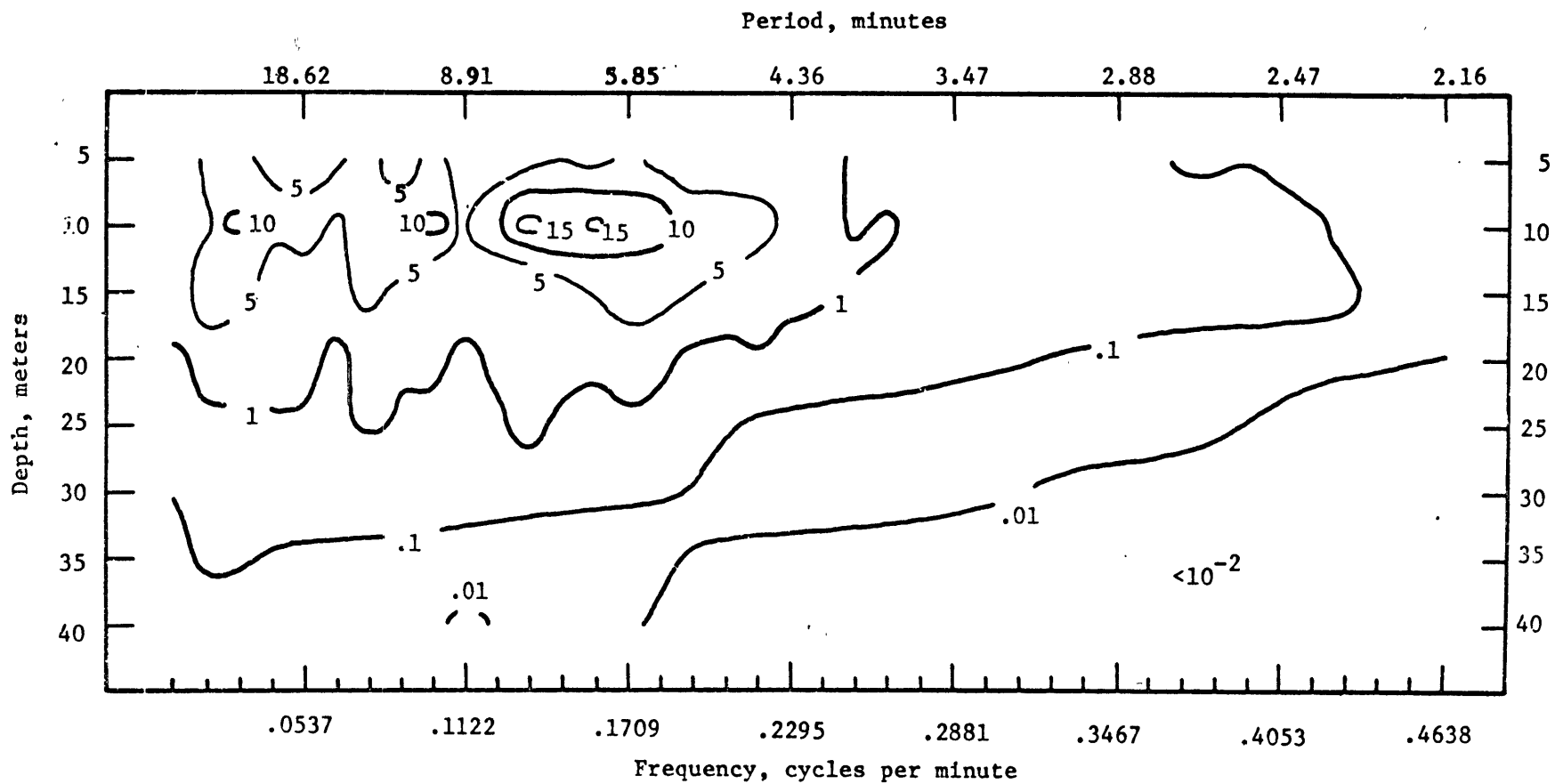


Figure 15. Contours of spectral density, $(^{\circ}\text{C})^2/\text{cpm}$, of the temperature fluctuations.
 $(\nu = 60; \Delta f = .01170 \text{ cpm})$

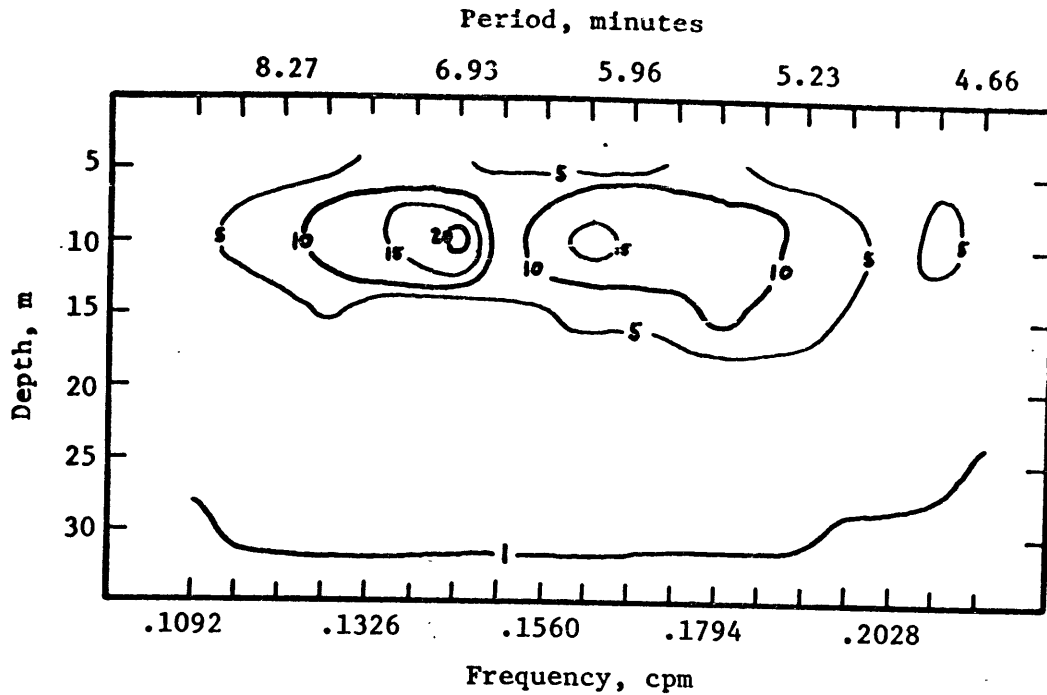


Figure 16a. Contours of equal power density, $(^{\circ}\text{C})^2/\text{cpm}$, on a frequency-depth plot of the high frequency temperature fluctuations. Each estimate has 30 degrees of freedom.

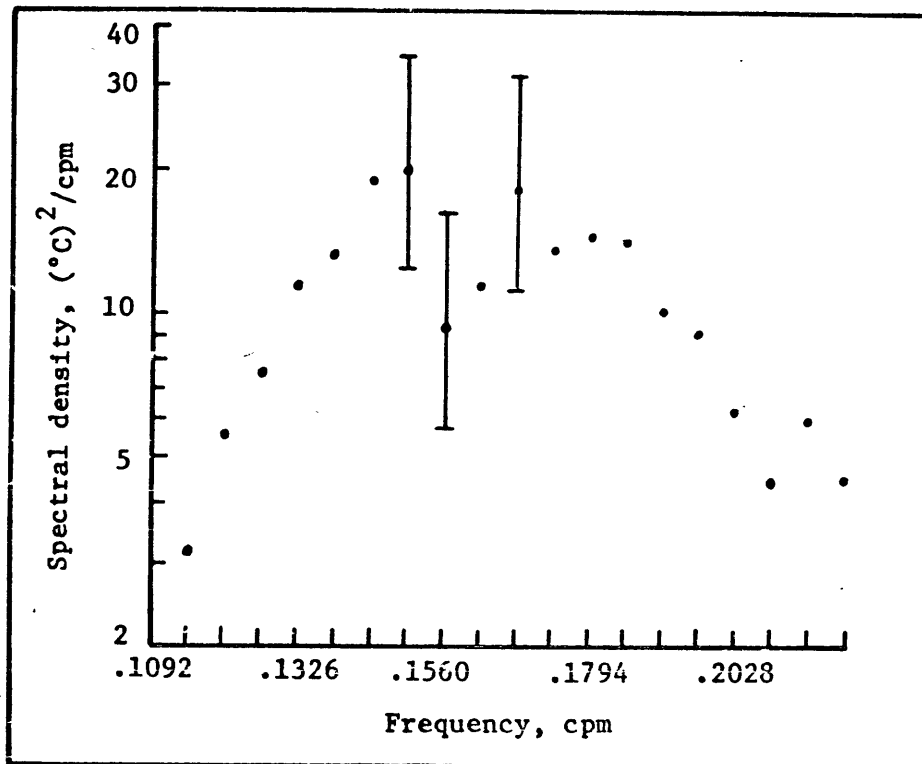
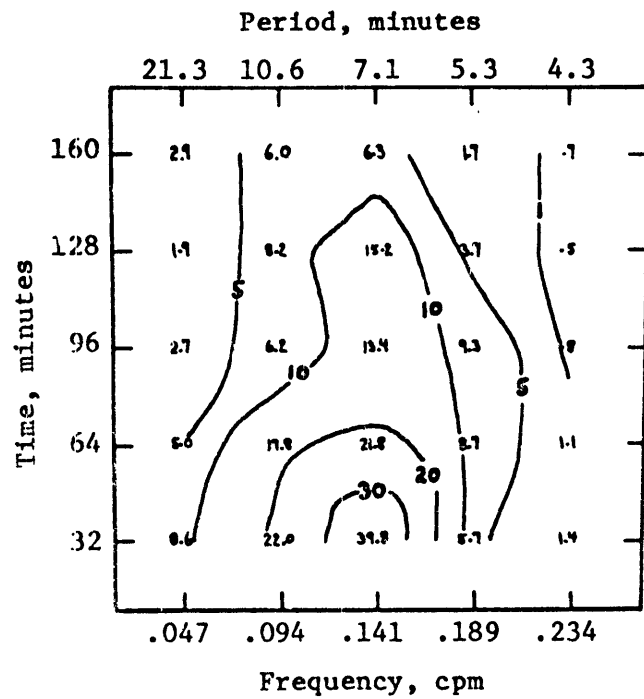


Figure 16b. Power density spectrum of the high frequency temperature fluctuations at the 10m level. Each pair of horizontal bars represent the 95% confidence limit. ($\nu = 30$; $\Delta f = .00585$ cpm)

the frequency change with time noted in figure 11, are not significant relative to each other at the 95% confidence level (figure 16b). For a particular confidence level, a peak in the spectral density function is considered significant and therefore representative of a sinusoid if the variation of the peak as defined by the χ^2 (chi-square) distribution does not overlap the variation of the estimate of the closest spectral trough. The 95% confidence limits for this case are .62 and 1.73 (Munk et al, 1959) of each spectral estimate, which means that there is a 95% probability that the true value of the spectral density lies within the stated proportions of the measured value. In figure 16b a pair of horizontal bars represent the 95% confidence limits of the estimate.

Dispersion of the high frequency temperature fluctuations was investigated from the time rate of change of the spectrum. Five independent, successive 32-minute groups of ensemble averaged spectral density estimates of 20 degrees of freedom at 10 m below the surface are shown on a contour diagram (figure 17) in which frequency and time are coordinates. The first 32-minute interval began at the initiation of the high frequency fluctuations, and each interval was adjusted to zero mean and zero linear trend by subdividing it into four equal sections. Neither an increase nor a decrease in frequency with time can be inferred from figure 17.



Contours of equal power density, $(^{\circ}\text{C})^2/\text{cpm}$, on a frequency-time plot for 160 minutes of (ensemble-averaged) measurements at 10m. The tick marks on the time axis indicate successive 32-minute intervals following the initiation of the high frequency fluctuations.

Figure 17.

Spectral density estimates of 120 degrees of freedom were computed at depths from 5 m to 25 m below the surface (figure 18). For this case the 95% confidence limits are .795 and 1.30 of each estimate. Below 5 m, significant spectral density peaks are centered at periods of about 7 minutes. The rms vertical displacements of the temperature fluctuations occurring between 8.5 minutes and 5.3 minutes (the 6th, 7th, and 8th harmonics of figure 18) were evaluated from the conservation of temperature (Kraus, 1966).

$$\eta_{rms} = \frac{T_{rms}}{\left(\frac{dT}{dz}\right)_{mean}} \quad (9)$$

The derivation of equation (9) assumes small amplitude motion in a resting fluid. The mean temperature gradient was evaluated using the average temperature of the five sections. Because the temperature in the thermocline decreases in a series of irregular steps (Cooper and Stommel, 1968), the computed value of the temperature gradient and the local value may be different. The apparent rms vertical displacements shown in Table 3 were greater than displacements arising from motion of the thermistors.

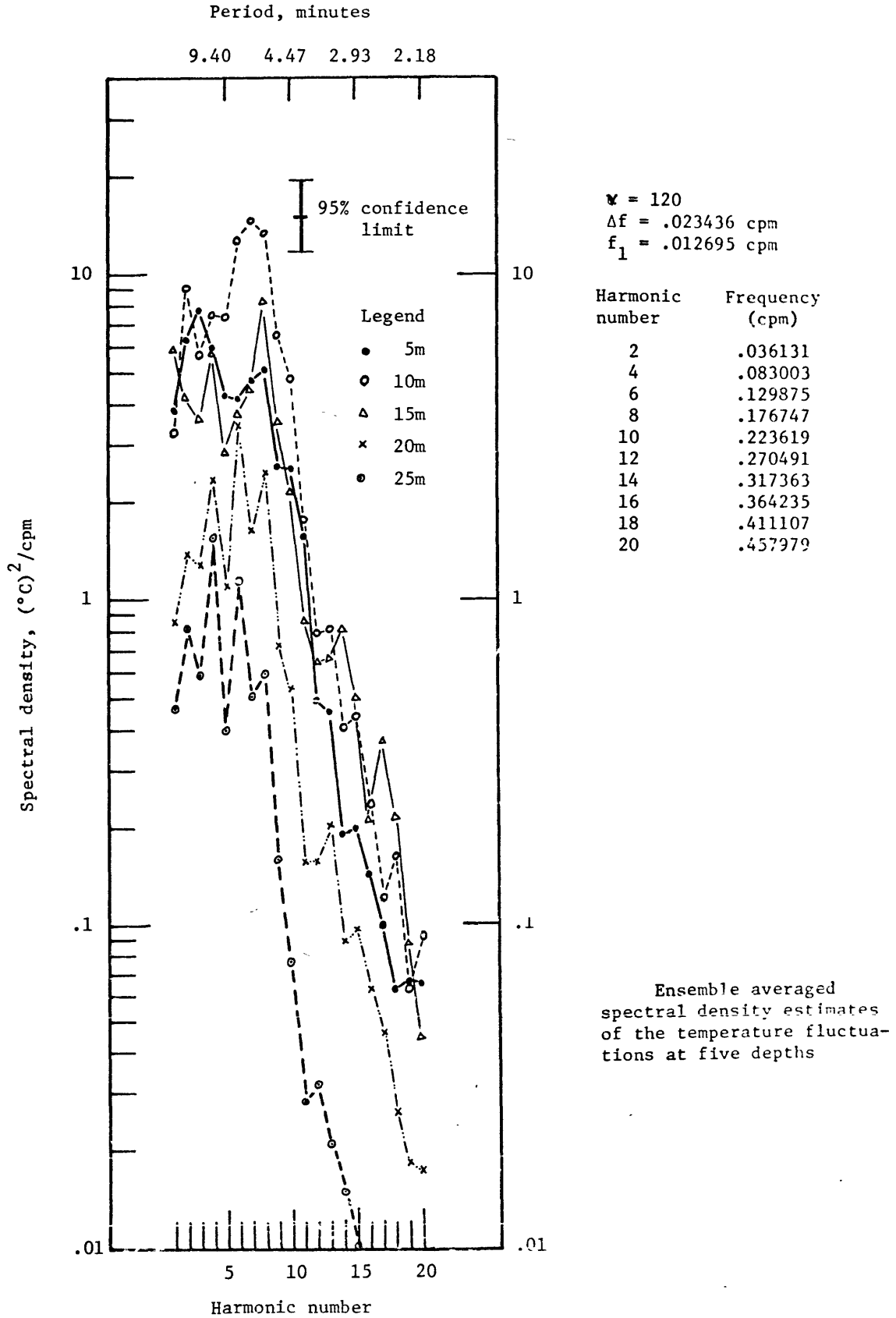


Figure 18.

Table 3

ENSEMBLED AVERAGED STATISTICS
OF THE HIGH FREQUENCY TEMPERATURE FLUCTUATIONS

Depth	Mean temp.	Mean vertical temp. gradient	RMS temp.	RMS vertical displacement for periods between 5.3 and 8.5 minutes
m	°C	°C/m	°C	m
10	9.84	.670	.982	1.47
15	7.64	.349	.625	1.79
20	6.35	.215	.421	1.96
25	5.49	.130	.231	1.77
30	5.05	.073	.131	1.79

2. Coherency Analysis

The normalized complex coherency function is a measure of the degree of linear relationship between harmonic constituents at different locations. It is defined by (Madden, 1963; Davidson and Heirtzler, 1968)

$$R_{12}(n) = \frac{\bar{\Phi}_{12}(n)}{[\bar{\Phi}_{11}(n) \cdot \bar{\Phi}_{22}(n)]^{1/2}} \quad 1 \leq n \leq \frac{N}{2} - 1 \quad (10)$$

$\bar{\Phi}_{12}(n)$ is the cross spectral density function between two time series designated as "1" and "2", and $\bar{\Phi}_{11}(n)$ and $\bar{\Phi}_{22}(n)$ are the

auto spectral density functions of each series. A substitution into equation (10) of the polar form of the cross and auto spectral functions, which are products of the complex Fourier transform (Robinson, 1967), yields

$$R_{12}(n) = \text{ave} \left\{ 1 e^{i\Theta_{12}(n)} \right\} \quad (11)$$

where $\text{ave} \{ \}$ means independent averages of successive values (e.g., Daniell estimates). The unit vector $1 e^{i\Theta_{12}(n)}$ represents the normalized Fourier transform of the n^{th} constituent evaluated from the two time series. The relative phase between constituents is given by

$$\Theta_{12}(n) = \Theta_1(n) - \Theta_2(n) \quad (12)$$

The phase of a Fourier transform constituent is given by

$$\Theta = \text{Tan}^{-1} \left(\frac{b_n}{a_n} \right) \quad (13)$$

A complex coherency estimate of 2ν degrees of freedom is formed by a vector summation of 2ν consecutive unit vectors. The magnitude of the summation is called the coherence, and the coherence and phase estimates each have ν degrees of freedom. A coherence estimate of unity over a frequency interval results when the unit vectors have the same directions; a coherence of

zero occurs when the vectors have opposite directions and therefore sum to zero. To quote Madden (1963, p.19): "The heart of the measure of coherency comes from the consistency of the phase relationship between the two sets of data."

The vertical coherency of the high frequency temperature fluctuations measured from July 25 to July 27, 1967 was computed directly from the modified Fourier coefficients used in the spectral analysis. For each section the phase difference between the measurements at 15 m and the other depths was calculated from equation (12). Daniell estimates of coherence and phase with 5 degrees of freedom were computed by averaging the unit vectors with a box car filter of width five, and an ensemble average of the Daniell estimates yielded estimates having 25 degrees of freedom.

With probability P , a phase angle ϕ lies between $\phi \pm \Delta\phi$ (Munk et al, 1959); values of $\Delta\phi$ for $P = 95\%$ are listed in Table 4a. The confidence limits of a coherence estimate (Table 4b) were interpolated from Groves and Hannan (1968, p.157). Significant coherences are determined by the null hypothesis, i.e., with probability P , $(1 - P) \cdot 100\%$ of the coherence estimates will be greater than R^* when their true value happens to be zero. R^* is defined by (Groves and Zetler, 1964)

$$R^* = \sqrt{1 - (1 - P)^{\frac{2}{v-2}}} \quad (14)$$

A correlation exists between constituents in a frequency band when the phase difference remains constant and coherence is significant.

The vertical coherency of the high frequency temperature fluctuations is shown in figure 19. Phase spectra have been drawn only when the coherence was significant, and the dashed horizontal line on the coherence plots indicates $R^* = .47$. Only the first 60 of the 102 estimates are shown. For the remaining 42 estimates, the harmonic numbers associated with coherence values greater than R^* are contained in Table 5. From about 8 m to 30 m below the surface the harmonic constituents in the frequency interval .1133 cpm to .2010 cpm (8.8 minutes to 5.0 minutes) have significant vertical coherency at the 95% confidence level. Zero phase difference occurs between the constituents at 10 m, 20 m, 25 m, and 30 m below the surface, and a uniform phase results throughout the thermocline region when the confidence limit $\Delta\phi$ is applied to the phase difference between those levels and the 15 m level. A different transfer characteristic of the thermistor at 15 m could have caused the 310° phase difference between the 15 m level and the other levels. The vertical coherency analysis indicates that the high frequency temperature fluctuations are coherent and in phase in the region above the sill depth. The whole thermocline heaves up and down in phase with periods from six to eight minutes.

Table 4a

VALUES OF $\Delta\phi$ FOR DIFFERENT COHERENCES ($\nu = 25$, $P = 95\%$)

Coherence	$\Delta\phi$
.5	66°
.6	45°
.7	32°
.8	23°

Table 4b

VALUES OF UPPER AND LOWER LIMITS FOR DIFFERENT COHERENCES
($P = 95\%$)

Coherence	(Coherence) _{upper limit}	(Coherence) _{lower limit}
.326	.600	0.0
.447	.693	0.0
.548	.76	0.1
.632	.81	.26
.707	.85	.37
.774	.88	.51
.837	.92	.62

Table 5

HARMONIC NUMBER OF COHERENCE ESTIMATES GREATER THAN .47

	Harmonic number of coherence estimates greater than .47
R ₃₁	81
R ₃₂	71, 81, 101
R ₃₄	66, 75, 87, 97, 101
R ₃₅	67, 71, 74, 79, 81, 82, 97, 98, 101
R ₃₆	nil
R ₃₇	nil
R ₃₈	98

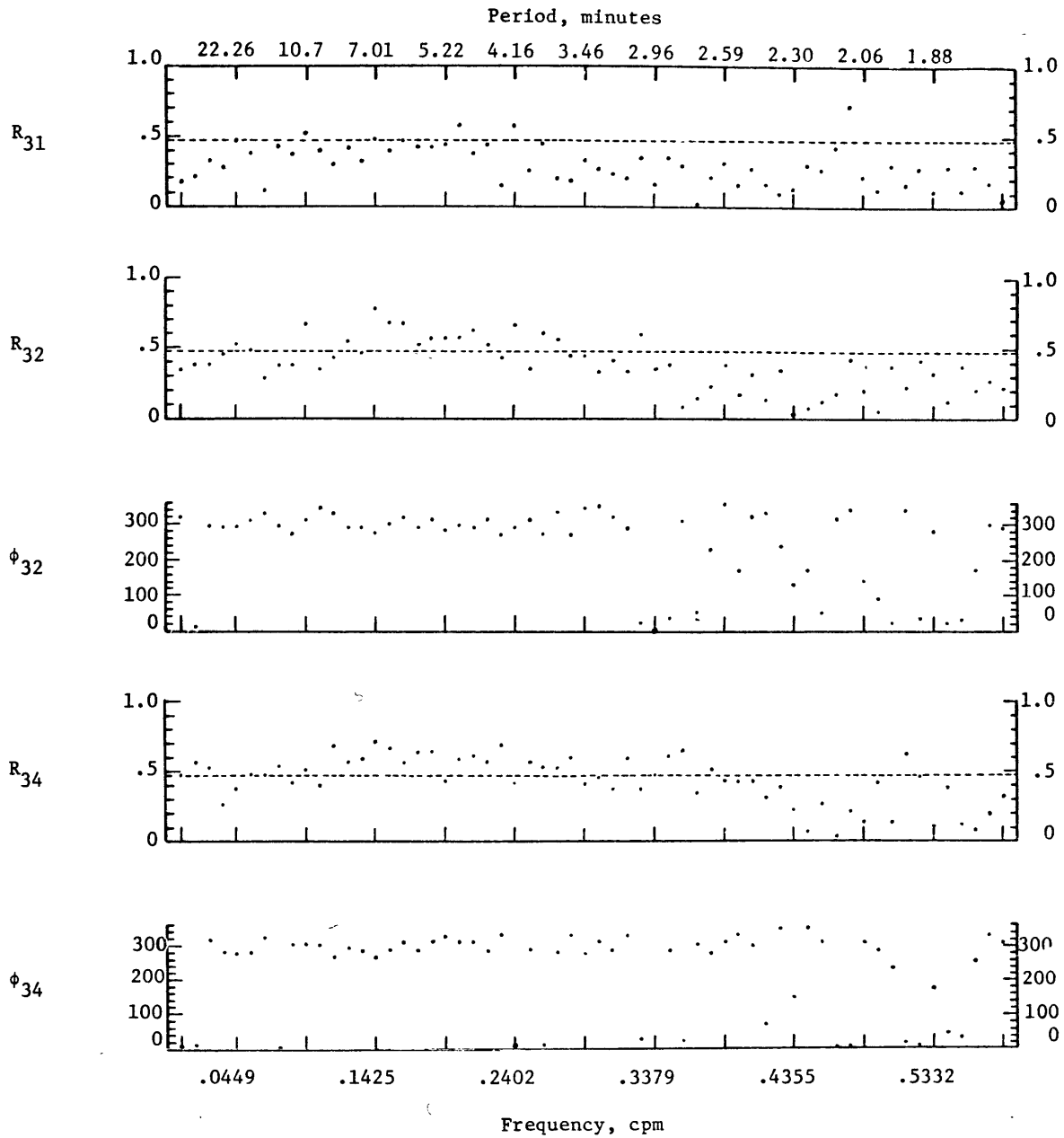


Figure 19. Ensemble averaged coherence and phase at different depths relative to the temperature fluctuations at the 15m level.
 $(\alpha = 25; \Delta f = .009765 \text{ cpm}; f_1 = .005859 \text{ cpm})$

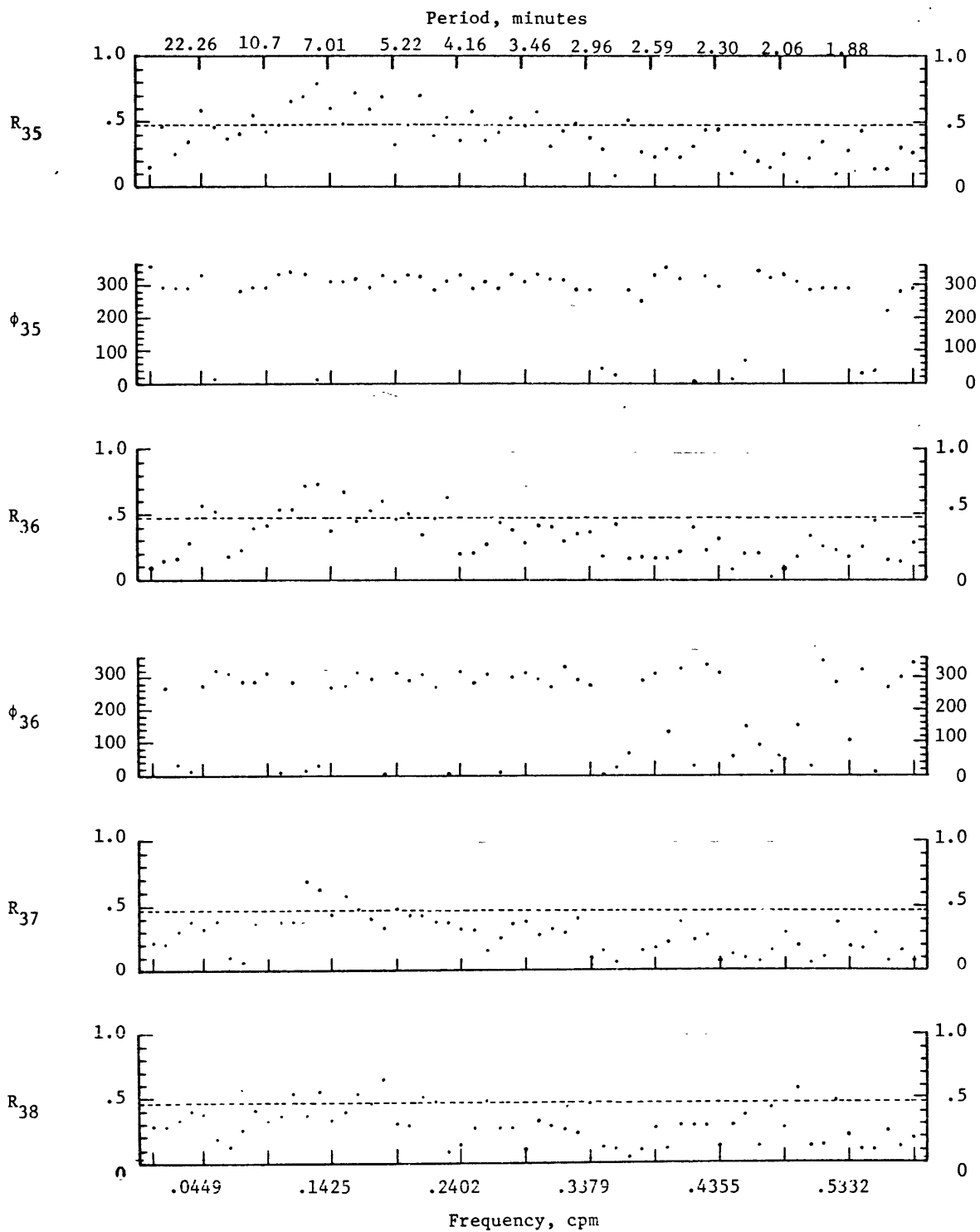


Figure 19. Ensemble averaged coherence and phase at different depths relative to the temperature fluctuations at the 15m level.
 $(\alpha = 25; \Delta f = .009765 \text{ cpm}; f_1 = .005859 \text{ cpm})$

Internal Wave Model

The Eulerian equation describing the vertical velocity of small amplitude two-dimensional motion in a stably stratified Boussinesq fluid which has a basic velocity distribution $U(z)$ is (Bretherton, 1966)

$$\left(\frac{\partial}{\partial t} + U \frac{\partial}{\partial x}\right)^2 (w_{xx} + w_{zz}) - \left(\frac{\partial}{\partial t} + U \frac{\partial}{\partial x}\right) (U_{zz} w_x) + N^2 w_{xx} = 0 \quad (15)$$

The x-axis has been oriented in the direction of propagation and the vertical axis z is positive upwards. A possible solution is a sum of simple harmonic (progressive) waves. Let one such constituent of frequency $\sigma (= \frac{2\pi}{\text{period}})$ and horizontal wavenumber $k (= \frac{2\pi}{\text{wavelength}})$ be represented by the real part of

$$w(x, z, t) = W(z) e^{i(kx - \sigma t)} \quad (16)$$

where $W(z)$ is the amplitude of the vertical component of the perturbation velocity. Substitution of equation (16) into equation (15) yields

$$\frac{d^2 W}{dz^2} + \left[\frac{N^2 k^2}{(\sigma - kU)^2} + \frac{k U_{zz}}{(\sigma - kU)} - k^2 \right] W = 0 \quad (17)$$

Equation (17) and two vertical boundary conditions form an eigenvalue problem. Along a rigid horizontal bottom the vertical velocity equals zero.

$$W = 0 \quad \text{at} \quad z = 0 \quad (18)$$

At the free surface the total (atmospheric) pressure is constant, say zero.

$$P_{\text{total}} = 0 \quad (19)$$

Since the frequency of internal waves is much less than the frequency of surface waves with the same wavenumber, the free surface condition can be approximated as (Phillips, 1966, p.165)

$$W = 0 \quad z = H \quad (20)$$

When $U = 0$ at all depths, equation (17) reduces to

$$\frac{d^2 W}{dz^2} + \frac{k^2(N^2 - \sigma^2)}{\sigma^2} W = 0 \quad (21)$$

In regions where $\sigma < N$ the function $W(z)$ has an oscillating behavior. Internal gravity waves (in a resting medium) with vertical wavenumber γ are then described by $w(x, z, t)$.

$$\gamma^2 = \frac{k^2 (N^2 - \sigma^2)}{\sigma^2} \quad (22)$$

Internal gravity waves are vertical oscillations which propagate horizontally and have maximum vertical displacements between the surface and the bottom. For each mode, σ is a monotonic increasing function of k . The amplitude of the vertical velocity of internal wave mode one contains a single maximum between the top and bottom, and the entire water column oscillates in phase. For this mode the horizontal velocity reverses direction once between the top and bottom.

Equation (17) was solved by a method that was suggested by Haskell (1953). The continuous vertical distributions of velocity and density are represented by many horizontal layers of constant U and ρ_0 . In a layer denoted by m , equation (17) becomes

$$\frac{d^2 W_m}{dz^2} - k^2 W_m = 0 \quad (23)$$

and

$$W_m = A_m e^{kz} + B_m e^{-kz} \quad (24)$$

In order that σ and k remain unchanged at each interface between successive layers, two conditions must be satisfied at each interface. The kinematic condition requires continuity of

the vertical displacement,

$$\frac{W_m}{(\sigma - k U_m)} = \frac{W_{m-1}}{(\sigma - k U_{m-1})} \quad (25)$$

The dynamic condition requires continuity of total pressure. To first order, the total pressure at the displaced position of a fluid particle is given by (Hines and Reddy, 1967)

$$p_{\text{total}} = p_0 + p + \eta \frac{dp_0}{dz} \quad (26)$$

where p_0 is the hydrostatic pressure which is continuous at an interface. The disturbance pressure (within a layer) p is evaluated from the horizontal component of the equation of motion, and to first order the vertical displacement η is given by

$$w = \frac{\partial \eta}{\partial t} + U \frac{\partial \eta}{\partial x} \quad (27)$$

The continuity of pressure at an interface is expressed by

$$\begin{aligned} & p_{0m} (\sigma - k U_m) \left(\frac{dW_m}{dz} - \frac{gk^2 W_m}{(\sigma - k U_m)^2} \right) \\ &= p_{0m-1} (\sigma - k U_{m-1}) \left(\frac{dW_{m-1}}{dz} - \frac{gk^2 W_{m-1}}{(\sigma - k U_{m-1})^2} \right) \end{aligned} \quad (28)$$

Equations (25) and (28) reduce to the interfacial conditions for the case $U = 0$.

The interfacial conditions were cast in a matrix formulation suggested by Haskell (1953): The surface and bottom boundary conditions were related by a 2×2 matrix A_{ij} , and for free surface and rigid bottom the matrix element $A_{22} = 0$.

The matrix element A_{22} was computed from prescribed values of σ , k , $U(z)$ and $\rho_0(z)$. Values of $U(z)$ and $\rho_0(z)$ were evaluated in the middle of the layers. Twenty-three layers were used to approximate the vertical distributions of velocity and density. The solution is obtained by varying k until $A_{22} = 0$.

For $U(z) \neq 0$ the eigenfunction of mode one was computed for periods between six and eight minutes. The spectral and vertical coherency analysis has shown that for periods from six to eight minutes the temperature fluctuations recorded between 10 m and 30 m below the surface contained significant (at the 95% confidence level) vertical displacements which were coherent and had a uniform phase.

Figure 20 contains the vertical distribution of W (mode one) computed for the case $U(z) = 0$ and for the $U(z)$ profile shown in the lower portion of that figure. The mean velocity profile $U(z)$ was estimated from the speeds measured at 10.6 m, 25.8 m, and 42.6 m below the surface during the time of the large amplitude high frequency speed fluctuations. The directions corresponding to these measurements were parallel to the wave crests and therefore use of $U(z)$ may be meaningless. These measurements were: $U(10.6 \text{ m}) = 40 \text{ cm/sec}$, $U(25.8 \text{ m}) = 15 \text{ cm/sec}$, and $U(42.6 \text{ m}) = 10 \text{ cm/sec}$. The density distribution used in the computation of W is also shown in

the lower portion of figure 20. Density was determined from the ensembled averaged values of mean temperature which had been computed in connection with the spectral analysis and from the salinity measurements made on July 28, 1967. The vertical distribution of the ratios of the rms vertical displacements (Table 3) to their maximum value have been plotted alongside the eigenfunction W . From 10 m to 30 m below the surface the rms vertical displacements of the temperature fluctuations and the eigenfunction computed for mode one with $U(z) \neq 0$ agree within 10%.

The horizontal wavelength, period and horizontal phase velocity corresponding to the eigenfunction shown in figure 20 are listed in the upper right portion of that figure. Table 6 contains additional eigenvalues computed for periods near 7-minutes. For the eigenvalues given in Table 6 the vertical distribution of the eigenfunction for mode one remained unchanged for the cases $U(z) = 0$ and $U(z) \neq 0$. In both cases the frequency increased with wavenumber. The constancy of the computed phase speed for 10% variations in wavelength and period is further (see figure 17) indication that these short period internal waves are non-dispersive.

The propagation speed computed for 7-minute period internal waves when $U(z) \neq 0$ was the same as the speed measured for individual narrow surface bands. The propagation speed of the high frequency temperature fluctuations measured with the towed thermometer also had the same magnitude as the computed speed. (The measurement of propagation speed from the temperature records obtained at buoys T1 and T2 was unsuccessful. Although the buoy spacing was less than one-half the computed wavelength, the buoys

were too close together to measure travel times, which were smaller than those foreseen because of the large (and previously unknown) tidal current. The thermistor cable suspended from the third buoy, located 525 m east of buoy T2 failed to operate.) The wavelength computed for 7-minute period internal waves when $U(z) \neq 0$ was twice the distance separating the narrow surface bands, suggesting that two narrow surface bands are associated with each wavelength of the internal waves measured at Station T. There is doubt concerning the direction of the mean current $U(z)$. If the current is parallel to the wave crests then eigenfunction calculations using $U(z)$ are meaningless. When $U(z) = 0$ the (theoretical) wavelength computed for 7-minute internal waves of mode one agrees with the spacing measured between individual surface bands but the observed speed of the bands does not agree with the computed (theoretical) phase speed.

Table 6

EIGENVALUES COMPUTED FOR VELOCITY AND
DENSITY DISTRIBUTIONS SHOWN IN FIGURE 20

L m	$U(z) = 0$		$U(z) \neq 0$		
	T min.	c cm/sec	L m	T min.	c cm/sec
134	6.7	35.0	301	6.6	76.3
158	7.5	35.3	321	7.0	76.7
173	8.0	36.1	344	7.5	77.0
			371	8.0	77.5

$k = 1.6 \times 10^{-2} \text{ m}^{-1}$
 $\sigma = 1.3 \times 10^{-2} \text{ s}^{-2}$

L = Horizontal wavelength
T = Period
c = Horizontal phase velocity

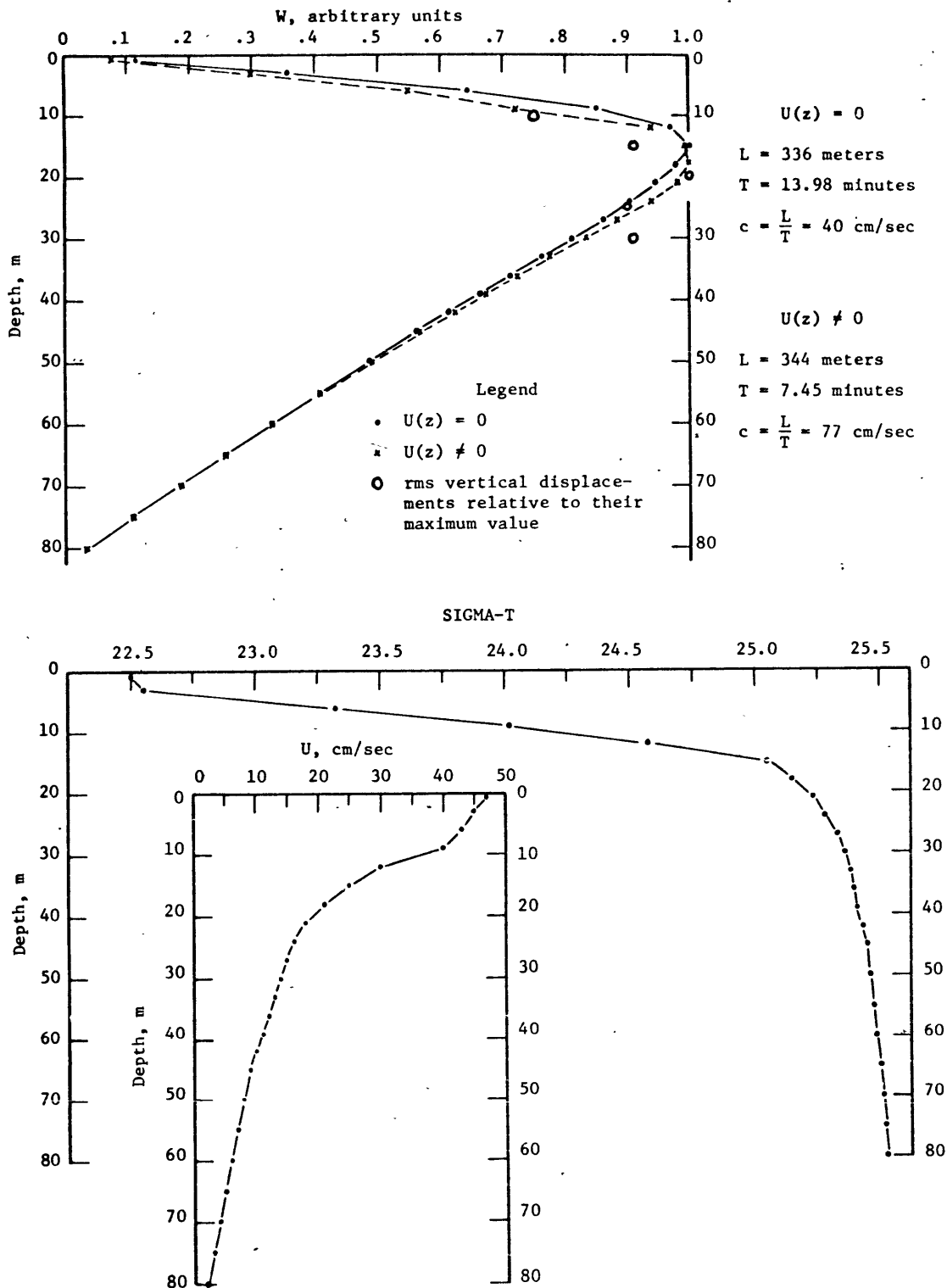


Figure 20. Upper: Vertical distribution of the amplitude of the vertical velocity (in arbitrary units) for internal wave motion of mode one in a fluid at rest and in a fluid moving with the profile $U(z)$. The eigenvalues corresponding to W are shown on the right. Lower: Vertical distribution of density (SIGMA-T) and velocity used in computing W .

In conclusion it must be said that there are many unanswered questions which arise from a study of the data. For example, we would like to know what generates the 7-minute waves. It is tempting to suppose that they are a result of shearing instability in the tidal flow. At Station T the Richardson number does drop almost to $1/4$ for very short intervals, but further upstream the Richardson number appears to be somewhat higher, so that this speculation is inconclusive. According to Miles (1961) and Howard (1961), a sufficient condition for small amplitude stable motion in parallel stably stratified inviscid flow is a Richardson number everywhere greater than $1/4$. A Richardson number was evaluated at Station T for 10-minute averages between 1148 EST, July 14 and 2000 EST, July 16 (1967) using: (1) 10-minute temperature averages calculated from the thermistor measurements at 15 m and 20 m below the surface, (2) 10-minute averages of velocity recorded at 10.6 m and 25.8 m, and (3) a single salinity measurement made at 15 m and 20 m. Figure 21 contains a Calcomp plot of 10-minute averages of Richardson number, vertical shear, and Brunt-Väisälä frequency. Variations of the Brunt-Väisälä frequency were smaller than variations in shear. When the shear decreased, the Richardson number increased. The Richardson number, though always greater than $1/4$, was less than unity and as low as .3 prior to the initiation of the short period internal waves.

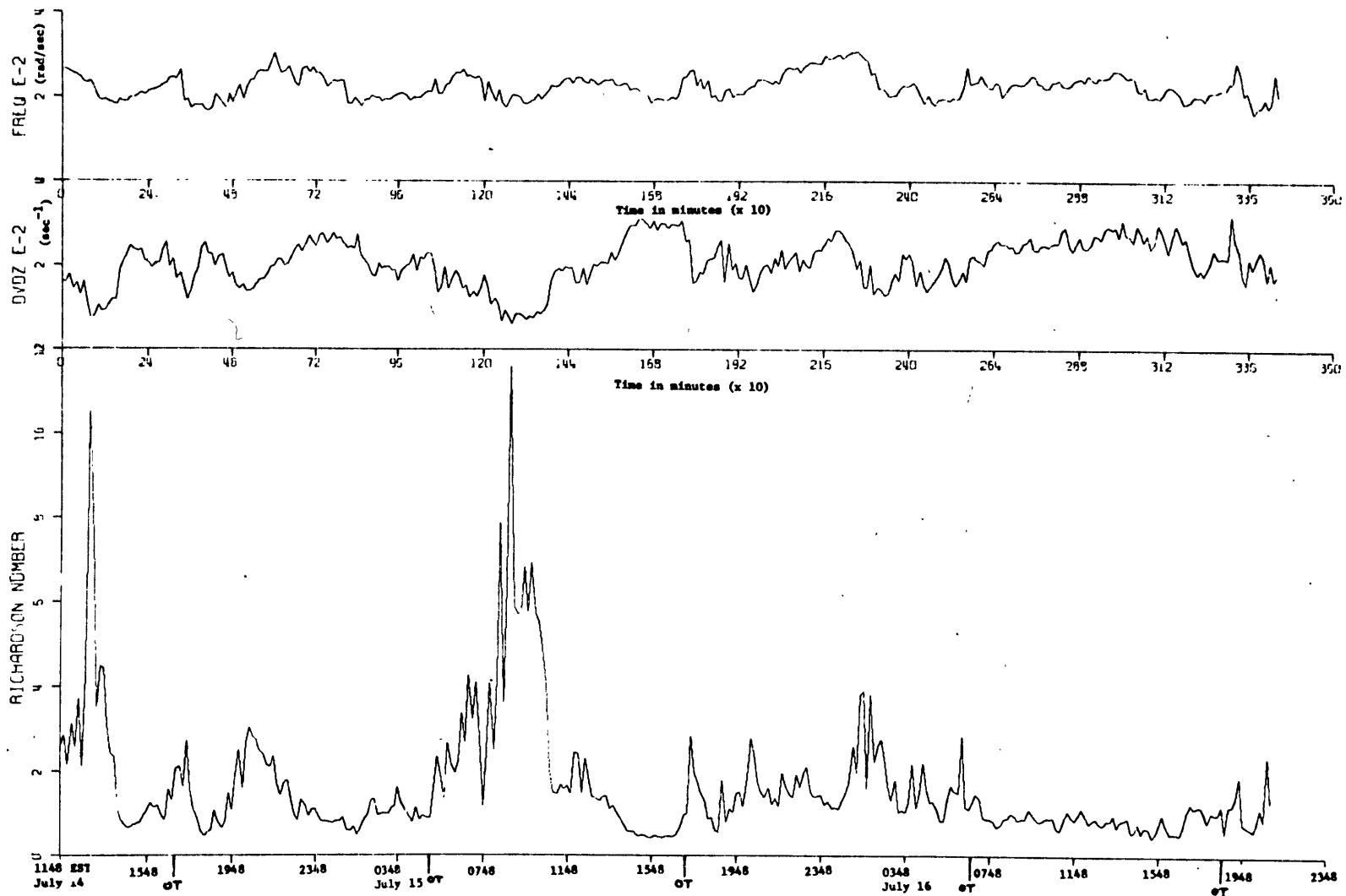
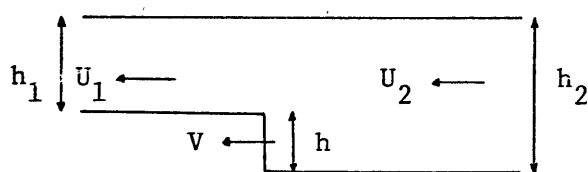


Figure 21. Ten minute averages of Richardson number (lower curve), vertical shear (middle curve) and Brunt-Väisälä frequency (upper curve). On the lower abscissa, a tick mark labelled OT is the onset time of a group of short period internal waves measured at Station T.

Another feature of the phenomenon which is not clearly explicable is the actual mechanism of the banded structure. Internal waves are cellular and contain alternating zones of convergence and divergence (Eckart, 1961). Bands of calm water in a rippled sea (Lafond, 1962) and bands of ruffled water in a smooth sea (Pickard, 1961) have been associated with convergence zones of short period internal waves occurring near the surface.

It is difficult to say much definite about the abrupt rise in temperature accompanying the first wave. The kinematics is fairly clear. Figure 22 describes the vertical displacement occurring at the onset of the abrupt temperature rise (figure 12) and the speeds occurring before and after a group of short period waves (figure 8).



$$\begin{array}{ll} h_1 = 15 \text{ m} & U_1 = 35 \text{ cm/sec} \\ h_2 = 25 \text{ m} & U_2 = 45 \text{ cm/sec} \\ h = 10 \text{ m} & \end{array}$$

Figure 22. Thermal front

The speed of the thermal front is

$$V = \frac{U_2 h_2 - U_1 h_1}{h} \quad (29)$$

Using the parameters listed in figure 22, $V = 60$ cm/sec, which is the same order as the measured propagation speed of the abrupt rise in temperature. The ultimate reason for flooding the surface from the east with a layer of deeper thermal structure is unknown.

Appendix A: Field Program

During the spring of 1965 equipment was gathered, a site selected, and a fishing vessel hired. The initial plan consisted of mooring a Richardson buoy with three nylon lines and recording on the buoy the temperature from thermistors placed along three multiconductor cables. The thermistor cables were to be anchored along the bottom at an angle from the buoy and buoyed vertically with subsurface floats. The first buoy launching took place at the end of June and was disastrous! The rented fishing boat was less than 35 feet in length and totally inadequate. For example, only two 1500 pound Stimson anchors could be loaded for fear of sinking the boat, and during the lowering of an anchor, the vessel nearly rolled over. At the beginning of July the project was in difficulty -- it was without a boat; two anchors had been lost; the buoy was shoaled at the Scituate Coast Guard Station; the equipment was stored in a garage in Scituate; and a 1500 pound Stimson anchor rested on the Scituate Town Pier against the wishes of the Harbormaster. Near the end of July a suitable vessel was hired. She was a 57-foot fishing dragger called the FRANCES ELIZABETH and was equipped with two winches, two windlasses, Loran, automatic pilot, fathometer, a knowledgeable skipper and a crew of two.

A single taut-wire mooring was used for the remainder of the 1965 summer when it became apparent that six lines extending at an angle from the buoy would inevitably result in chaos. Since internal waves had not previously been observed in Massachusetts Bay, their existence and not their directional properties would now be investigated. Wire cable was used to reduce the elasticity in the mooring and to keep each thermistor fixed in space. The thermistor cable hung from the buoy and was attached to the wire cable with swivel snap hooks.

A successful recording of temperature did not occur until late September due to failures of the electronic instruments. On that occasion four small surface floats, each having a net buoyancy of 100 pounds, buoyed up a wire cable and a thermistor cable attached to it. Recording took place on the fishing vessel stationed about 50 feet from the floats. The Richardson buoy had not been used because the mooring cable had parted near the anchor in mid-September. The buoy drifted towards the southwest and was retrieved by the Race Point (Massachusetts) Coast Guard when it was a mile offshore from their station.

The data collected in September, 1965 consisted of temperature measurements from nine depths sampled at 8-second intervals for a period of 2-1/2 hours. The data was plotted on the Calcomp plotter and fluctuations of 6-minute periods were observed in the upper 40 m.

In the spring of 1966 two additional temperature recording digitizers and two Richardson buoys were purchased. Each recorder was programmed to sample temperature at nine depths and pressure at one depth every two minutes. This sampling rate was chosen to obtain as long a series as possible (i.e., about eight days) with the minimum amount of aliasing. At the end of June, 1966 three temperature recording buoy systems were moored at Station T using the F/V FRANCES ELIZABETH. The buoys (A, B, and C) were located at the apexes of a right angled triangle (figure A1), although an equilateral triangular array had been planned. The buoys remained on station until their removal by the FRANCES ELIZABETH on September 1, 1966. The successes and failures in connection with the data obtained from the moored buoys during the 1966 summer have been summarized in Table A1.

Throughout the 1966 summer, data was collected from the MIT research vessel RR SHROCK. With it the digitizers were placed on (and taken off) the buoys; the buoy array was surveyed with magnetic compass, measured line, and sextant; water was collected in Van Dorn bottles for subsequent salinity determination at the Woods Hole Oceanographic Institution (WHOI); and BT's were run. On three separate occasions a Roberts current meter, on loan from the U.S. Naval Underwater Weapons Research and Engineering Station, Newport, R.I., failed to operate. Also, two flights were made over Station T in the WHOI heliocourier.

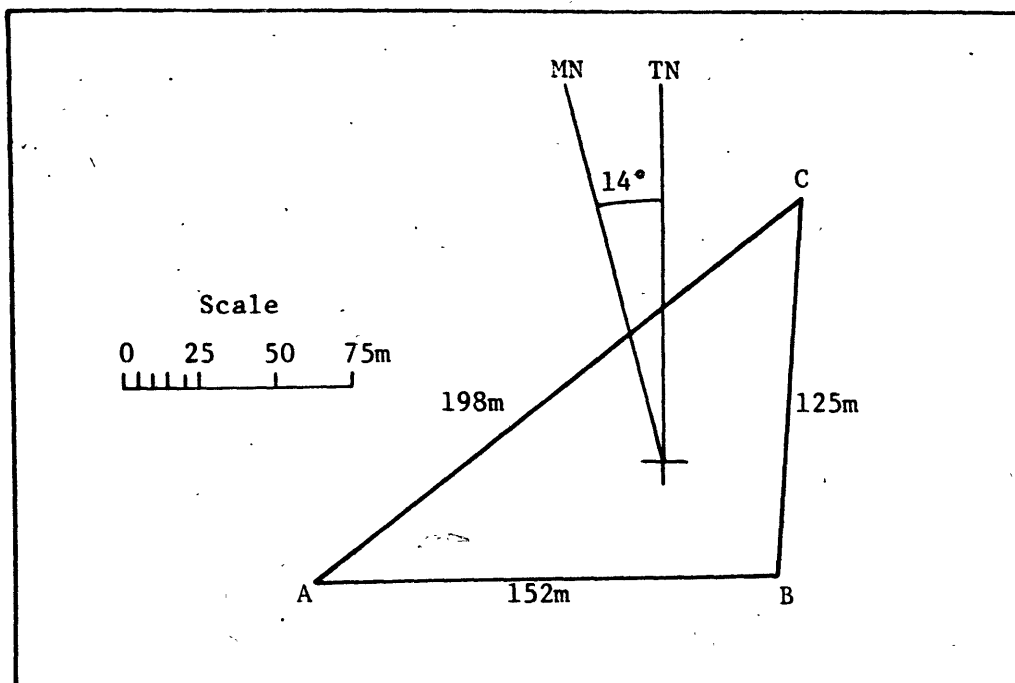


Figure A1. Location of buoys at Station T (1966)

Table A1.

STATION T MOORED BUOY RESULTS-1966

BUOY	EXPT 66-I	EXPT 66-II	EXPT 66-III
A	NO DATA Digitizer Failure	DATA July 28-Aug 3 Spurious Obs Aug 3-Aug 8	NO DATA Spurious Obs
B	NO DATA Digitizer Failure	NO DATA Digitizer Failure	NO DATA Severed Thermistor Cable
C	DATA July 6-July 9 Time Origin Lost	DATA July 28-Aug 3 Time Origin Lost	DATA Aug 24-Aug 30 Time Origin Lost

At the end of June, 1967 four moorings were established at Station T using the R/V RR SHROCK. Two of the three temperature recording buoy systems were set along a line perpendicular to Stellwagen Bank (figure A2). The fourth mooring contained three Geodyne current meters (Table A2). The buoys were removed in early September, but not before a fully instrumented temperature recording buoy system (buoy T1) was lost on the east side of Stellwagen Bank. Table A3 summarizes the data collected from the moorings.

The mooring system was launched by the anchor-first method. On arrival at Station T, the Richardson buoy with its chain bridle was lifted onto the water. Using the A-frame, the anchor was then gently lowered until the end of the wire cable came to a height about five feet above deck level. The mooring cable and an auxiliary winch-cable were connected through a pear-shaped ring. The thermistor cable was then attached to the wire cable and slid into the water by its own weight. The connector end of the thermistor cable was threaded through the center of the toroid and the cable fastened to the tension bridle. The pear-shaped ring was lowered to deck level and the chain leader from the buoy bridle was shackled to it. Half-inch (and larger sizes) round pin anchor shackles were used in the mooring. To disengage the vessel from the mooring the winch pulled in the wire cable a foot or two and a nylon stopper was secured to the ring. The winch released its hold on the mooring system and the auxiliary cable was removed. The nylon line was then cut

close to the ring dropping the anchor 1-2 m to the bottom.

Table A2

LOCATION OF VELOCITY MEASUREMENTS

Date (1967)	EXPT	Location	Water depth m	Amount of slack m	Current meter Ser. no.	Depth m
July 13-17	67-2	42°16'32" N 70°24'54" W	82	4	H879	10.6
					H880	25.8
					H881	45.6
July 24-28	67-3	42°16'12" N 70°16'36" W	29	2	H879	15.2
					H880	7.6
					H881	22.8
August 22-25	67-4	42°16'32" N 70°08'30" W	61	3	H879	45.6
					H880	25.8
					H881	10.6

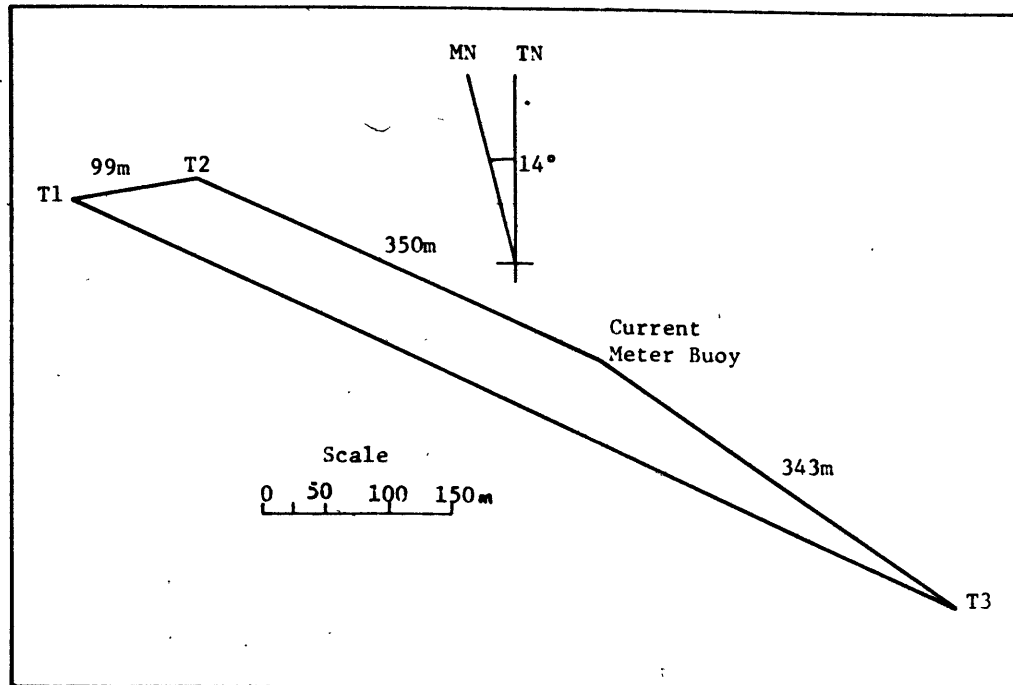


Figure A2. Location of buoys at Station T (1967)

Table A3. MOORED BUOY RESULTS-1967

BUOY	EXPT 67-II	EXPT 67-III	EXPT 67-IV
T1	DATA July 13-July 17 Location: Station T	DATA July 25-July 28 Location: Station T	DATA Aug 25-Aug 29 Location: Station T
T2	DATA July 13-July 17 Location: Station T	DATA July 25-July 28 Location: Station T	NO DATA Buoy Lost Location: 11 km East of Stellwagen Bank
(3) Current Meters	DATA July 13-July 17 Location: Station T	DATA July 24-July 28 Location: Stellwagen Bank	DATA Aug 22-Aug 25 Location: 11 km East of Stellwagen Bank
		Photographic survey over Station T, July 26	
EXPT 67-I failed because the buoys did not remain on station.			

Appendix B: Data Format

The format of the IBM-compatible magnetic tapes containing the temperature data is shown in Table B1. Each row or tape-record contains ten sequential measurements of a single sensor while a column of fourteen rows represents the fourteen sensors observed at a particular time. Uninterrupted time series belonging to various sensors are obtained by sorting the data as the tape is read into the computer, and a listing of the Fortran IV statements which perform this operation is given in Table B2. Prior to any type of analysis the temperature time series is scanned for obvious errors (i.e., temperature values greater than 20°C or less than 2°C) which are replaced by a linear interpolation using the preceding value and the next value. For example, if $T_i < 2^{\circ}\text{C}$, then T_i becomes $(T_{i-1} + T_{i+1})/2.0$. These errors result from 'bad' spots (dirt, wrinkles) occurring on the original 4-inch magnetic tape or Kodak film, or because bits were destroyed during the processing of the data by Geodyne. The data collected from the tape recording digitizers contained fewer of these errors.

The format of the 7-track tapes containing the velocity measurements is shown in Table B3. Each row contains a 50-second average value of the compass, vane, direction (= compass - vane), normalized unit vector of compass and vane, speed, and the angle of inclination of the meter from the vertical.

The compass, vane, and direction represent the angle of the instrument in the earth's magnetic field, the direction of the current relative to the instrument, and the direction of the current relative to magnetic north, respectively. By convention, the current direction is specified as the direction toward which the current is flowing. The normalized unit vectors provide a measure of dispersion occurring among the individual compass and vane values, i.e., a 1.0000 indicates that all twenty elements of the 50-second sample were identical.

Table B1.
A LISTING OF A TEMPERATURE-TAPE

9	23.	4.81	4.81	4.81	4.81	4.81	4.81	4.81	4.81	4.81	4.81
10	24.	4.64	4.64	4.64	4.64	4.64	4.64	4.64	4.64	4.64	4.64
11	0.	4.43	4.43	4.43	4.43	4.43	4.43	4.43	4.43	4.43	4.43
12	0.	4.39	4.39	4.39	4.39	4.39	4.39	4.39	4.39	4.39	4.39
13	0.4995	0.04997	0.04997	0.04997	0.04997	0.04997	0.04997	0.04997	0.04997	0.04997	0.04997
14	0.	179.64	175.78	172.92	173.23	176.57	175.77	178.07	179.00	174.09	177.27
1	24.	15.00	12.00	10.00	12.00	10.00	12.00	10.00	12.00	10.00	12.00
2	24.	14.12	14.12	14.11	14.12	14.13	14.16	14.16	14.19	14.16	14.22
3	24.	21.23	21.23	21.23	21.23	21.23	21.23	21.23	21.23	21.23	21.23
4	24.	13.55	13.29	13.13	13.04	13.06	12.99	12.90	12.80	12.72	12.66
5	24.	8.22	8.19	8.14	8.08	8.04	8.01	7.99	7.95	7.94	7.92
6	24.	7.45	7.45	7.45	7.45	7.45	7.43	7.41	7.39	7.35	7.33
7	24.	5.80	5.82	5.86	5.92	5.96	6.00	6.04	6.05	6.08	6.08
8	24.	5.24	5.24	5.24	5.24	5.24	5.24	5.24	5.24	5.24	5.24
9	24.	4.81	4.81	4.81	4.81	4.81	4.81	4.81	4.81	4.81	4.81
10	25.	4.64	4.64	4.64	4.64	4.64	4.64	4.64	4.64	4.64	4.64
11	0.	4.41	4.41	4.41	4.41	4.41	4.41	4.41	4.41	4.41	4.41
12	0.	4.37	4.37	4.37	4.37	4.37	4.37	4.37	4.37	4.37	4.37
13	0.4995	0.04997	0.04997	0.04997	0.04997	0.04997	0.04997	0.04997	0.04997	0.04997	0.04997
14	0.	179.14	175.10	173.34	172.85	172.63	172.70	172.74	174.17	173.55	180.45
1	25.	15.00	12.00	10.00	12.00	10.00	12.00	10.00	12.00	10.00	12.00
2	25.	14.22	14.22	14.26	14.27	14.27	14.27	14.27	14.27	14.28	14.35
3	25.	21.23	21.24	21.24	21.24	21.24	21.24	21.24	21.24	21.25	21.25
4	25.	12.57	12.50	12.49	12.53	12.75	13.16	13.33	13.19	13.07	13.01
5	25.	7.99	7.88	7.86	7.88	7.94	8.03	8.06	8.03	7.99	7.97
6	25.	7.29	7.29	7.31	7.33	7.39	7.41	7.43	7.41	7.37	7.39
7	25.	6.11	6.13	6.15	6.15	6.17	6.21	6.21	6.17	6.13	6.11
8	25.	5.24	5.24	5.24	5.24	5.24	5.24	5.24	5.22	5.22	5.20
9	25.	4.81	4.81	4.81	4.81	4.81	4.81	4.81	4.81	4.81	4.79
10	26.	4.64	4.64	4.64	4.64	4.64	4.64	4.64	4.64	4.64	4.64
11	0.	4.43	4.43	4.43	4.43	4.43	4.43	4.43	4.43	4.43	4.43
12	0.	4.37	4.37	4.37	4.37	4.37	4.37	4.37	4.37	4.37	4.35
13	0.4995	0.04997	0.04997	0.04997	0.04997	0.04997	0.04997	0.04997	0.04997	0.04997	0.04997
14	0.	180.35	179.28	180.27	172.84	175.42	175.42	175.94	177.09	179.21	173.09
1	26.	15.00	12.00	10.00	12.00	10.00	12.00	10.00	12.00	10.00	12.00
2	26.	14.35	14.35	14.35	14.35	14.35	14.37	14.40	14.40	14.40	14.40
3	26.	21.25	21.25	21.25	21.25	21.25	21.26	21.26	21.25	21.26	21.25
4	26.	12.93	12.87	12.83	12.98	13.12	13.25	13.16	12.99	12.80	12.62
5	26.	7.97	7.97	7.97	7.95	7.95	7.95	7.94	7.92	7.88	7.84
6	26.	7.37	7.39	7.41	7.43	7.43	7.43	7.41	7.33	7.26	7.18
7	26.	6.09	6.09	6.09	6.11	6.13	6.13	6.11	6.09	6.08	6.02
8	26.	5.20	5.20	5.20	5.20	5.20	5.20	5.20	5.20	5.20	5.20

LEGEND

A. Horizontal

Column	Remarks
1,2	Sensor number
3-7, inclusive	Sequential numbering of time series
8-77, inclusive	10 sequential measurements

B. Vertical

Sensor Number	Measurement	Depth (meters)	
		1966	1967
1	Reference resistor (5000 ohms)		Inside the digitizer
2	Time (hours)		Inside the digitizer
3	Temperature (°C)		Inside the digitizer
4	Temperature (°C)		
5	Temperature (°C)	5	5
6	Temperature (°C)	11.1	10
7	Temperature (°C)	17.2	15
8	Temperature (°C)	23.3	20
9	Temperature (°C)	29.4	25
10	Temperature (°C)	35.5	30
11	Temperature (°C)	41.6	35
12	Temperature (°C)	47.7	40
13	Temperature (°C)	53.8	45
14	Reference resistor (5000 ohms)	59.9	50
	Pressure (feet)	66.0	55

Table 82

A LISTING OF THE STATEMENTS THAT SORT THE DATA

```

C   A TAPE RECORD CONTAINS 10 DATA POINTS
C   NCARD = 1 TAPE RECORD
C   SENSORS 4 THRU 8 ARE TO BE SORTED FROM THE TAPE
C   IN THE READ STATEMENTS (10,900), THE SUBSCRIPT I
CC  DETERMINES WHICH OF THE 14 SENSORS WILL BE SORTED
C   THE ARRAY TEMP(J) CONTAINS A TOTAL OF NPOINT VALUES
CC  BELONGING TO SUBSCRIPT I, NFIRST BEING THE FIRST VALUE.
CCC THE FIRST VALUE IN TEMP(J) IS SUBSCRIPTED BY I
  
```

```

DATA IEND/'$$$$'/
READ (5,600) NCARD
600 FORMAT (I5)
C   SORTING OF THE PROBES
DO 10 K=1,NCARD
KK = K-1
READ (10,900) ((DUMMY(I,J),J=1,10),I=1,3)
READ (10,900) ((POINTS(I,J+KK*10),J=1,10),I=1,5)
READ (10,900) ((DUMMY(I,J),J=1,10),I=1,6)
900 FORMAT (7X,10F7.2)
10 CONTINUE
C   ESTABLISHMENT OF THE TEMP ARRAY
1 READ (5,901) NPOINT,NFIRST,NSENSE,(IHEAD(I),I=1,7)
901 FORMAT (3I5,7A4)
IF (IHEAD(1) .EQ. IEND) GO TO 100
NLASt = NFIRST + NPOINT
J=0
DO 20 I=NFIRST,NLASt
J=J+1
TEMP(J) = POINTS(NSENSE,I)
20 CONTINUE
  
```

* * * * *

EXAMPLE

1000 TEMPERATURE VALUES OF SENSORS 4,5,6,7, AND 8 ARE TO BE PLOTTED, AND THE FIRST VALUE OF SENSOR 4 BEGINS AT 500 DELT, 600 DELT FOR SENSOR 5, AND 700 DELT FOR SENSORS 6,7, AND 8, DELT IS THE SAMPLING INTERVAL. THE INPUT CARDS ARE

```

170
1000 500 1 THERMISTOR 1 (5 METERS)
1000 600 2 THERMISTOR 2 (10 METERS)
1000 700 3 THERMISTOR 3 (15 METERS)
1000 700 4 THERMISTOR 4 (20 METERS)
1000 700 5 THERMISTOR 5 (25 METERS)
  
```

\$\$\$\$

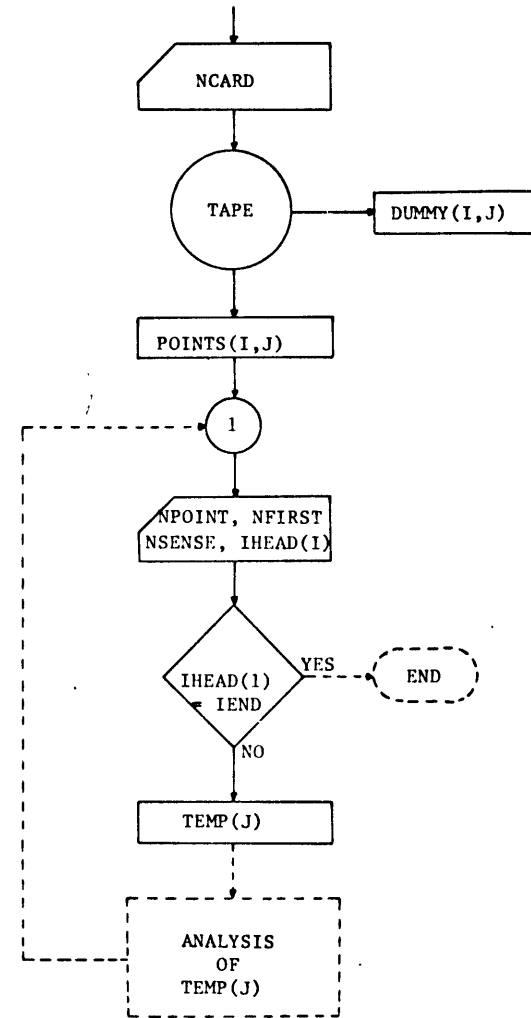


Table 83

A LISTING OF A CURRENT METER-TAPE

VALIDITY INDICATORS	INTERVAL NO.		COMPASS VANE		DIRECTION	NORMALIZED UNIT VECTOR		ROTOR SPEED IN KNOTS	INCLINOMETER READING IN DEGREES
			COMPASS	VANE		COMPASS	VANE		
**	101	AVERAGE	139	8	131	0.999	0.926	0.29	0
	102	AVERAGE	140	2	138	0.999	0.882	0.30	0
	103	AVERAGE	135	7	128	0.999	0.937	0.40	0
	104	AVERAGE	138	16	122	0.999	0.943	0.42	0
	105	AVERAGE	134	9	125	0.999	0.956	0.43	0
**	106	AVERAGE	132	11	121	0.998	0.985	0.43	0
	107	AVERAGE	132	7	125	0.999	0.970	0.40	0
	108	AVERAGE	137	13	124	0.998	0.947	0.28	0
	109	AVERAGE	136	10	126	0.999	0.928	0.42	0
	110	AVERAGE	142	24	118	1.000	0.913	0.42	0
**	111	AVERAGE	143	27	116	0.999	0.976	0.41	0
	112	AVERAGE	146	19	127	1.000	0.958	0.38	0
	113	AVERAGE	144	19	125	0.999	0.965	0.45	0
	114	AVERAGE	146	17	129	1.000	0.855	0.42	0
	115	AVERAGE	147	26	121	0.999	0.988	0.38	0
**	116	AVERAGE	145	21	124	0.999	0.975	0.45	0
	117	AVERAGE	141	22	119	0.999	0.964	0.45	0
	118	AVERAGE	143	24	119	0.999	0.983	0.43	0
	119	AVERAGE	140	18	122	0.999	0.924	0.46	0

Appendix C: Temperature and Salinity Measurements at Station T

The mean value of a series of (ungrouped) temperature measurements was computed from the formula

$$\bar{T}_0 = \frac{1}{N} \sum_{i=1}^N T_i \quad (C1)$$

where T_i is the value of the i^{th} temperature measurement, N is the total number of terms in the series¹, and for sequential measurements $N\Delta t$ is the length of the series in time. The overall variability of the measurements was described by the standard deviation

$$SD = \left[\frac{\sum_{i=1}^N (T_i - \bar{T}_0)^2}{N} \right]^{\frac{1}{2}} \quad (C2)$$

Vertical distributions of mean temperature and standard deviation computed from the thermistor measurements obtained at Station T in 1965 are shown in figure C1. Minima and Maxima temperature values are given in Table C1. Bathythermographs were lowered once or twice during each experiment to determine the deep water temperature (Table C2).

Water, collected in eight 2-liter Van Dorn bottles spaced

¹ The symbol N has also been used to represent the Brunt-Väisälä frequency.

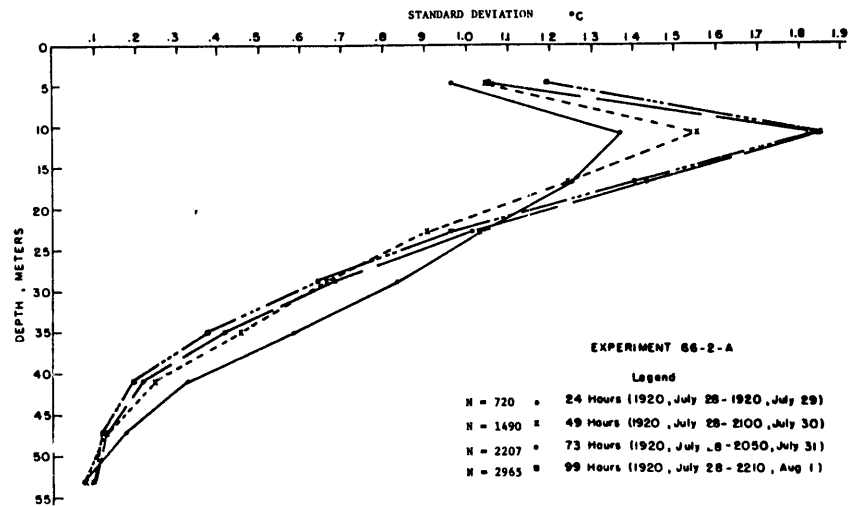
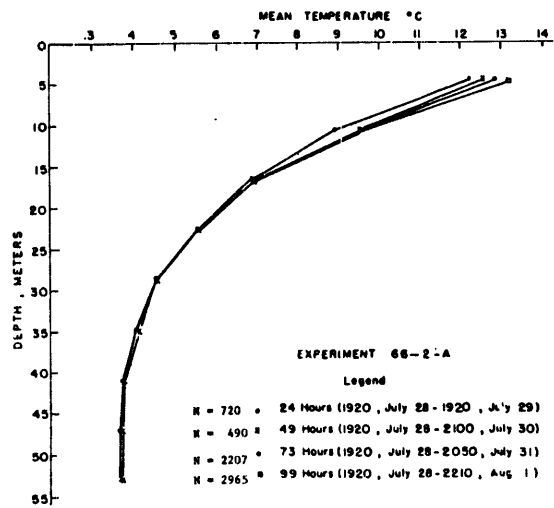
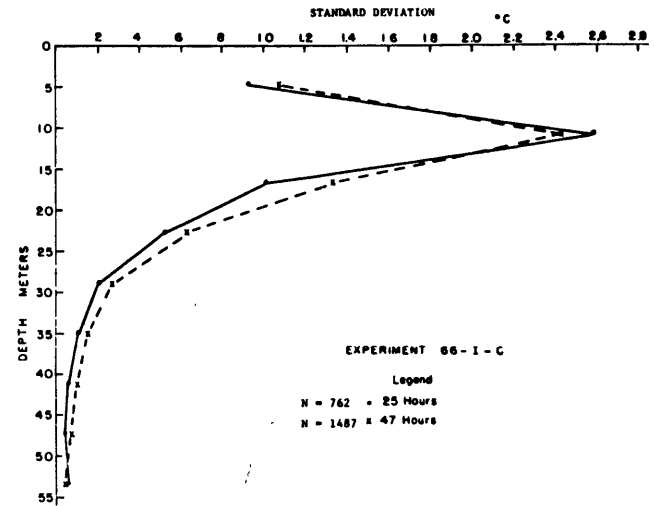
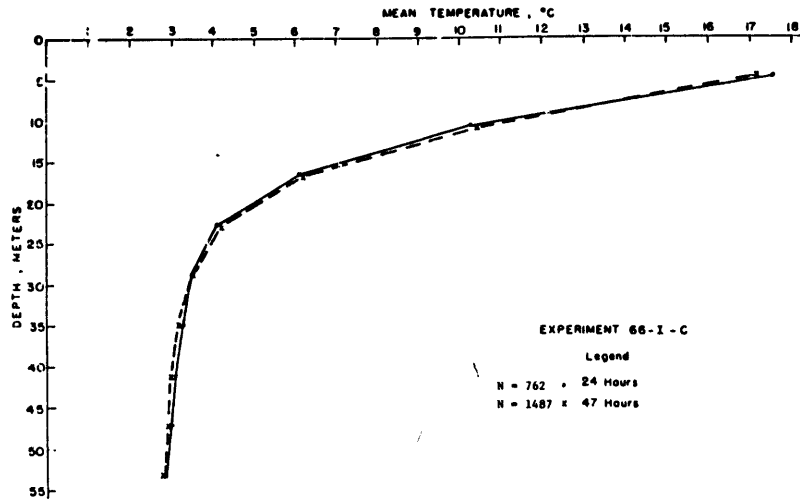


Figure C1

Table C2

AVERAGE TEMPERATURE DISTRIBUTION

Depth m	Experiment						Therm. Tow Sept. 19
	66-I	66-II	66-III	67-II	67-III	67-IV	
0	18.1	17.0	15.9	14.0	18.0	17.7	14.5
50				3.9	3.9	4.0	4.4
55	3.0	3.8	4.0	3.85	3.85	3.9	4.1
60	3.0	3.8	4.0	3.85	3.8	3.9	4.0
65	3.0	3.6	3.9		3.75	3.9	4.0
70	2.9	3.5	3.8		3.75	3.85	4.0
75	2.9	3.4	3.6				4.0

Table C1

MINIMUM AND MAXIMUM TEMPERATURES

Depth m	Expt 66-1-C		Expt 66-2-A	
	MIN	MAX	MIN	MAX
	°C		°C	
5	13.87	18.88	10.54	16.09
11.1	5.70	18.35	6.43	14.62
17.2	4.18	16.29	5.20	13.85
23.3	3.02	9.94	3.97	12.26
29.4	2.11	6.00	3.64	9.79
35.5	2.86	4.55	3.69	7.11
41.6	2.75	3.53	3.54	6.29
47.7	2.75	3.16	3.49	5.01
54.8	2.68	2.99	3.47	4.37

Depth m	Expt 67-2-T2		Expt 67-3-T2	
	MIN	MAX	MIN	MAX
	°C		°C	
5	7.83	16.48	10.48	18.75
10	6.19	15.02	7.11	16.39
15	5.52	14.02	5.96	14.66
20	4.85	13.36	5.34	13.04
25	4.47	12.14	4.87	9.91
30	4.47	11.47	4.60	7.39
35	4.43	8.01	4.35	6.44
40	4.41	6.15	4.31	5.54
45	4.35	5.28	4.29	4.91

10 m apart, was analyzed for salinity by the conductivity method at WHOI. The salinity measurements are given in Table C3 and vertical distributions of the average salinity are shown in figures C2 and C3.

Density was computed directly from Knudsen's Formula (Lafond, 1951, p.91) using the mean values of temperature and salinity. The density gradient was computed from the formula

$$\left(\frac{d\rho}{dz}\right)_j = \frac{(\rho)_{j-1} - (\rho)_{j+1}}{2 \Delta h} \quad z \approx j \quad (C3)$$

where subscript j represents a thermistor (e.g., $j = 1$ being the uppermost thermistor) and Δh is the spacing between thermistors. Gravity, calculated from the International Gravity Formula (Jacobs et al, 1959, p.91), was equal to 980.401 c.g.s. units.

The statistics of the temperature measurements recorded between July 25 and July 27 (49 hours) at buoys T1 and T2 are compared in Table C4.

Figures C4, C5, and C6 are Calcomp plots of the actual temperature measurements. The times of initiation of the high frequency temperature fluctuations are summarized in Table C5.

Table C3

SALINITY MEASUREMENTS AT STATION T

Date (1966)	July 7	July 7	July 8	July 8	July 9	July 9	July 14
Depth (feet)	Salinity (%)						
30	31.189	31.577	31.614	31.657	31.520	31.575	31.597
60		32.037	32.103	32.110	31.890	31.744	31.980
90	32.151	32.202	32.199	32.222	32.179		32.173
120		32.241	32.247	32.242	32.238	32.348	32.225
150	32.248	32.271			32.267		32.252
180		32.286	32.270	32.272		32.287	32.299
210		32.301			32.306	32.303	32.330
240					32.336		32.320

Date (1966)	Aug 11	Aug 11	Aug 23	Aug 23	Aug 24
Depth (m)	Salinity (%)				
10	31.940	31.942	31.679	31.660	31.872
20	32.112	32.158	31.962	32.049	32.126
30	32.180	32.175	32.110	32.156	32.173
40	32.194		32.163	32.186	32.220
50	32.215		32.189	32.217	
60	32.255		32.233	32.232	32.229
70	32.240		32.228	32.228	32.239
80	32.264			32.257	32.252

Date (1967)	July 13	July 17	July 25	July 28	Aug 29
Depth (feet)	Salinity (%)				
5	30.938	30.994	30.508	30.794	31.038
35	31.284	31.379	31.386	31.671	31.519
65	31.700	31.700	31.858	31.858	31.806
95	31.817	31.916	31.983	31.984	31.942
125	31.935	31.987	32.029		
155	32.022	32.023	32.067	32.037	32.030
185		32.025	32.112	32.048	
215	32.038	32.034	32.120		

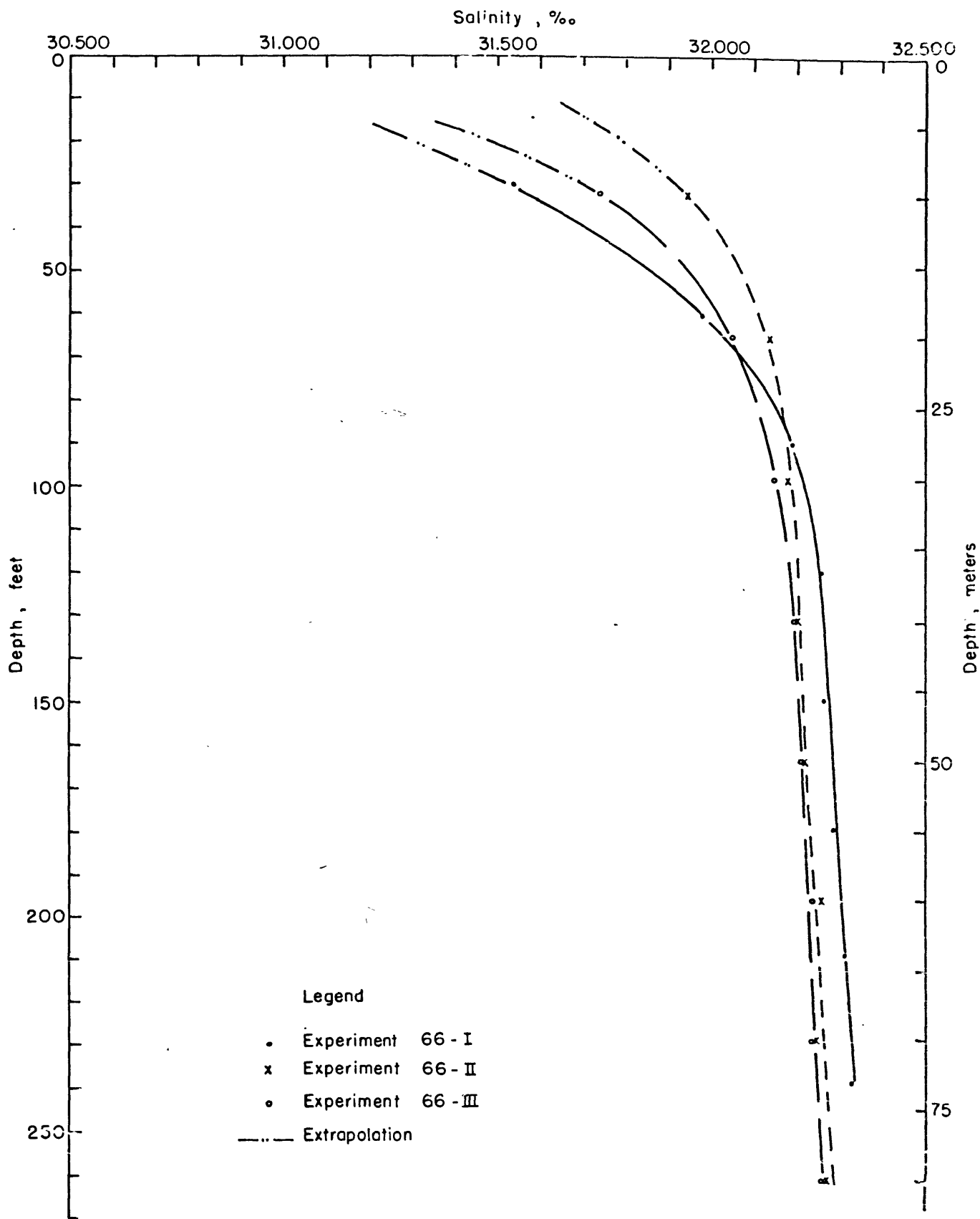


Figure c2. Salinity Observations, 1966

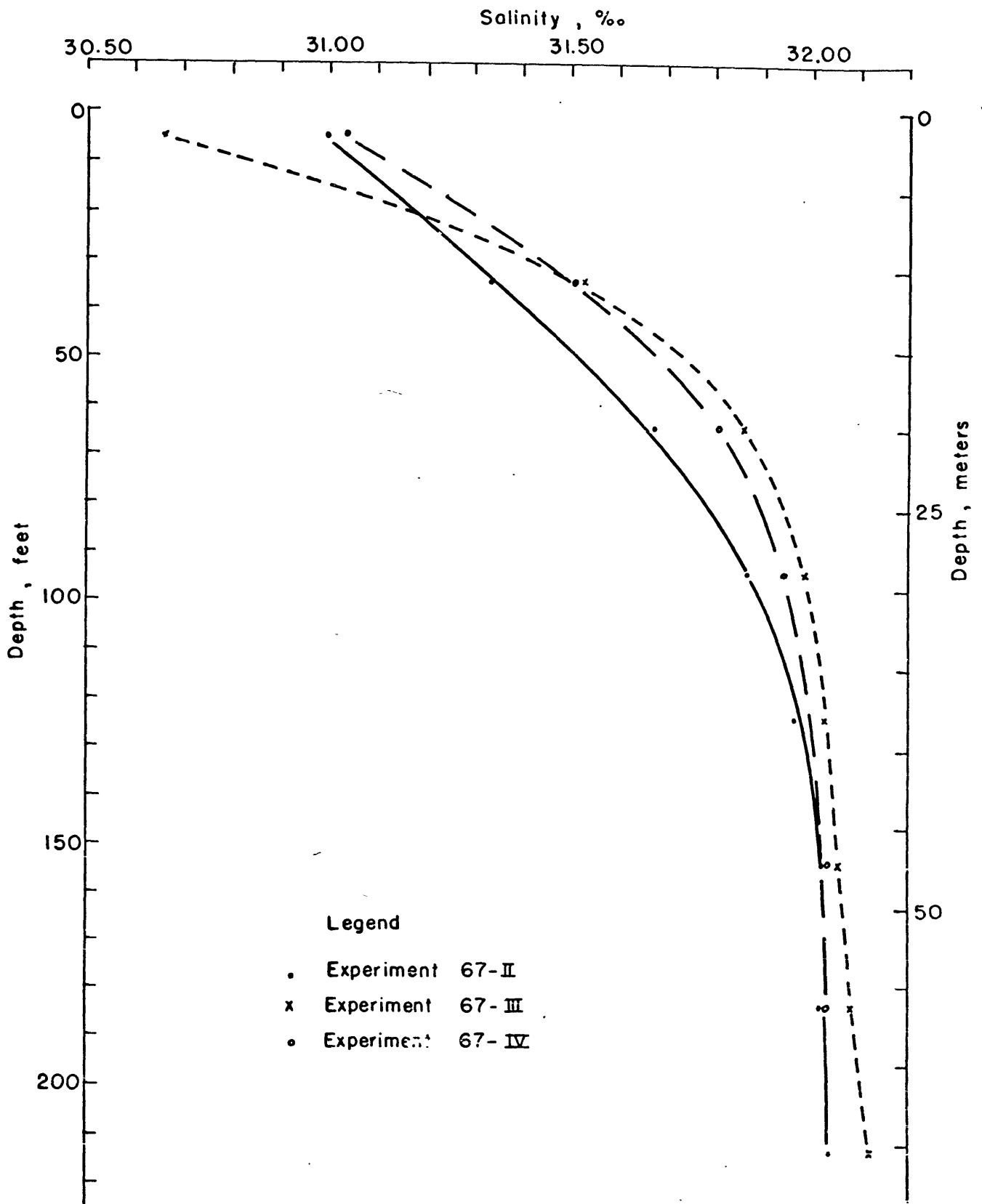


Figure C3. Salinity Observations, 1967

Table C4

A COMPARISON OF 49 HOURS (N = 5900) OF MEASUREMENTS
RECORDED AT BUOYS T1 AND T2 DURING EXPT 67-3

Depth m	Buoy	Mean	SD	Max	Min	Brunt-Väisälä Frequency cpm
5	T1	15.36	1.66	19.16	11.25	
	T2	13.91	1.64	18.75	10.48	
10	T1	10.71	1.66	18.08	7.77	.397
	T2	9.73	1.52	16.39	7.11	.371
15	T1	8.21	1.15	15.31	6.02	.281
	T2	7.69	0.96	14.66	5.96	.262
20	T1	6.70	0.69	13.36	5.48	.211
	T2	6.35	0.63	13.04	5.34	.200
25	T1	5.63	0.44	10.44	4.93	.159
	T2	5.46	0.41	9.91	4.87	.149
30	T1	5.13	0.30	7.59	4.60	.119
	T2	5.04	0.27	7.39	4.60	.112
35	T1	4.72	0.22	6.68	4.29	.0871
	T2	4.71	0.19	6.44	4.35	.0847
40	T1	4.57	0.14	5.90	4.29	.0704
	T2	4.52	0.12	5.54	4.31	.0697
45	T1	4.35	0.09	5.15	4.18	
	T2	4.41	0.08	4.91	4.29	

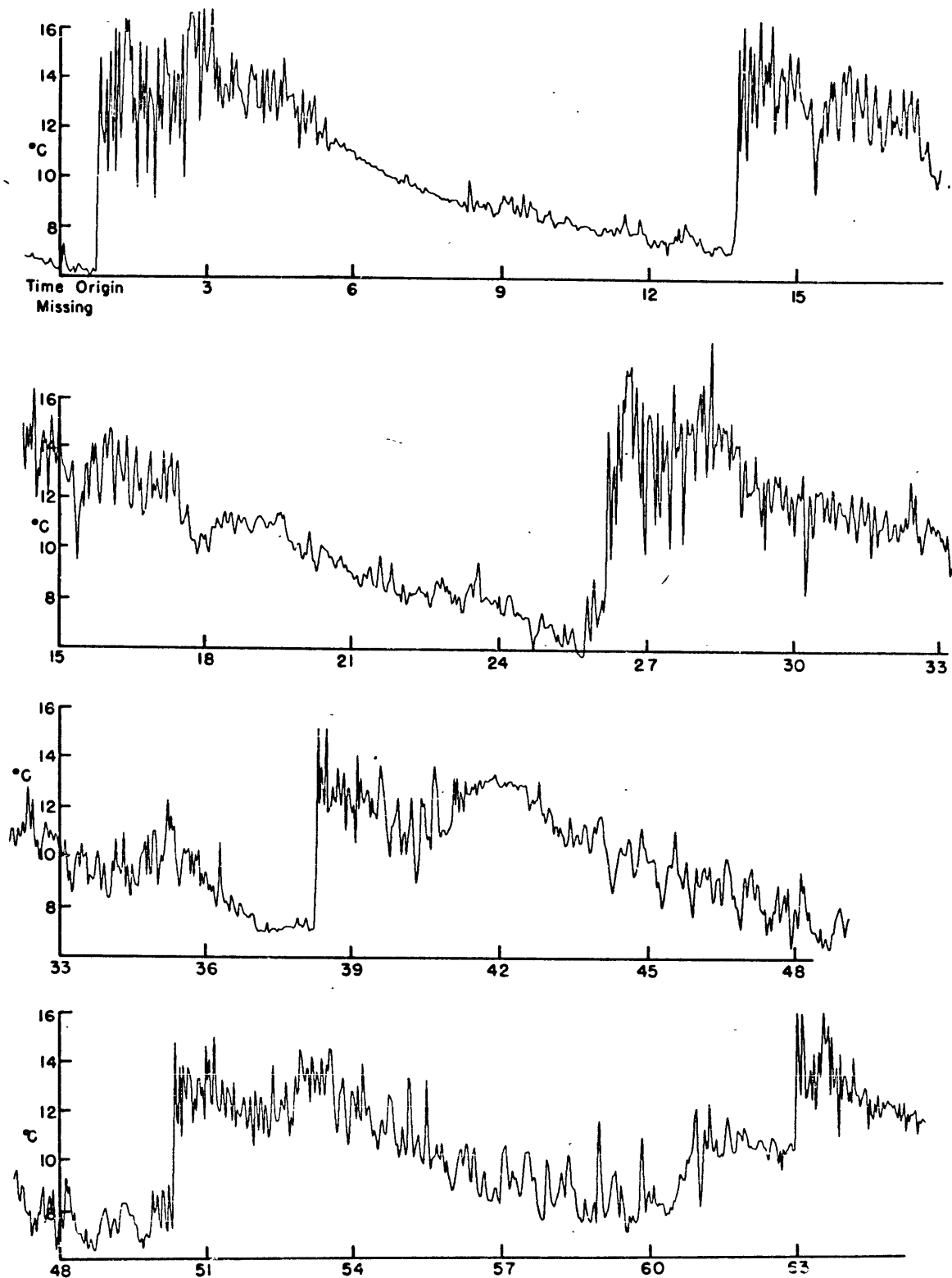


Figure C4. A Calcomp plot of 1950 temperature measurements at 11.1m at Station T (buoy C) between July 6 and July 9, 1966. Sampling interval was 2-minutes. The time origin is missing and the interval between tick marks on the abscissa is 3-hours.

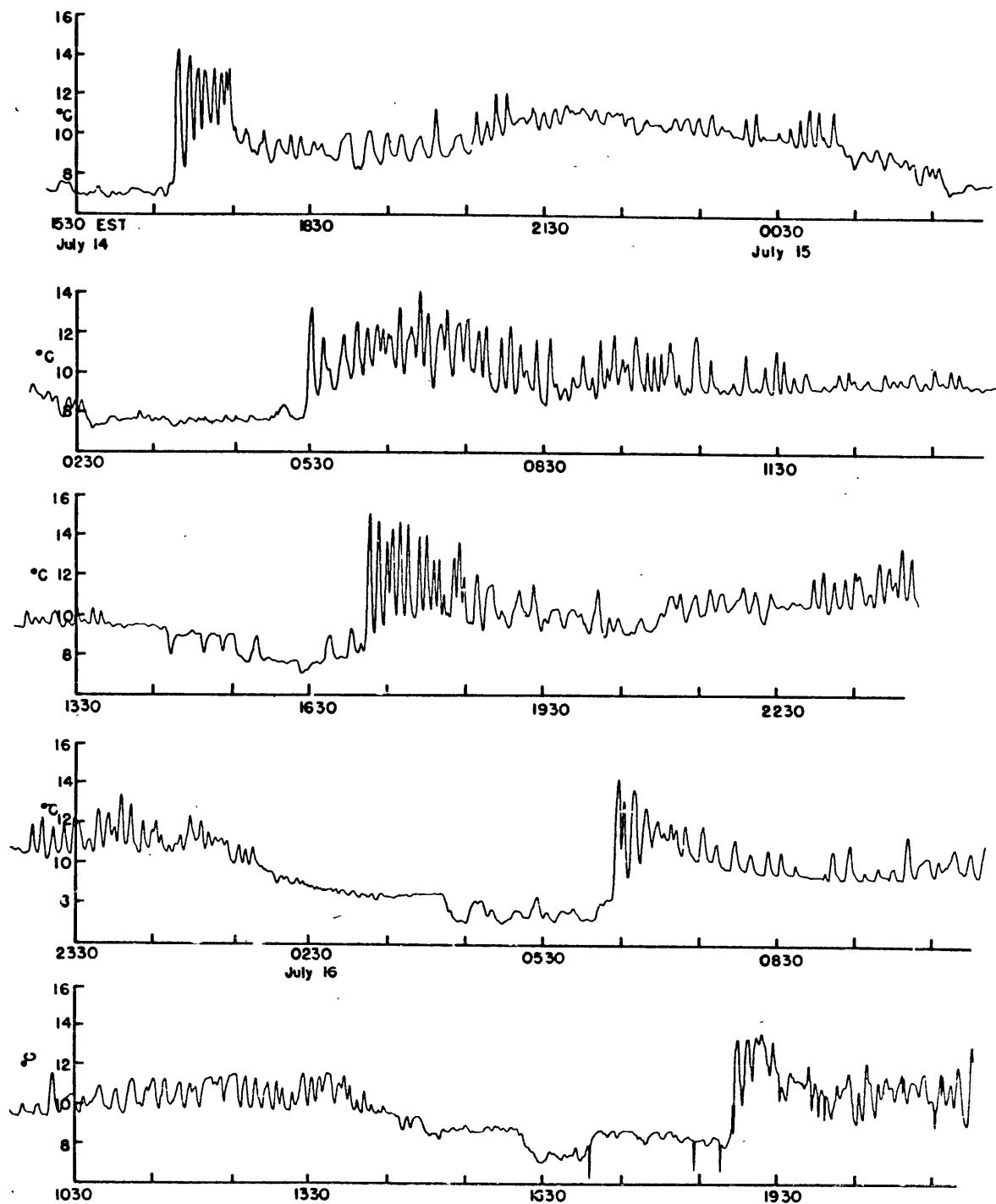


Figure 05. A Calcomp plot of 6500 temperature measurements at 10m at Station T (buoy T2) between July 14 and July 17, 1967. Sampling interval was 30-seconds.

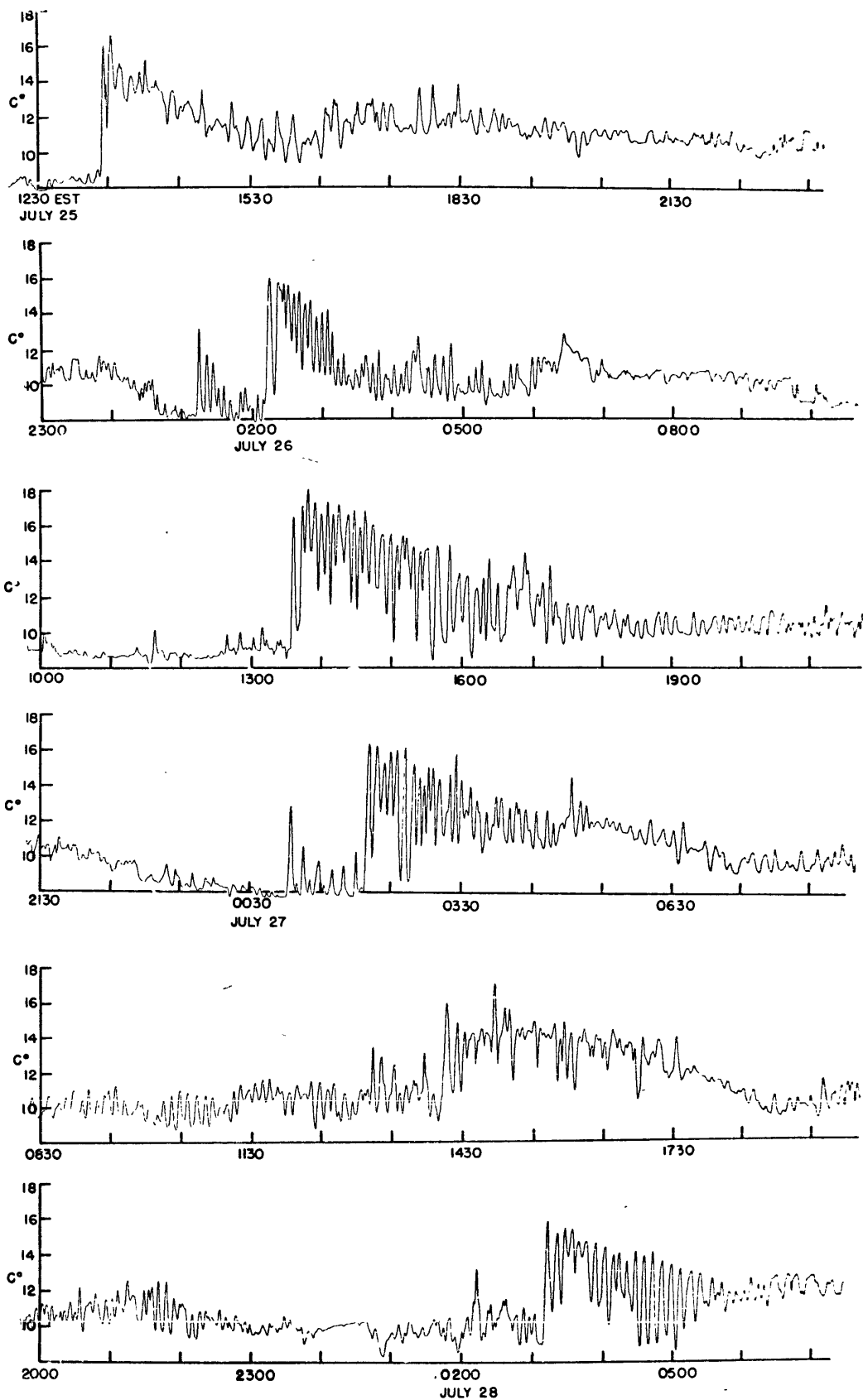


Figure c6 . A Calcomp plot of 7900 temperature measurements at 10m at Station T (buoy T1) between July 25 and July 27, 1967. Sampling interval was 30-seconds.

Table C5

TIMES OF INITIATION OF THE HIGH FREQUENCY TEMPERATURE FLUCTUATIONS

EXPT 66-2A		EXPT 67-2		EXPT 67-3	
EST	Date	EST	Date	EST	Date
1919	July 28	1645	July 14	1325	July 25
0752	29	0526	14	0212	26
1919	29	1713	15	1336	26
0731	30	0626	16	0209	27
2058	30	1855	16	1415	27
0909	31			0316	28
2054	31				
0927	August 1				
2212	1				
1026	2				

Appendix D: Velocity Measurements

Bigelow (1927), using drift bottle measurements, described the circulation in Massachusetts Bay as being dominated entirely by tidal currents such that any non-tidal (geostrophic) drift would be easily obscured. In the Gulf of Maine the tide flows northward along Cape Cod but runs westward into Massachusetts Bay drawing southward around the northern tip of Cape Cod and reaching a speed of 75 cm/sec in the narrow channel between Provincetown and Stellwagen Bank. Haight (1942) has reported that the maximum speed of a current rose measured on Stellwagen Bank for 60 days in 1919 was 8 cm/sec. Although commercial fishermen from Scituate speak of a strong current (about a knot) on Stellwagen Bank, recent Coast and Geodetic Survey Tidal Current Tables have indicated that the current on the Bank is variable and too weak to measure.

The speed and direction measurements from each experiment were organized into histograms (figures D1, D2, D3, D4, D5, and D6). A histogram contains no reference to the frequency constituents nor to the time sequence of the data, and it can be interpreted if a large enough sample is used although its description becomes less reliable as the number of processes contributing to the measurement increases. The speed histograms at Station T are bimodal and the smaller high speed mode occurring at the lower depths represents the resultant of tidal

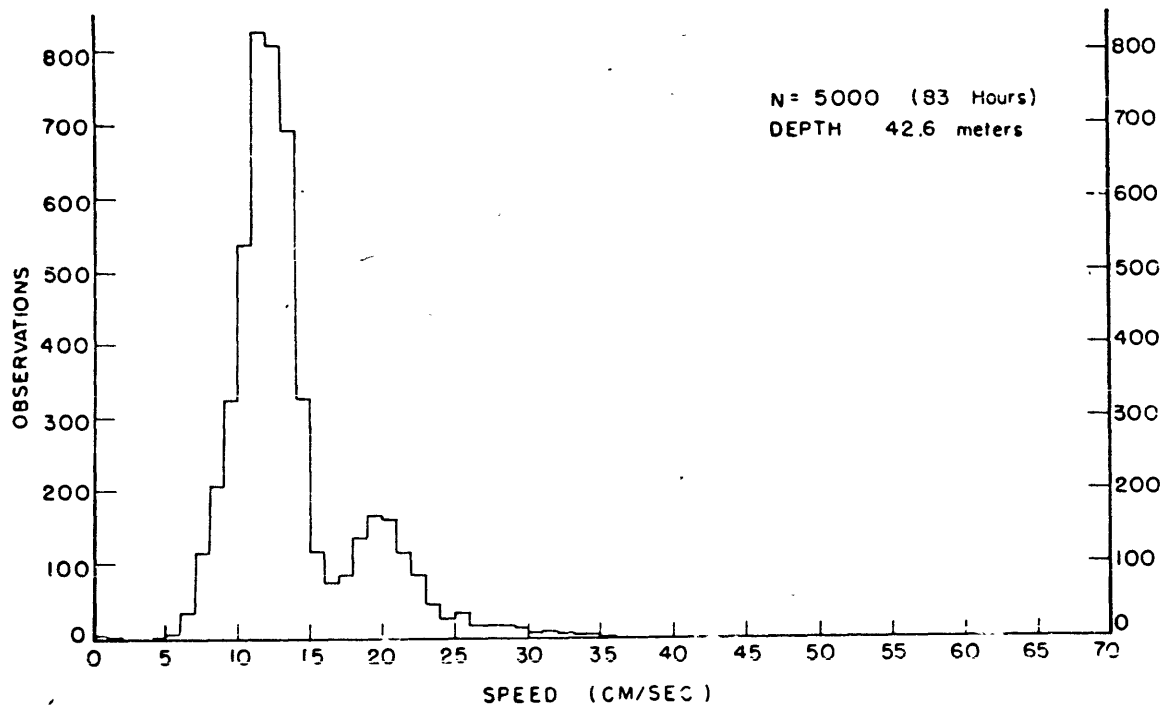
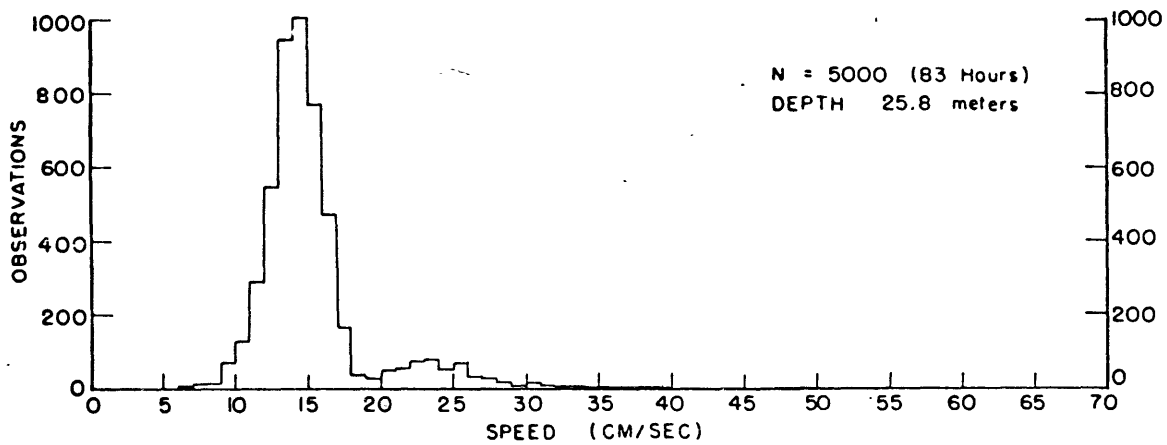
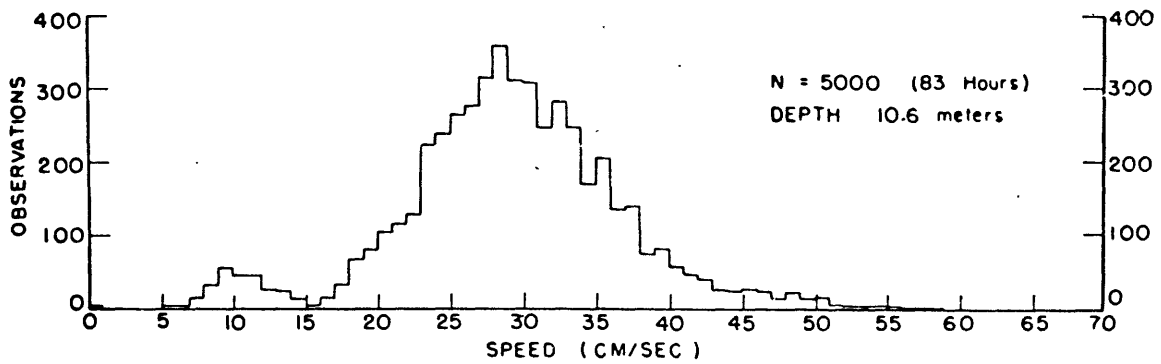


Figure 31. SPEED HISTOGRAM (EXPT 67-2)

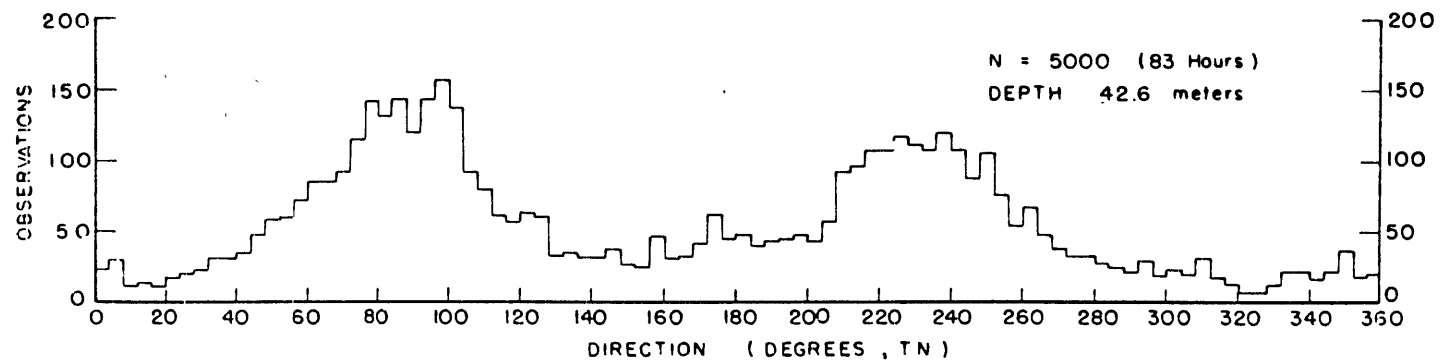
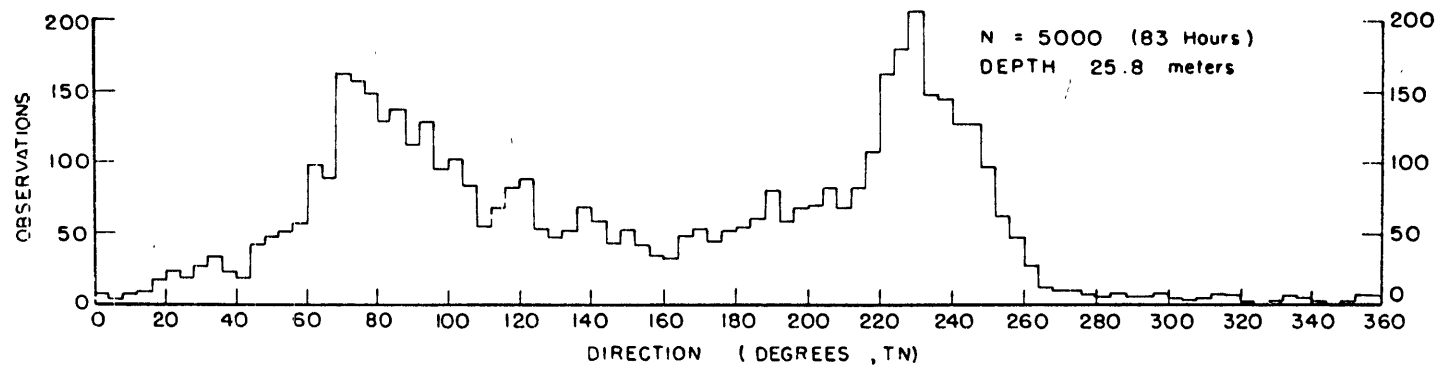
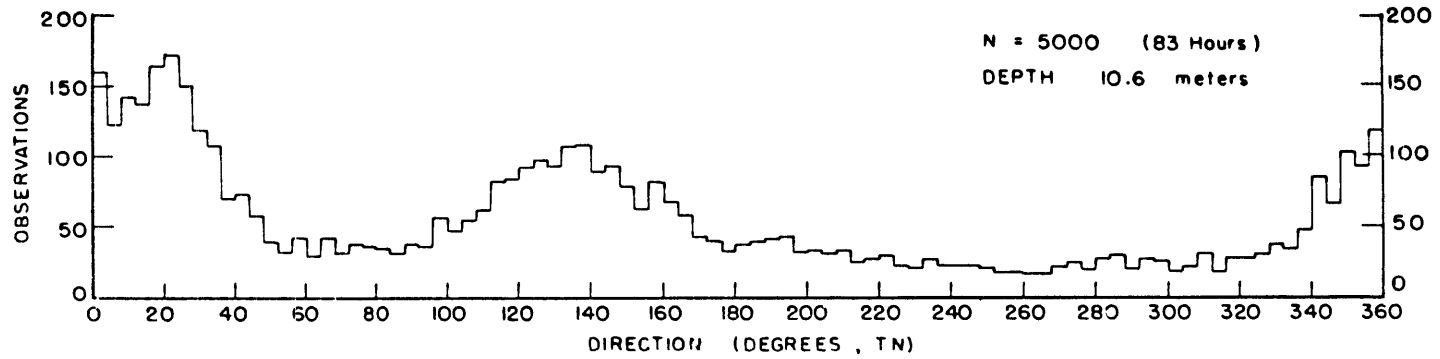


Figure 32. DIRECTION HISTOGRAM (EXPT 67-2)

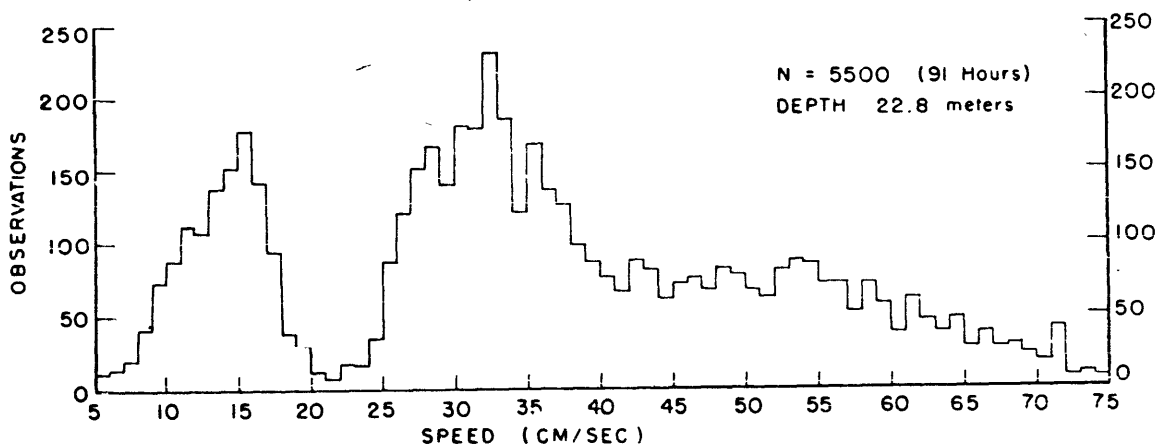
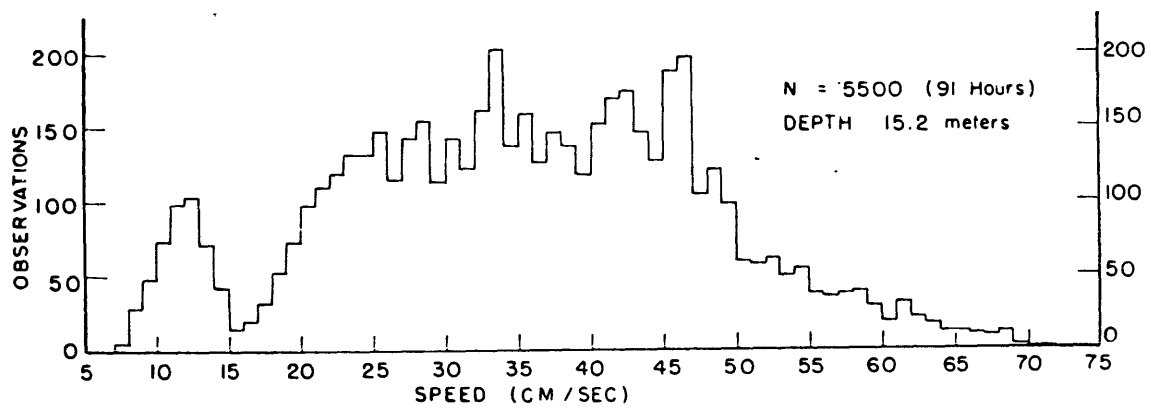
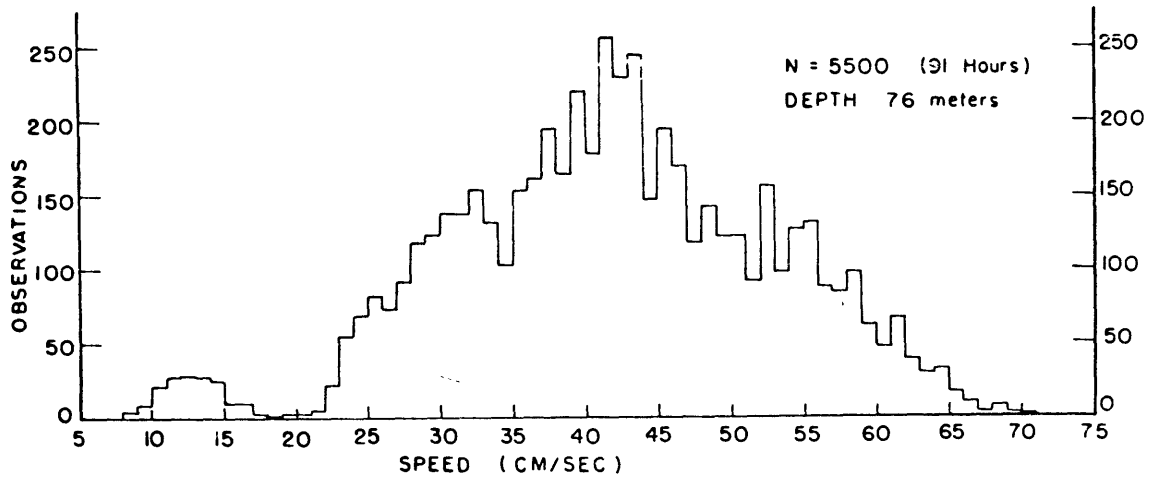


Figure 23. SPEED HISTOGRAM (EXPT 67-3)

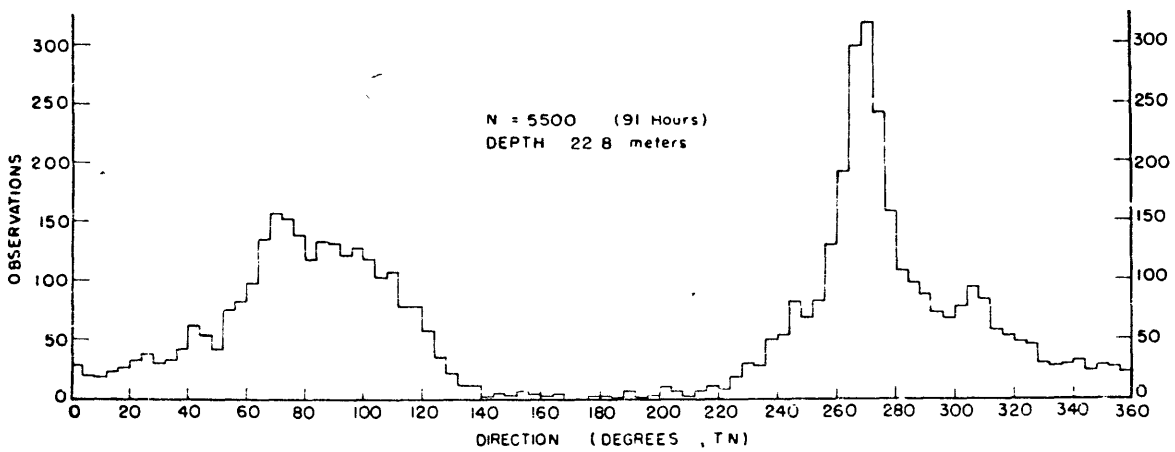
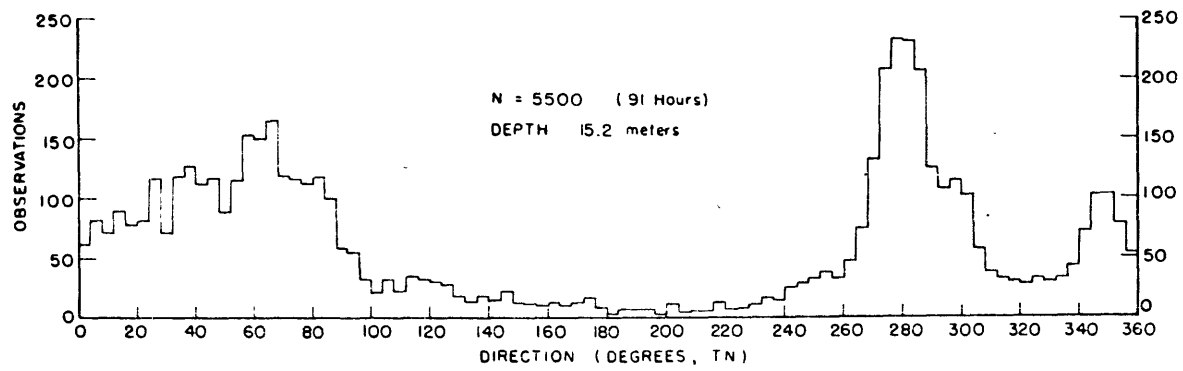
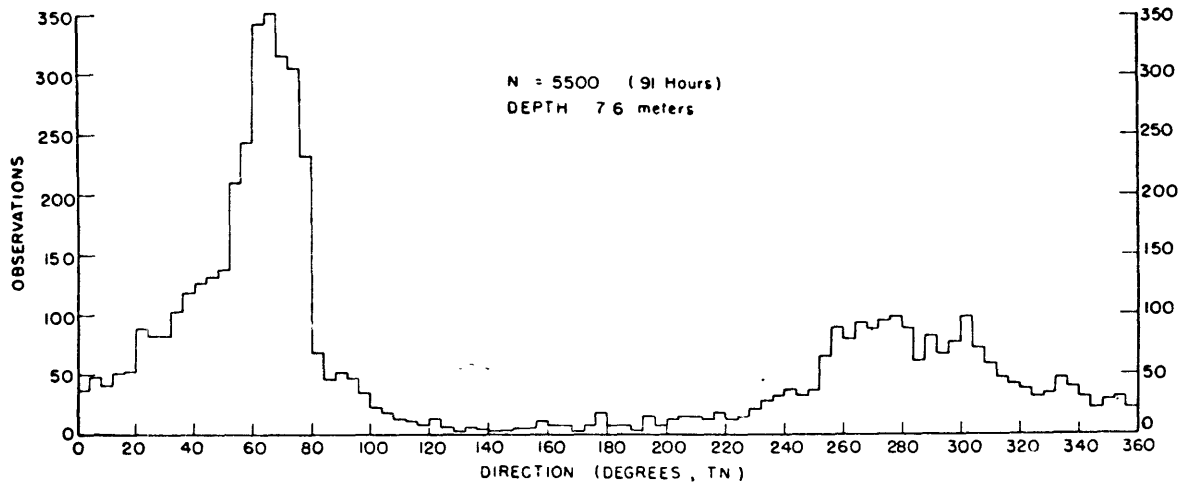


Figure 34 DIRECTION HISTOGRAM (EXPT 57-3)

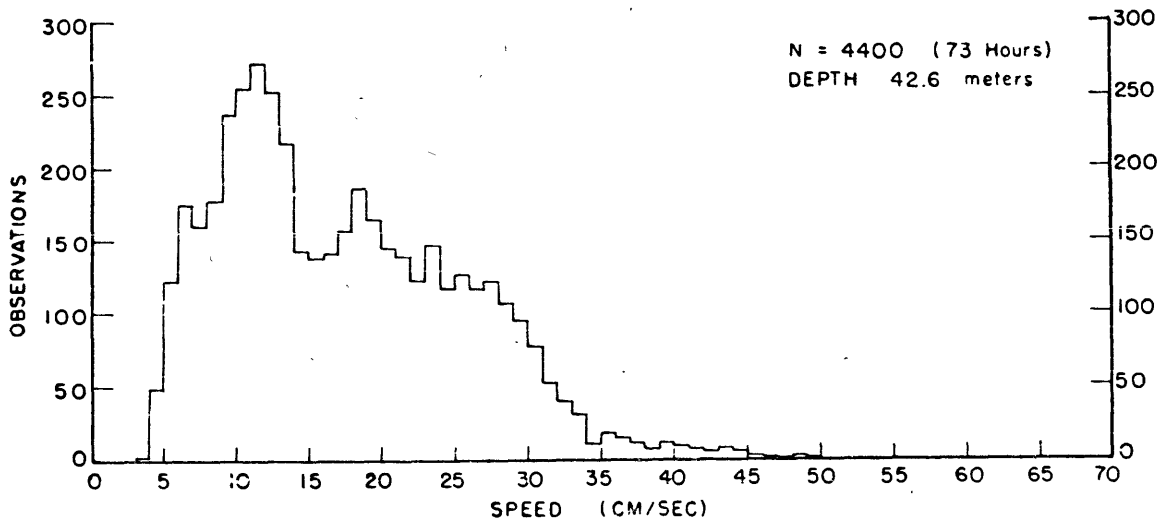
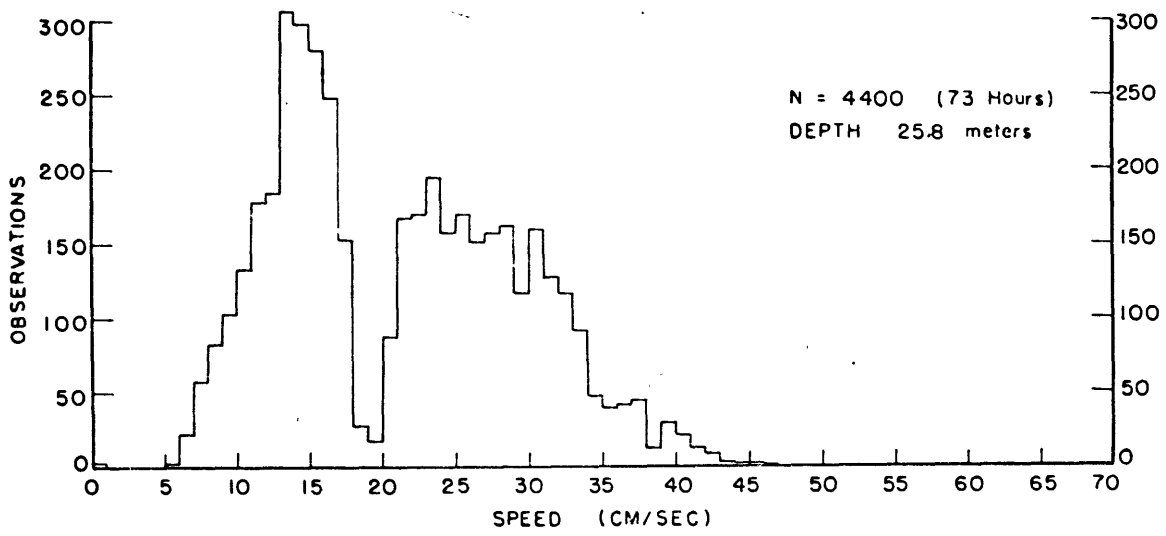
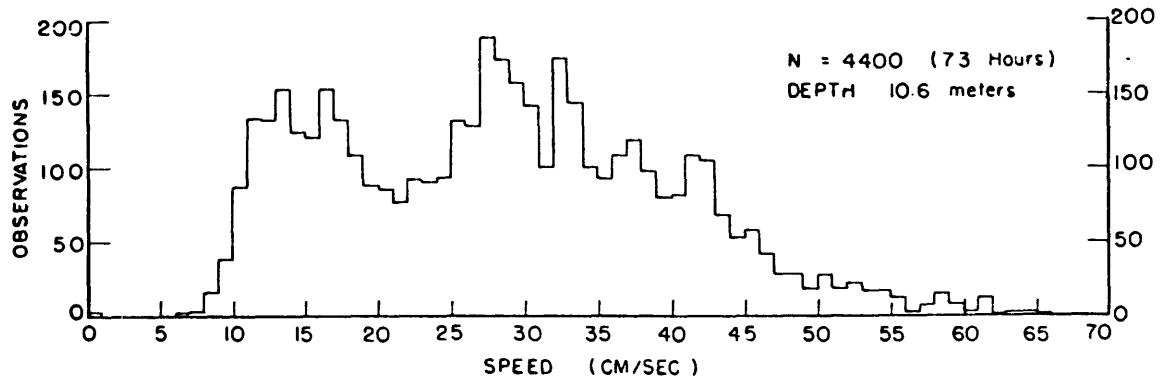


Figure 35. SPEED HISTOGRAM (EXPT 67-4)

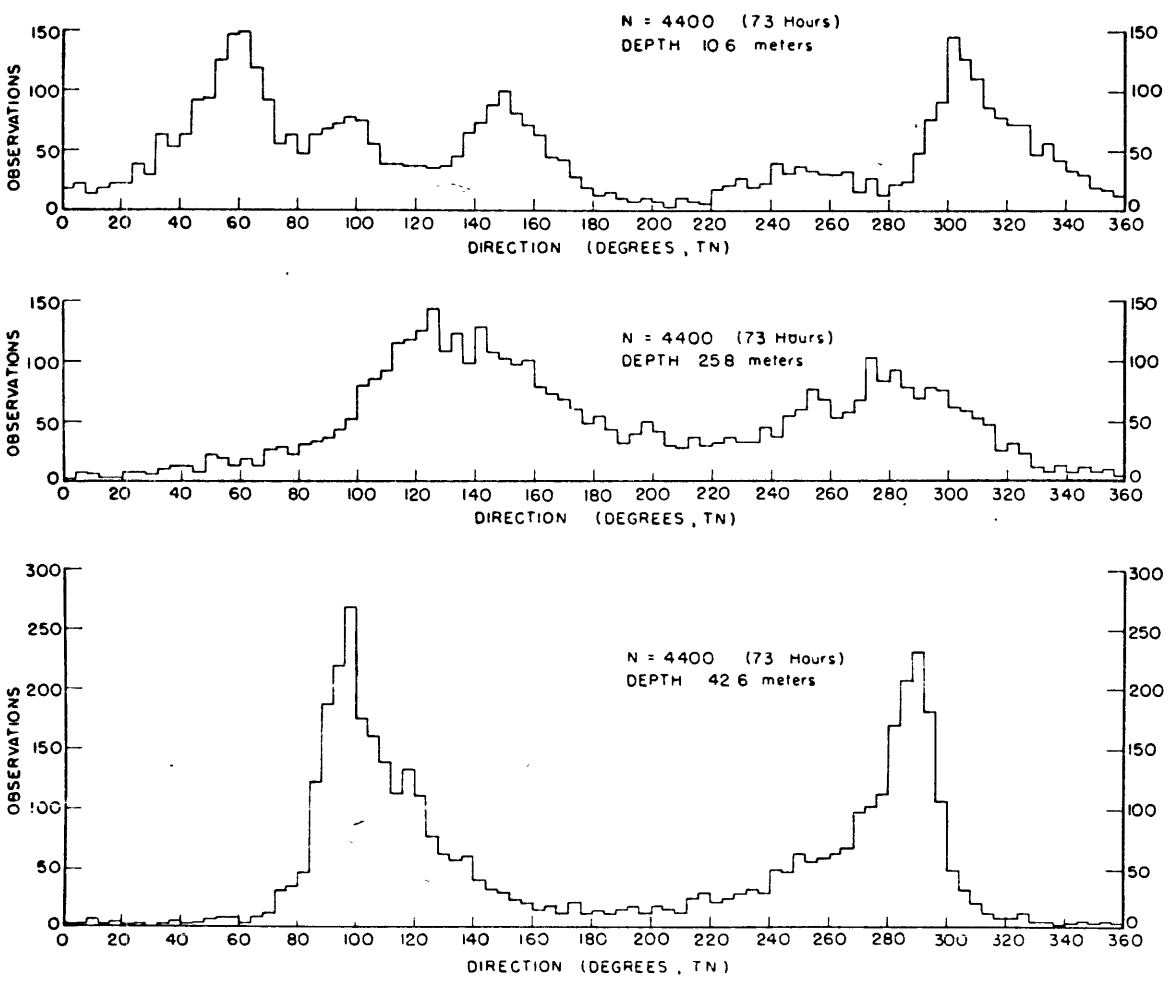


Figure 36. DIRECTION HISTOGRAM (EXPT 67-4)

current and internal wave motion. The large modes describe the tidal currents which are present all the time.

Direction histograms were plotted on a linear scale to eliminate the polar distortion inherent in a polar plot (Webster, 1964), and 0° refers to true north. The crest of Stellwagen Bank trends about 15° west of true north. In each of the three experiments the histogram of the lowermost instrument shows a back-and-forth type of motion suggestive of shallow water flood and ebb tidal currents. This is best exemplified at the mouth of Massachusetts Bay (EXPT 67-4) where two similar modes occur at 095° and 290° .

Figures D7 and D8 contain Calcomp plots of the speed measurements at Station T at 25.6 m and 42.8 m.

The time origin of the velocity data was destroyed by film exposure at the beginning of an experiment. Also, the film was all used before the current meters were taken from the water, removing any possibility of attaching a time origin at the termination of the experiment. It was assumed that the initiation of a distinct group of large amplitude high frequency speed fluctuations occurred simultaneously throughout the depth, as was seen in the temperature data. The difference in time in the arrival of the phenomena at the instruments arising from horizontal separation due to cable curvature is neglected because the maximum horizontal separation between the instruments was 4.5 m or a maximum of 2 to 3 minutes arrival time

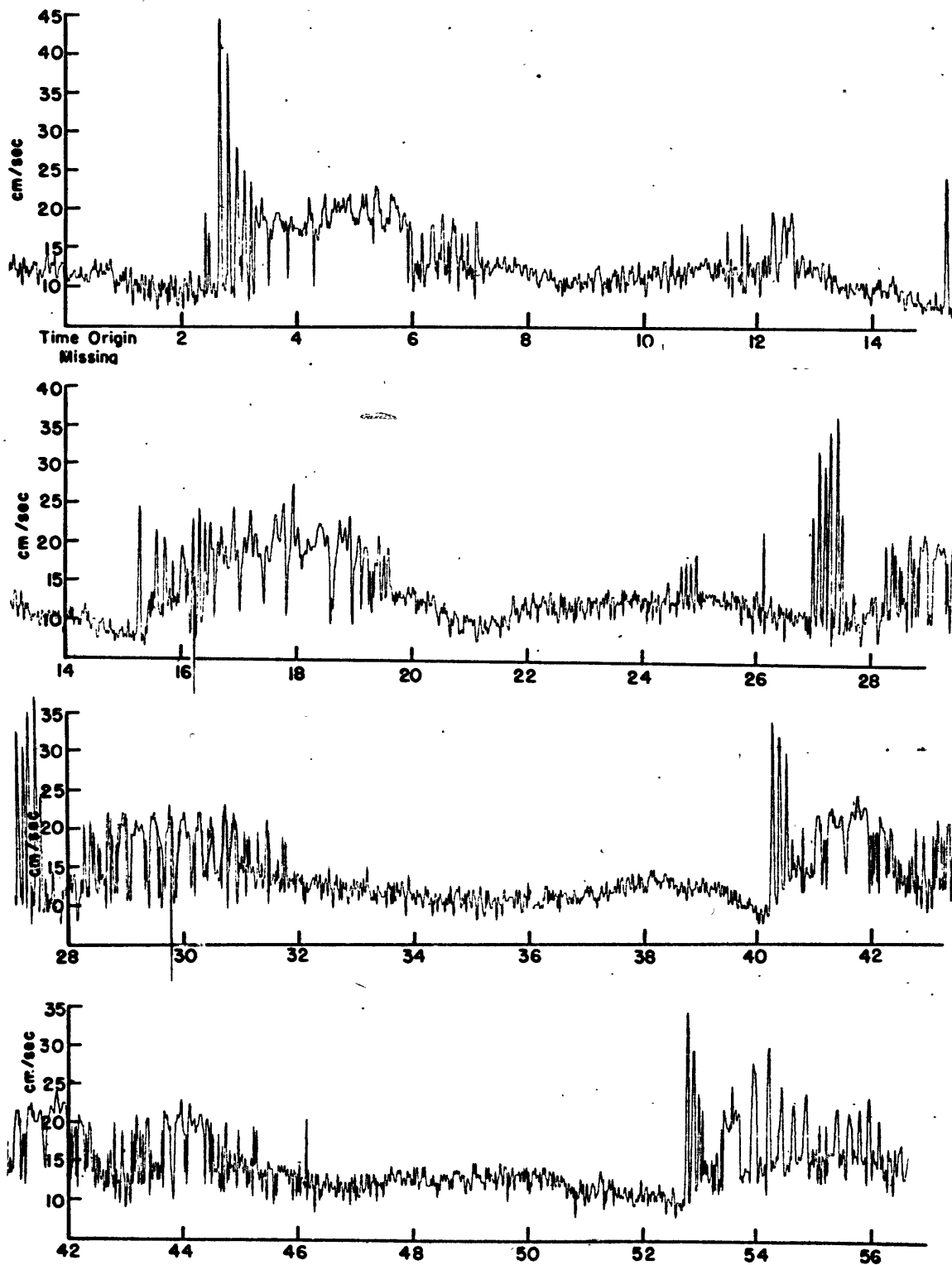
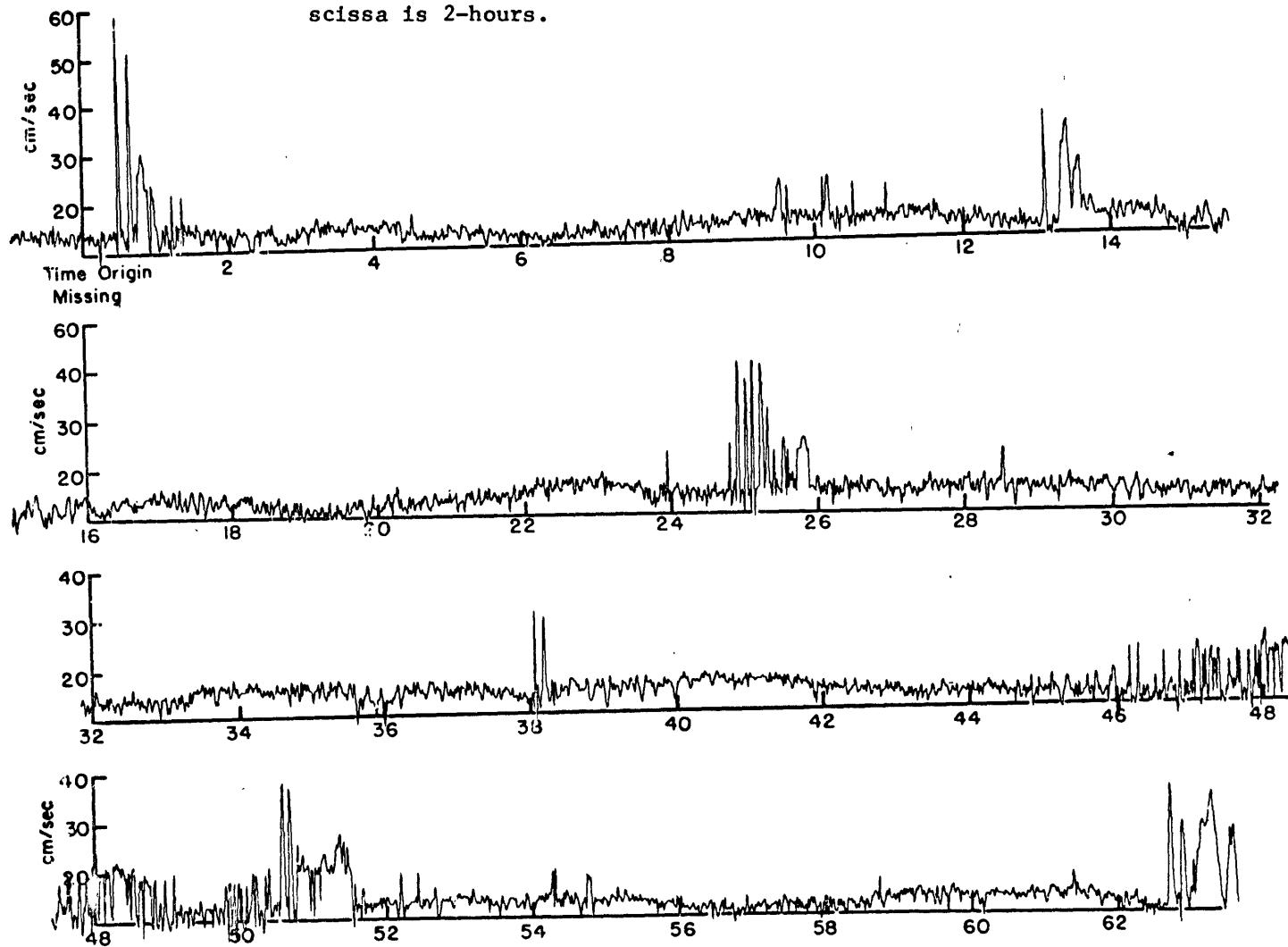


Figure D7. A Calcomp plot of 3900 speed measurements at 42.6m at Station T between July 13-17, 1967. The time origin is missing and the interval between tick marks on the abscissa is 2-hours.

Figure D8. A Calcomp plot of 3900 speed measurements at 25.8m at Station T between July 13-17, 1967. The time origin is missing and the interval between tick marks on the abscissa is 2-hours.



difference. A real-time origin for the data collected at Station T is based upon two features. The temperature measurements do not contain a well-defined abrupt increase in temperature until 1648 EST, July 14 which was 28 hours and 31 minutes after the temperature recording began; also, the speed records do not contain any distinct groups until about 28.5 hours have elapsed from the start of their data. All instruments had begun operating within three hours of one another. The second feature is that time intervals between the successive groups of large amplitude high frequency fluctuations in the speed records were similar to the time intervals between successive groups of short period internal waves. Therefore, the three sets of velocity measurements were aligned so that their first distinct group coincided in time with 1648 EST, July 14. Using 1648 EST, July 14 as a real-time reference, the length of data lost from film exposure was 128 minutes (H880) and 106 minutes (H879). The fact that three full turns of film around the supply spool corresponds to 126 minutes of recording time indicates that the choice of the simultaneous time for the data can be considered valid, since exposure of film at the beginning of an experiment usually arises from a hurried LOAD procedure. In the future, the instrument should be turned ON (prior to recording data) until the supply spool has completed three full turns.

Appendix E: Temperature Measurements from a Towed Thermistor

A thermistor, enclosed in a Braincom Navitherm assembly just above a V-fin, was towed at 16 m below the surface on the western side of Stellwagen Bank on September 19, 1967. The towing occurred from the stern of the R/V RR SHROCK. Temperature was recorded continuously on a Leeds-Northrup strip chart recorder. The time constant of the thermistor and its attachment was about .5 minutes; the vessel travelled at about 6.5 knots. Figure E1 portrays the pattern of towing and identifies the temperature sections. Navigation was accomplished by dead reckoning, by following bottom topography although the fathometer was inoperative 15% of the time, and with two small floats located approximately 12 km west of Stellwagen Bank. The small floats were sighted on only three occasions, and it is reasonable to assume that at any time the position error of the vessel was at least 3 km.

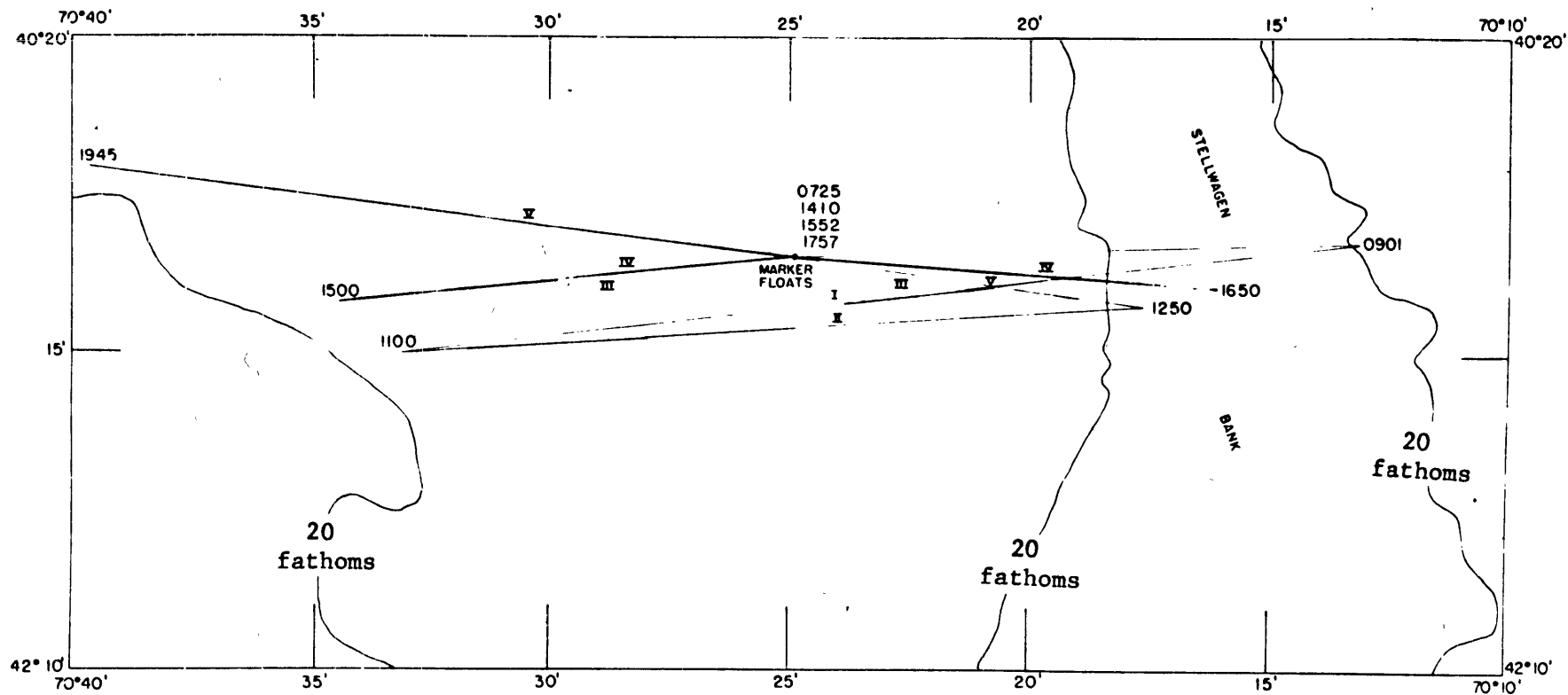


Figure E1. The pattern of thermistor towing on September 19, 1967, and the identification of thermal structure data sections. Times (EST) shown are when the vessel changed course and when the marker floats were passed.

Appendix F: Problems for Further Investigation

1. What is the mechanism generating the surface bands?
2. What is the mechanism generating regularly occurring groups of short period internal waves?
3. Are internal waves a sink for the ordinary tide?

Acknowledgements

I am grateful to Professor Henry Stommel for suggesting this investigation and for his continual support. The critical comments of Professors Stommel, Carl Wunsch, and Norman Phillips were most helpful. I wish to thank Professor Wunsch for the use of his computer program to calculate the eigenfunctions.

I am indebted to Mr. Dan Arnold, captain of the fishing vessel FRANCES ELIZABETH, for rescuing the project from despair in August, 1965 and thereafter helping immensely with the buoy moorings. Mr. Tony Cella's continual aid at Lewis Wharf was highly valued. The help of Captain Harold Payson is acknowledged. To the many graduate students who assisted in the field program I express my sincere thanks. I thank Miss Diane Lippincott for typing many of the diagram labels.

My wife Tema was a constant source of love, understanding, and encouragement. She also typed many drafts of the thesis as well as the final manuscript.

The computations were done on an IBM 360/65 at the MIT Computation Center. This work was supported by the Office of Naval Research under research grant 1841(74).

References

Bigelow H.B. (1927) Physical oceanography of the Gulf of Maine. Bull. U.S. Bur. Fish. 40, 511-1027.

Bingham C., M.D.Godfrey and J.W.Tukey (1967) Modern techniques of power spectrum estimation. IEEE Trans. on Audio and Electroacoustics. AU-15, 56-66.

Blackman R.B. and J.W.Tukey (1958) The measurement of power spectra. Dover, 190pp.

Bretherton F.P. (1966) The propagation of groups of internal gravity waves in a shear flow. Quart. J. Royal Meteor. Soc. 92, 466-480.

Cooley J.W. and J.W.Tukey (1965) An algorithm for the machine calculation of complex Fourier series. Math. Computation. 19, 297-301.

Cooper J.W. and H.Stommel (1968) Regularly spaced steps in the main thermocline near Bermuda. J. Geophys. Res. 73, 5849-5854.

Cox C.S. and H.Sandstrom (1962) Coupling of internal waves and surface waves in water of variable depth. J. Oceanog. Soc. Japan, 20th Anniv. Vol. 499-513.

Davidson M.J. and J.R.Heirtzler (1968) Spatial coherence of geomagnetic rapid variations. J. Geophys. Res. 73, 2143-3162.

Defant A. (1961) Physical oceanography. Pergamon Press, 2, 598pp.

Ewing G.C. (1950) Slicks, surface films and internal waves. J. Mar. Res. 9, 161-187.

Fofonoff N.P. (1967) Variability of ocean circulation. Trans. Am. Geophys. Un. 48, 575-578.

Frassetto R. (1964) Short-period vertical displacements of the upper layers in the Strait of Gibraltar. NATO Technical Report No. 30.

Fritzlaff J.A. and J.P.Laniewski (1964) Development of a self-contained deep moored buoy system. In: Transactions of 1964 Buoy Technology Symposium, MTS, 73-111.

- Groves G.W. and E.J.Hannan (1968) Time series regression of sea level on weather. *Rev. of Geophys.* 6, 129-174.
- Groves G.W. and B.D.Zetler (1964) The cross spectrum of sea level at San Francisco and Honolulu. *J. Mar. Res.* 22, 269-275.
- Haight F.J. (1942) Coastal currents along the Atlantic coast of the United States. U.S.Coast and Geodetic Survey special publication 230.
- Hansen P. (1964) Note on the omnidirectionality of the Savonius rotor current meter. *J. Geophys. Res.* 69, 4419.
- Haskell N.A. (1953) The dispersion of surface waves on multi-layered media. *Bull. Seism. Soc. Am.* 43, 17-34,
- Haurwitz B. (1953) Internal tidal waves in the ocean. Woods Hole Oceanographic Institution Technical Report, Ref. No. 53-69. Unpublished manuscript.
- Haurwitz B., H.Stommel and W.H.Munk (1959) On the thermal unrest in the ocean. In: *The atmosphere and the sea in motion*, B.Bolin, editor, Rockefeller Institute Press, 74-94.
- Hines C.O. and C.A.Reddy (1967) On the propagation of atmospheric gravity waves through regions of wind shear. *J. Geophys. Res.* 72, 1015-1034.
- Hinich M.J. and C.S.Clay (1968) The application of the discrete Fourier transform in the estimation of power spectra, coherence, and bispectra of geophysical data. *Rev. of Geophys.* 6, 347-363.
- Hunkins K. (1967) Inertial oscillations of Fletcher's Ice Island (T-3). *J. Geophys. Res.* 72, 1165-1174.
- IBM (1967) System/360 scientific subroutine package, version II.
- Krauss W. (1966) *Interne wellen*. Gebrüder Borntraeger, 248 pp.
- Lafond E.C. (1951) Processing oceanographic data. U.S.Navy Hydrographic Office Publication 614.
- Lafond E.C. (1962) Internal waves. In: *The sea*, M.N.Hill, editor, Interscience Publications, 1, 731-751.
- Long R.R. (1954) Some aspects of the flow of stratified fluids, II. Experiments with a two-fluid system. *Tellus*, 6, 97-115.

- Madden T. (1963) Spectral, cross-spectral, and bispectral analysis of low frequency electromagnetic data. Geophys. Lab. MIT, 44pp.
- Munk W.H. (1966) Abyssal Recipes. Deep-Sea Res. 13, 707-730.
- Munk W.H. and G.J.F. Macdonald (1960) The rotation of the earth. Cambridge Univ. Press, 323pp.
- Munk W.H., F.E. Snodgrass and M.J. Tucker (1959) Spectra of low-frequency ocean waves. Bull. Scripps Inst. of Oceanog. 7, 283-362.
- Paquette R.G. and B.E. Henderson (1965) The dynamics of simple deep-sea moorings. General Motors Corporation Report TR65-79.
- Perry K.E. and P.F. Smith (1965a) Digital methods of handling oceanographic transducers. In: Marine sciences instrumentation, W.C. Knopf and H.A. Cook, editors, Plenum Press, 3, 25-39.
- Perry K.E. and P.F. Smith (1965b) The importance of digital techniques for oceanographic instrumentation. In: Ocean science and ocean engineering, 1, Mar. Tech. Soc. 398-413.
- Pickard G.L. (1954) Oceanography of British Columbia inlets, III. Internal waves. In: Progress reports of the Pacific coast stations of the Fisheries Research Board of Canada, Issue 98, 13-16.
- Pickard G.L. (1961) Oceanographic features of inlets in the British Columbia mainland coast. J. Fish. Res. Bd. Canada, 18, 907-999.
- Pode L. (1951) Tables for computing the equilibrium configuration of a flexible cable in a uniform stream. David Taylor Model Basin Report 687.
- Press F. and D. Harkrider (1962) Propagation of acoustic-gravity waves in the atmosphere. J. Geophys. Res. 67, 3889-3908.
- Richardson W.S., P.B. Stimson and C.H. Wilkins (1963) Current measurements from moored buoys. Deep-Sea Res. 10, 369-388.
- Robinson E.A. (1967) Predictive decomposition of time series with application to seismic exploration. Geophysics, 32, 418-484.
- Sabinin K.D. and V.A. Shulepov (1965) Short-period internal waves of the Norwegian Sea. Okeznologiiz, 5, 264-275. (Trans., Scripta Technica for AGU.)

Shand J.A. (1953) Internal waves in Georgia Strait. Am. Geophys. Un. Trans. 34, 849-856.

Tidal current tables, Atlantic coast of North America (1967)
U.S. Government Printing Office, 199pp.

Van Dorn W. (1956) Large-volume water samplers. Am. Geophys. Un. Trans. 37, 682-684.

Webster F. (1964) Some periods of measurement from moored ocean buoys. In: Transactions of 1964 Buoy Technology Symposium, MTS, 33-48.

Welch P.D. (1967) The use of fast Fourier transform for the estimation of power spectra: a method based on time averaging over short, modified periodograms. IEEE Trans. on Audio and Electroacoustic, AU-15, 70-73.

White R.A. (1967) The vertical structure of temperature fluctuations within an oceanic thermocline. Deep-Sea Res. 14, 613-623.

Woods J.D. (1968) Wave-induced shear instability in the summer thermocline. J. Fluid Mech. 32, 791-800.

Biographical Sketch

The author was born in Montreal, Canada on June 24, 1942. During high school, he served as a member of the Students' Council and was elected its president in his senior year. In September, 1959 he entered Mc Gill University, where he was a member of Sigma Alpha Mu fraternity. Mr. Halpern received a Bachelor of Science degree with Honours in Geology and Physics in May, 1964. While an undergraduate he did analytical chemistry for a pharmaceutical firm and participated in geological field work in the Gaspé Peninsula of Quebec, the Rocky Mountain foothills of northern Alberta, and the Canadian Arctic Islands north of 74° N.

In September, 1964 he enrolled at MIT. The author presented a paper titled "Observations of Short Period Internal Waves" at the 49th Annual Meeting of the American Geophysical Union in April, 1968.

Mr. Halpern is a member of the American Geophysical Union, American Society for Oceanography, and Society of the Sigma Xi.

On May 29, 1966 the author married the former Tema Kovack of Milton, Massachusetts.